

Sigurjón Jónsson

A survey of active landslide movement in east Iceland from satellite radar interferometry

Summary

Landslides in Iceland have caused both fatalities and considerable economic loss during the past centuries. Knowledge of creeping landslides near towns in eastern and northern Iceland led to the initiation of this project that has the following two primary objectives: To assess the monitoring capabilities of Synthetic Aperture Radar Interferometry (InSAR) from satellites on these known landslides and to survey large areas in eastern and central-north Iceland to search for other creeping landslides that may exist. In this report I focus on results from eastern Iceland.

I ordered and processed radar data from the European Space Agency's archives that were collected by the ERS-1 and ERS-2 satellites during 1993-1999. I also requested new data acquisitions from the Envisat satellite during summers in 2004 and 2005. A total of 44 interferograms were processed and they have variable time-spans from 1 day to four years. Some problems were encountered in the data processing, which were mainly due to an inaccurate digital elevation model (DEM), but no adequate high-resolution DEM was available for the project, and due to high-elevation snow cover in several of the images, which corrupts the signal. However, my results indicate that while inter-annual interferograms often provide only limited information, single- and multi-month summer interferograms are very useful to study landslides in eastern Iceland.

Prior to the start of this project, two landslides were known to be active in eastern Iceland: The Þófi landslide near the town of Seyðisfjörður and the Urðarbotn landslide above Neskaupstaður town. Repeated GPS measurements from 2001-2 revealed that these landslides were moving at rates of up to 40 cm/year. No suitable ERS radar data exist from 2001-2002, but interferograms from 1998 and 1999 show a few cm of displacement on the Þófi landslide while interferograms from 1995-1997 and 2004-2005 exhibit no signs of displacement. These measurements demonstrate that the Þófi landslide started creeping two years before surface cracks were discovered in 2000 and that the landslide movement is episodic. The 2004-2005 data are the only suitable data that exist for imaging the Urðarbotn landslide and these data do not suggest any movement on the landslide.

In my search for other active landslides I found more than ten locations of previously unknown landslide creep. The search extended from Vopnafjörður in the north to Breiðdalur in the south. The most prominent landslides were discovered in Vopnafjörður and in Loðmundarfjörður, which both are about 1 km wide. The other landslides are somewhat smaller or only several hundreds of meters wide. The Vopnafjörður landslide creep shows variations in both displacement rate and aerial extent during the observation period, which further demonstrates the episodic behavior of landslides in eastern Iceland.

The results of this project show that InSAR is a useful technique to both search for and monitor landslides in eastern Iceland that are larger than 1-200 m in aerial extent. Radar data acquisitions of eastern Iceland are neither regular nor frequent and the 2004-2005 data exist only because of my request to European Space Agency. Therefore, a monitoring policy and an observation plan for eastern Iceland is needed to secure future data acquisitions.

Contents

| | |
|---|-----------|
| List of Figures | 7 |
| Abbreviations | 9 |
| 1 Introduction | 11 |
| 2 Data Availability and Data Processing | 13 |
| 2.1 Limitations due to the Radar Viewing Geometry | 13 |
| 2.2 ERS-1 and ERS-2 Data Availability and Baselines | 16 |
| 2.3 Envisat Acquisitions and Baselines | 18 |
| 2.4 Data Processing Steps | 23 |
| 3 General Results | 25 |
| 3.1 General Interferogram Results | 25 |
| 3.2 Coherence Conditions | 28 |
| 3.3 Limitations due to the inaccurate Digital Elevation Model | 32 |
| 4 Observed Landslide Motion at Various Locations | 35 |
| 4.1 The Þófi Landslide in Seyðisfjörður | 37 |
| 4.2 The Urðarbotn Landslide above Neskaupstaður | 46 |
| 4.3 The Vopnafjörður Area | 48 |
| 4.4 Other Locations in Descending Interferograms | 55 |
| 4.4.1 Ytri-Þverhryggir in Lambadalur, Borgarfjörður | 55 |
| 4.4.2 Reykjadalur in Mjóifjörður | 56 |
| 4.4.3 Barðsnes | 56 |
| 4.4.4 Jökulbotnar in Reyðarfjörður | 59 |
| 4.4.5 Eyvindarárdalur | 60 |
| 4.4.6 Suðurdalur | 60 |
| 4.5 Detected Deformation in Ascending Interferograms | 63 |
| 4.5.1 Loðmundarfjörður | 63 |
| 4.5.2 Surtssstaðatunga in Kaldárgil, Jökulsárhlíð | 63 |
| 4.5.3 Þingmúli in Skriðdalur | 68 |
| 4.5.4 Lambadalur and Beinageitarfjall | 69 |
| 4.5.5 Breiðdalur | 70 |

| | |
|---|-----------|
| 5 Discussion | 71 |
| 6 Conclusions | 73 |
| Acknowledgements | 74 |
| A Appendix | 77 |
| A.1 Descending interferograms from ERS-1/2 data 1993-1999 | 77 |
| A.2 Descending interferograms from Envisat data 2004-2005 | 81 |
| A.3 Ascending interferograms from Envisat data 2004-2005 | 83 |

List of Figures

| | | |
|----|---|----|
| 1 | A schematic figure of an ascending ERS-2 pass above Iceland | 14 |
| 2 | A schematic figure of layovers and shadows in radar imaging | 15 |
| 3 | Topography and slopes in central-east Iceland | 16 |
| 4 | Layovers in central-east Iceland | 17 |
| 5 | A map of satellite tracks covering eastern Iceland | 19 |
| 6 | ERS spatio-temporal baseline information for eastern Iceland tracks | 20 |
| 7 | Spatio-temporal baseline information for descending track 424 | 21 |
| 8 | Envisat baseline information for ascending track 187 | 22 |
| 9 | Envisat baseline information for descending track 195 | 23 |
| 10 | Descending InSAR image of eastern Iceland | 27 |
| 11 | An ascending InSAR image of eastern Iceland | 29 |
| 12 | SAR amplitude image and a tandem interferogram of Vopnafjörður | 30 |
| 13 | Examples of coherence | 31 |
| 14 | Coherence as a function of temporal and perpendicular baselines | 31 |
| 15 | Tandem interferograms showing decorrelation due to snow | 33 |
| 16 | Examples of differential interferograms influenced by the poor DEM | 34 |
| 17 | An example of how interferograms are displayed in this report | 35 |
| 18 | An example of the interferogram post-processing | 36 |
| 19 | Seyðisfjörður map | 37 |
| 20 | SAR amplitude image and a tandem interferogram of Seyðisfjörður | 38 |
| 21 | Seyðisfjörður interferograms from 1993-1997 | 39 |
| 22 | Seyðisfjörður interferograms from 1995-7 | 40 |
| 23 | Seyðisfjörður interferogram from 1998 | 41 |
| 24 | Geocoded Seyðisfjörður interferogram from 1998 | 42 |
| 25 | Seyðisfjörður interferogram from 1999 | 43 |
| 26 | Seyðisfjörður interferograms from 2004-5 | 44 |
| 27 | SAR amplitude images from Neskaupstaður | 46 |
| 28 | Two interferograms of Neskaupstaður from 2004-5 | 47 |
| 29 | Vopnafjörður map | 48 |
| 30 | Vopnafjörður interferograms from 1995 | 49 |

| | | |
|----|--|----|
| 31 | Geocoded Vopnafjörður interferogram from 1995 | 50 |
| 32 | Vopnafjörður interferograms from 1996-9 | 51 |
| 33 | Vopnafjörður interferograms from 2004-5 | 53 |
| 34 | Precipitation and deformation in Vopnafjörður | 54 |
| 35 | Deformation in Borgarfjörður | 55 |
| 36 | Interferograms from Mjóifjörður | 57 |
| 37 | Interferograms of Barðsnes peninsula | 58 |
| 38 | A map and an interferogram of Jökulbotnar in Reyðarfjörður | 59 |
| 39 | Interferograms of Eyvindarárdalur | 61 |
| 40 | A map and an interferogram from Suðurdalur | 62 |
| 41 | Loðmundarfjörður map and interferograms | 64 |
| 42 | Two interferograms of Loðmundarfjörður | 65 |
| 43 | A map and an amplitude image of Kaldárgil | 66 |
| 44 | Two interferograms of Kaldárgil from 2004 | 66 |
| 45 | Two interferograms of Kaldárgil from 2004-5 | 67 |
| 46 | Blowups of three interferograms from Kaldárgil | 67 |
| 47 | A map and an interferogram of Þingmúli | 68 |
| 48 | Beinageitafjall and Lambadalur interferograms | 69 |
| 49 | Breiðdalur map and interferograms | 70 |

Abbreviations

| | |
|---------|---|
| ALOS | Advanced Land Observing Satellite |
| DEM | Digital Elevation Model |
| DLR | German Aerospace Center |
| CSA | Canadian Space Agency |
| ERS | European Remote Sensing Satellite |
| ESA | European Space Agency |
| GPS | Global Positioning System |
| IMO | Icelandic Meteorological Office |
| InSAR | Interferometric Synthetic Aperture Radar |
| JPL | Jet Propulsion Laboratory |
| LOS | Line of sight |
| NASA | National Aeronautics and Space Administration |
| NLSI | National Land Survey of Iceland |
| ROI_PAC | Repeat Orbit Interferometry Package |
| SAR | Synthetic Aperture Radar |
| SLC | Single-Look Complex |
| SNR | Signal to Noise Ratio |
| SRTM | Shuttle Radar Topography Mission |
| UTM | Universal Transverse Mercator |
| WGS | World Geodetic System |

1 Introduction

Landslides and avalanches mainly occur in three regions of Iceland: The Eastern Fjords, central part of North Iceland, and the Western Fjords [*Jóhannesson and Arnalds, 2001*]. These areas are geologically the oldest parts of Iceland and consist of valleys and fjords bounded by steep sided mountains, a landscape shaped by glaciers during the past ice ages. Two snow avalanches in the Western Fjords in 1995 caused 34 fatalities and led to a complete revision of laws and regulations related to hazard and risk evaluation for landslides and avalanches in Iceland. These new laws and regulations initiated various projects to study, catalogue, map, and evaluate landslides and avalanches near towns, mostly in these three regions. In addition, a recent discovery of active landslide movement near the towns of Seyðisfjörður and Neskaupstaður in East Iceland has also prompted extra efforts to assess if a catastrophic event could occur. These efforts include landslide mapping and geodetic observations of the landslide movement. GPS measurements of the Þófi landslide in Seyðisfjörður and in Urðarbotn above Neskaupstaður, have shown displacement rates of up to 33 and 138 cm/year, respectively [*Jensen and Jóhannesson, 2002; Jensen and Hjartarson, 2002*].

The results of the Seyðisfjörður and Neskaupstaður GPS measurements, among other things, led to the initiation of a new project focussing on using satellite radar interferometry (InSAR) to study Icelandic landslides. This project started in 2003 and it was decided to focus on landslides in East Iceland and in the central part of North Iceland. The project has three main goals:

1. To investigate the feasibility of satellite radar interferometry (InSAR) to detect and monitor landslides in Iceland.
2. To use InSAR to measure landslide motion on landslides that are known to be active, such as the Þófi landslide in Seyðisfjörður, Urðarbotn above Neskaupstaður, and the landslides along the road to Siglufjörður in North Iceland, and to compare InSAR results with ground based measurements.
3. To survey both East and North Iceland to search for other landslides that may be creeping at present.

In this report I present results from East Iceland. I begin by discussing general conditions of InSAR and the satellite radar data availability for the region. I then move on and review the main data processing steps involved followed by more detailed analysis on how interferometric correlation degrades with time for this area, which is a fundamental limitation of InSAR. Next I discuss the general results of the measurements in East Iceland and then move on to describe results at the different sites, starting with the Þófi landslide in Seyðisfjörður, followed by findings above Neskaupstaður and in other areas.

2 Data Availability and Data Processing

The satellite radar data used in this project are from the ERS-1, ERS-2, and Envisat satellites operated by the European Space Agency (ESA). ERS-1 was launched in 1991 and was operated for nine years or until 2000. ERS-2 and Envisat were launched in 1995 and 2002, respectively, and both are still in operation. However, the precise pointing of the ERS-2 radar antenna failed in 2001 and since then ERS-2 data are of limited use for radar interferometry. All these satellites transmit radar signals at C-band (wavelength ≈ 5.6 cm) that interact with and reflect from objects on the ground that have a roughness of a similar dimension. The ERS-1 and ERS-2 radar wavelengths are identical and data from these two satellites can be combined to form interferograms. The Envisat radar, on the other hand, operates on a slightly different wavelength so Envisat data cannot easily be combined with ERS data for interferometry. Other radar data of Iceland exist, including data from the Japanese L-band (wavelength ≈ 23.5 cm) JERS-1 satellite (1992-1998) and the Canadian C-band Radarsat-1 (launched in 1995 and still in operation). However, these data were not investigated in this project. Other recent and future radar missions include the Japanese L-band ALOS satellite (launched in January 2006), the Canadian Radarsat-2 (scheduled launch in March 2007), and the German TerraSAR-X mission (scheduled launch in April 2007) .

My investigation focussed on two classes of data. First, I surveyed what data have been acquired in the past and exist in the ESA archives, which include primarily ERS-1 and ERS-2 data from the 1990s, and selected a number of these scenes for this study. Second, I requested new Envisat radar acquisitions above east Iceland during summers of 2004 and 2005. In this section I first discuss how the rough topography of east Iceland limits satellite radar observations, then I report on the ERS-1/ERS-2 data availability and baselines of the different satellite tracks that cover the study area, and finally I describe what data were collected during summers of 2004 and 2005 that I requested as a part of this project.

2.1 Limitations due to the Radar Viewing Geometry

Radar imaging is fundamentally different from conventional passive remote sensing techniques that typically acquire near-nadir photographs in the visible or near-visible bands. Radar imaging is an active remote sensing technique where radar pulses are transmitted and the ground reflections of these pulses are collected again by the same antenna (see e.g. *Hanssen* [2001] for a review). The primary advantage of this technique over other remote-sensing techniques is that radar imaging is not limited to daylight acquisitions nor to cloud-free conditions, and in addition it can be used to detect ground displacement. The ERS-1/2 satellites cover in each pass a swath that is about 100 km wide and the incidence angle varies from about 19° to about 26° across the swath (Figure 1). The Envisat satellite can be operated in several different modes with different incidence angles. However, the data requested for East Iceland were acquired in the IS-2 mode, which is similar to the ERS mode.

The average incidence angle of 23° has limitations and it means that slopes tilting away

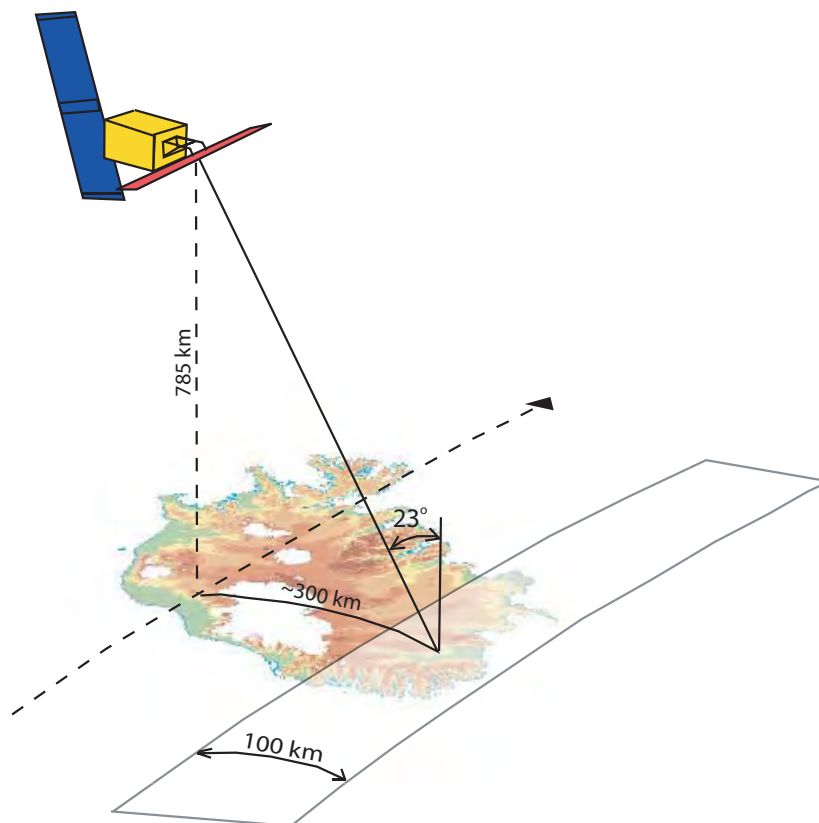


Figure 1. Schematic figure of an ERS-2 ascending pass covering East Iceland. The incidence angle is 23° in the middle of the 100 km wide swath the satellite covers in each pass. The viewing azimuth during ascending passes is about $N78^\circ E$ for ascending passes and $N78^\circ W$ for descending passes.

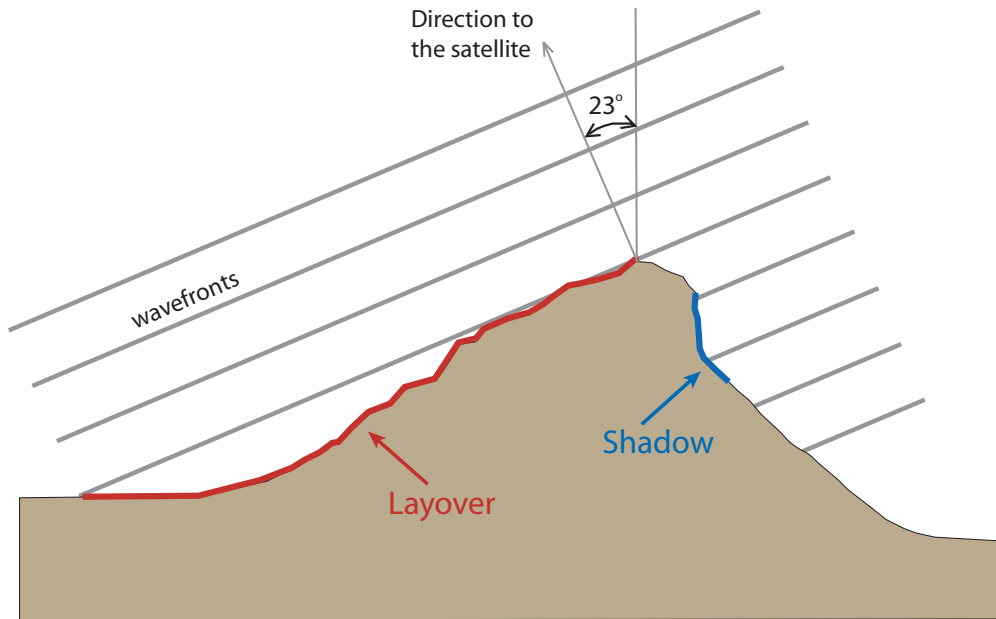


Figure 2. Schematic figure showing shadowing and layovers in radar imaging. The gray straight lines indicate incoming wavefronts from a radar satellite looking down from the left. When slopes facing the satellite are steeper than 23° reflected signals from the top of the mountain return before reflections from further down the slope, resulting in a "layover". Slopes facing away from the radar are better imaged, although shadowing can occur on very steep slopes.

from the radar and are steeper than 67° are in a 'shadow' and cannot be imaged by the radar satellite (Figure 2). However, not many slopes are so steep. More important is the imaging limitation of slopes that incline towards the radar look direction. When the tilt of these slopes exceeds 23° , radar returns from the top of the mountain will arrive at the same time or before radar reflections from further down the slope, which makes it impossible to distinguish between these signals (Figure 2). This phenomena is called a 'layover' and is much more limiting than shadowing, as it excludes virtually all significant slopes facing the radar look direction. Fortunately, radar satellites can acquire radar data from approximately opposite directions, i.e. during ascending and descending passes, so most slopes can be imaged using one of these two viewing directions.

The topography of the Eastern Fjords in Iceland is relatively rough with steep-sided valleys and fjords and with mountains exceeding 1000 m in elevation (Figure 3). A large part of the area consists of slopes exceeding 23° and some slopes even exceed 67° . Figure 4 shows a map of layovers in the central part of the eastern fjords for the ascending and descending viewing directions, assuming the average ERS incidence angle of 23° . The steep topography clearly limits the capability of the radar imaging at many slopes, showing that slopes facing ESE result in a layover during descending passes and WSW slopes cannot be imaged during ascending passes. The Þófi landslide in Seyðisfjörður is only visible in

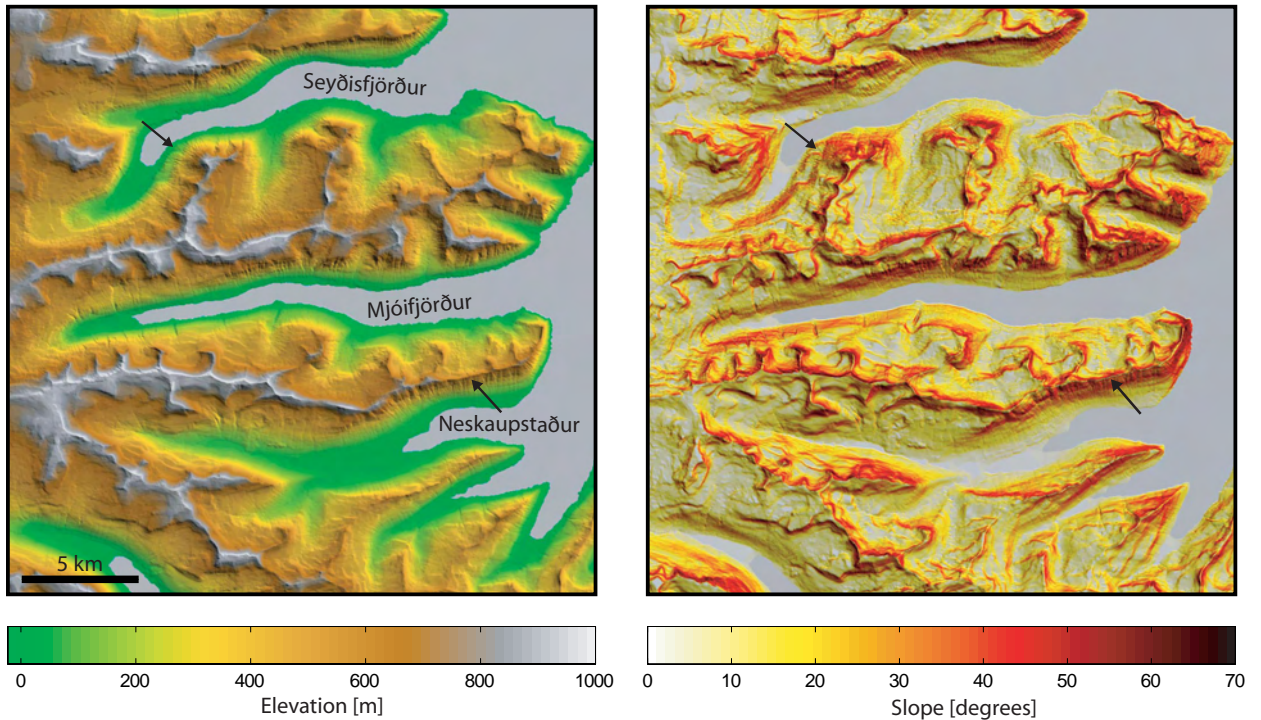


Figure 3. *An example of the topography (left) and slopes (right) in the central part of the Eastern Fjords. The topography of the Eastern Fjords is typically rough with many steep slopes. The locations of the Þófi landslide in Seyðisfjörður and the Urðarbotn landslide above the town of Neskaupstaður are indicated by black arrows.*

descending data, while the landslide above the town of Neskaupstaður can only be imaged from ascending tracks.

2.2 ERS-1 and ERS-2 Data Availability and Baselines

Thousands of ERS-1 (1991-2000) and ERS-2 (1995-) radar images have been acquired over Iceland since 1991 with multiple acquisitions for any given location from several different tracks and from both the ascending and descending directions. The repeat time of these satellites is 35 days, which means that they orbit along the same track every 35 days. The revisit time is shorter, as any given point on ground can be imaged more frequently, i.e. from overlapping tracks and from ascending and descending tracks. Although many acquisitions of Iceland exist, most of these data have been acquired during descending passes. Other limitations include a gap in ERS-1 data from 12/1993 to 4/1995, when the satellite was operated in different orbits. After the launch of ERS-2 in 1995 the satellite trailed ERS-1 by only a day, providing an opportunity to form one-day (tandem) interferograms that have been extensively used to generate digital elevation models and to study glacier motion.

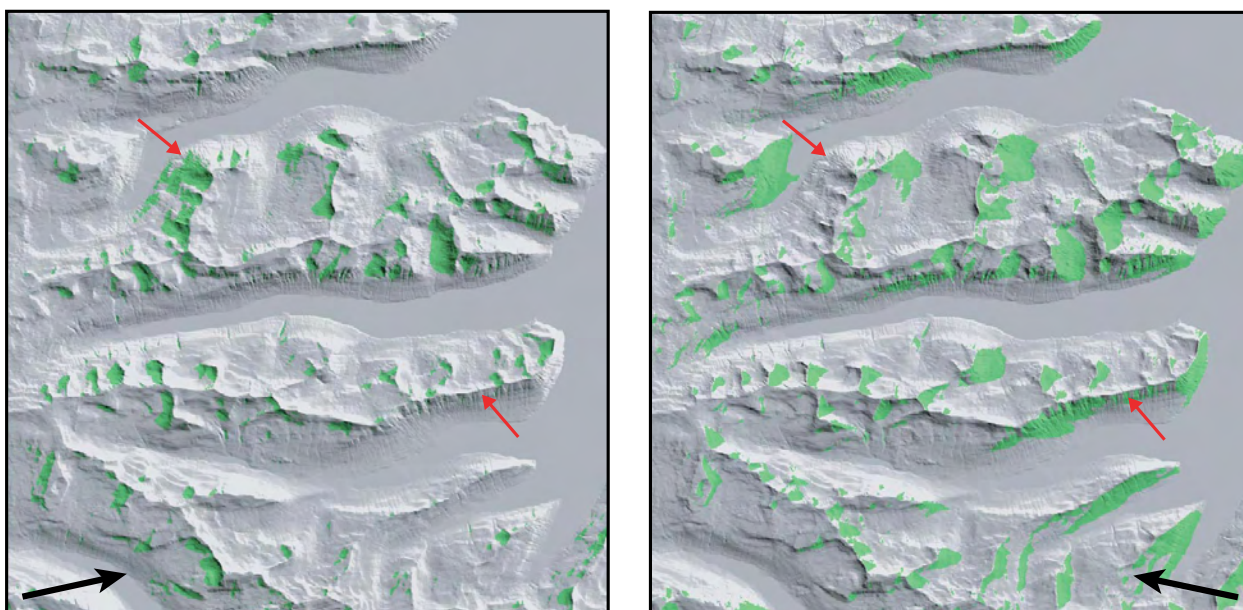


Figure 4. Map of ERS-1/2 layovers (shown as green) from the ascending (left) and descending (right) viewing directions for the same area as in Figure 3. Black arrows indicate the look direction of the satellite. The figures show clearly that many slopes cannot be imaged using only one look direction. The Þófi landslide in Seyðisfjörður can only be imaged using descending data while the Urðarbotn landslide in Neskaupstaður is only visible from ascending tracks (see red arrows).

However, after 1997 ERS-1 was only used as a backup for ERS-2 until its operation was stopped in 2000. In addition, the precise pointing capabilities of ERS-2 failed in early 2001 and after that time ERS-2 data are of limited use for interferometry.

I searched the ESA data archives for ERS-1/2 data of East Iceland from three parallel ascending tracks (tracks: 187, 416, and 144) and three parallel descending tracks (tracks: 195, 424, and 152, see Figure 5). These tracks all cover the Eastern Fjords as there is about 65% overlap between adjacent tracks at this latitude. The amount of existing ascending data from 1991 to 2006 is limited; only 5, 10, and 9 radar images have been acquired from tracks 187, 416, and 144, respectively (Figure 6). The perpendicular baseline information for these limited datasets reveals that no small-baseline summer pairs exist that span less than half a year and only one feasible inter-annual pair exist, from track 416. Therefore, no ascending ERS data were ordered for this project due to this limited data availability.

The amount of acquired descending data is much greater, or 34, 85, and 35 radar images from tracks 195, 424, and 152, respectively (Figure 6). The spatio-temporal baseline distribution indicates that many potentially usable interferograms can be formed using data from any of these three tracks, especially from track 424, where the amount of acquired data is the largest. Therefore, I decided to focus on descending track 424 and order data from this track for the project.

The ordered data were acquired mainly during the summers of 1995, 1997-1999, but a few additional scenes were ordered from 1993, 1996, 2002-2003. The data were selected based on acquisition date (summer) and the possibility to combine multi-month and multi-year scenes with a relatively small perpendicular baseline (<200 m) due to the steep topography in East Iceland. In addition, three one-day tandem pairs were ordered to generate a high-resolution DEM of the area. I ordered 24 radar images from descending track 424 and the selected dates can be seen in Figure 7. From these images I have generated 23 interferograms with variable perpendicular baselines from 10 to 260 m and with temporal baselines from one day to four years.

2.3 Envisat Acquisitions and Baselines

Within this project I submitted requests to ESA for Envisat acquisitions above East Iceland during summers 2004 and 2005. It is important to note that these data were only acquired because of my request and would otherwise not have been collected. The Envisat satellite has also a revisit time of 35 days which makes 10-11 acquisitions possible each year of any given area from a certain track. However, to avoid potential problems due to snow cover I only asked for acquisitions from May to early October. My request included about 4-5 image acquisitions from one ascending and one descending track each summer, or a total of 18 acquisitions during the 2 years. Unfortunately, there is limited prior knowledge about how the satellite orbit is going to be during each pass and thus outlier scenes are acquired that are not well suited for interferometry.

For ascending track 187 I requested four acquisitions in 2004 (from 30 May to 12 Septem-

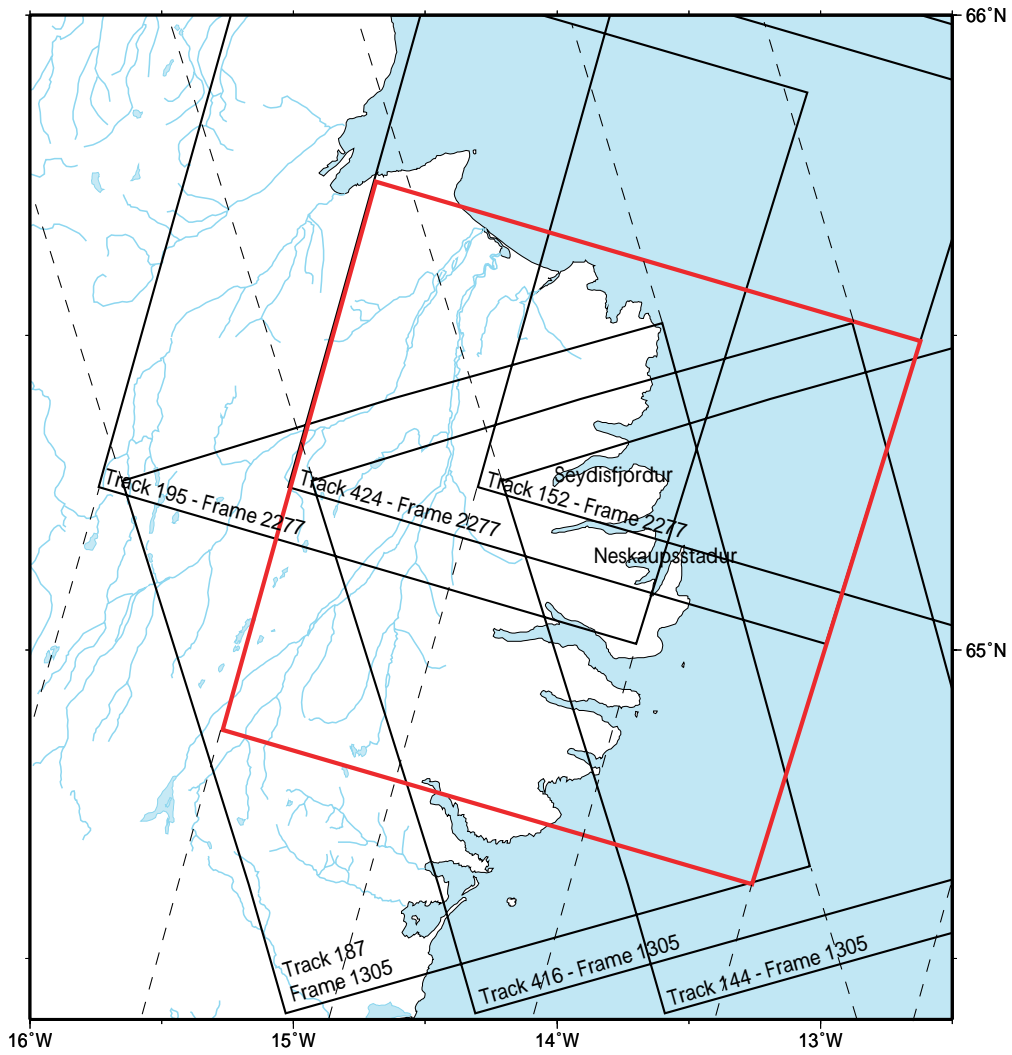


Figure 5. A map of East Iceland showing the coverage by three ascending tracks (187, 416, and 144) and three descending tracks (195, 424, and 152). The standard ascending frames 1305 and descending frames 2277 are also shown. I ordered ERS-1/2 data from a shifted frame along descending track 424 as indicated by the red rectangle. The available data from these tracks is shown in Figure 6. The Envisat data used in this project are from ascending track 187 and descending track 195.

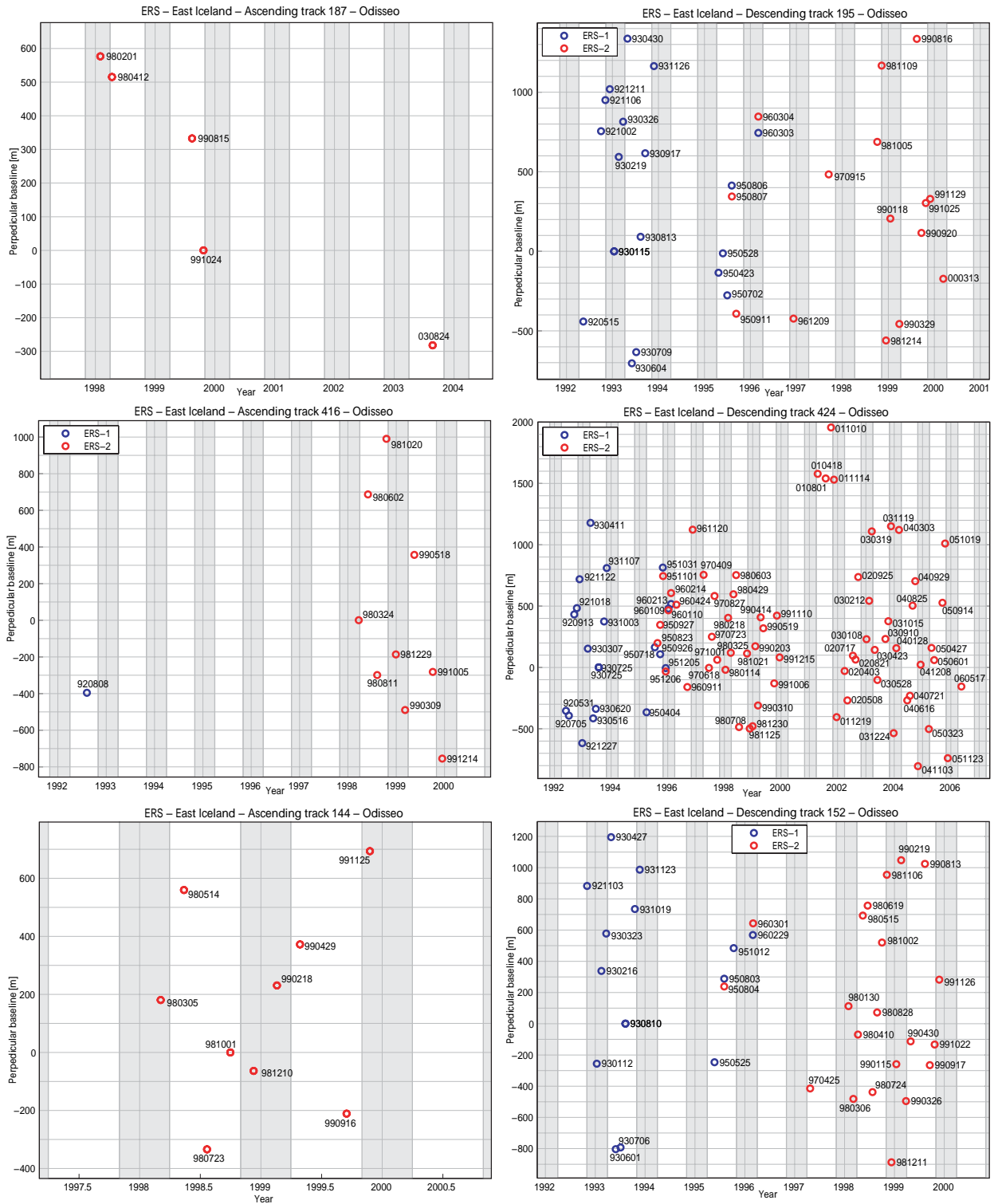


Figure 6. Spatio-temporal baseline information for East Iceland radar images acquired from ascending (left) and descending tracks (right), with perpendicular baseline plotted as a function of acquisition date. The plots include all ERS-1/2 images acquired during 1991-2006 according to the online Odisseo database of ESA. Gray shading indicates winter months November-April.

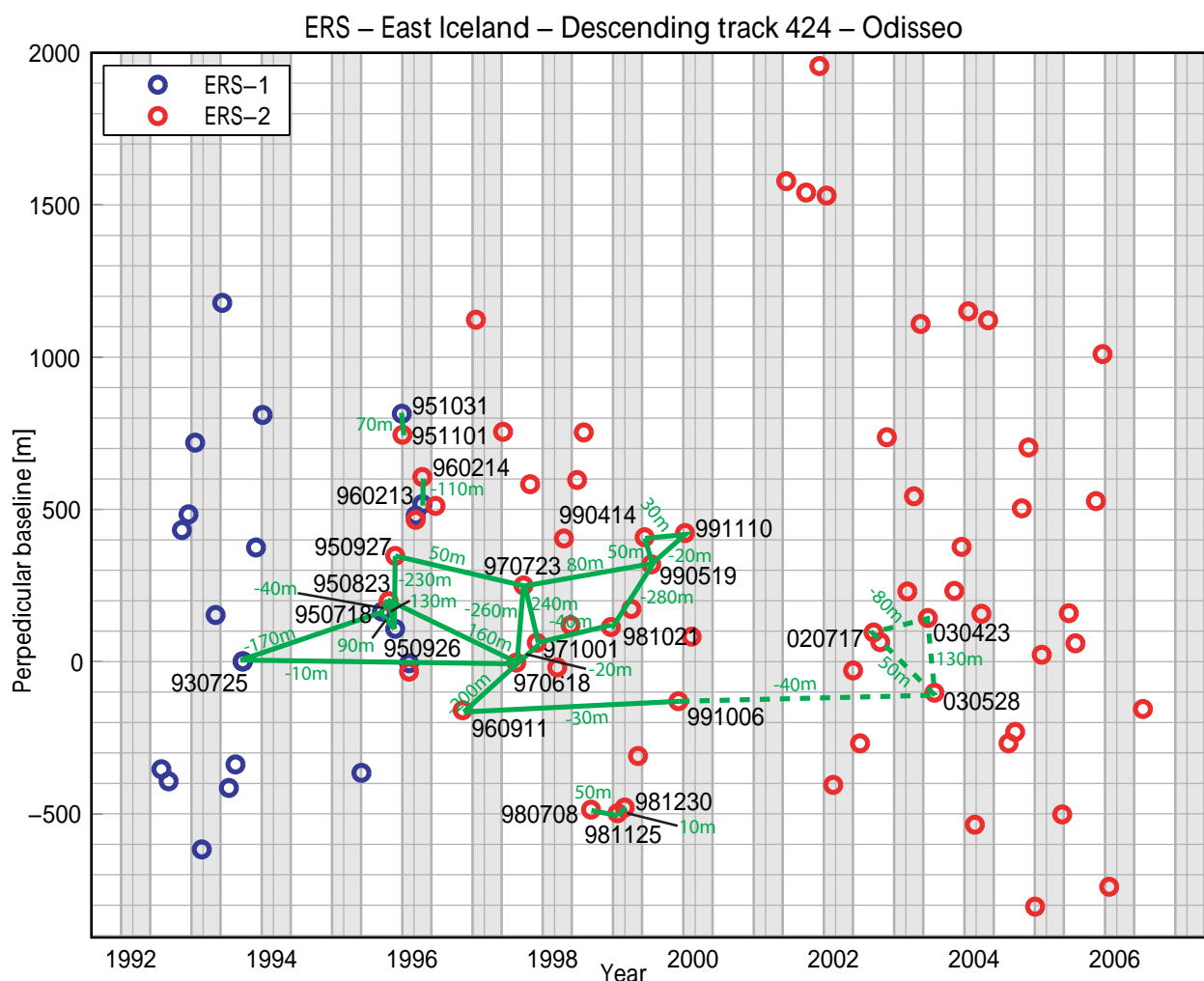


Figure 7. Spatio-temporal baseline information for ERS descending track 424 in East Iceland. The information comes from ESA's Odisseo online database. Labelled scenes were ordered for the project and green lines indicate the interferograms formed. Green numbers show the perpendicular baseline as calculated from the precise Delft orbital information. The data from 2002-3 proved to be not usable due to the pointing problems the ERS-2 satellite has had since 2001.

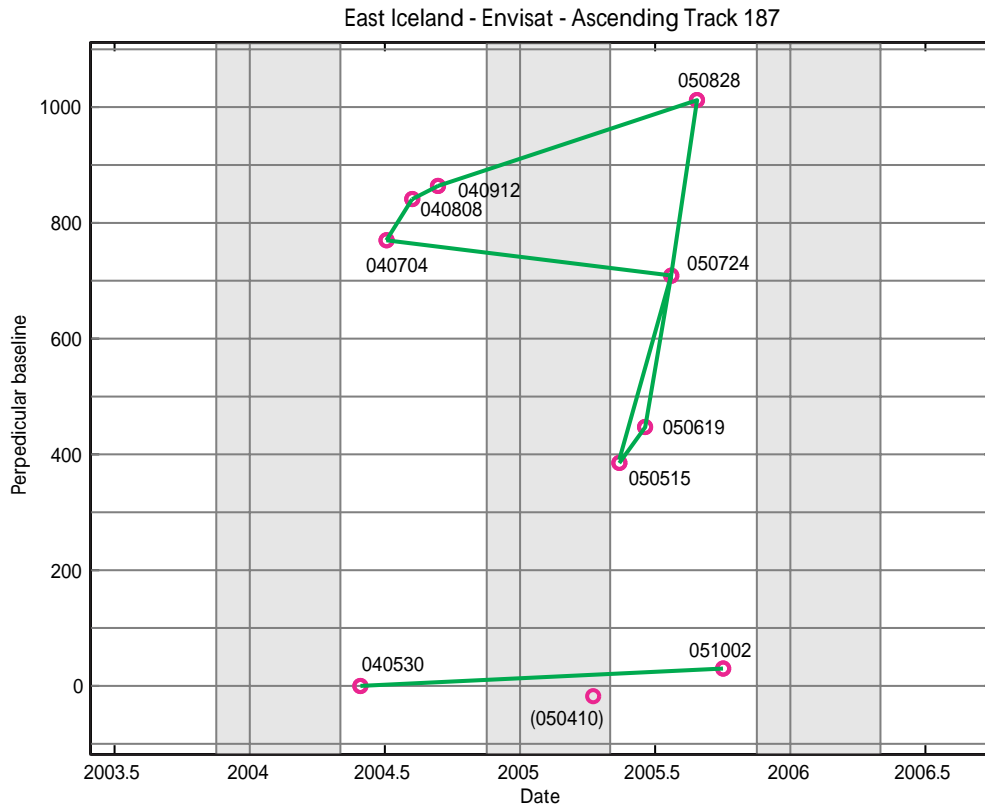


Figure 8. A spatio-temporal baseline diagram for Envisat radar data acquired along ascending track 187 above East Iceland. Green lines connecting the scenes indicate pairs for which interferograms were calculated, a total of 9 interferograms for this set. The image date in parenthesis indicates a scene that exist in the ESA archives but was not ordered for this project.

ber) and five acquisitions in 2005 (from 15 May to 2 October). The perpendicular baseline distances between the passes show a range of about 1000 m (Figure 8). The baseline distribution during 2004 is quite favorable resulting in small baselines between scenes acquired on 4 July, 8 August, and 12 September. The scene acquired on 30 May, on the other hand, is an outlier that cannot really be combined with the other three 2004 scenes (Figure 8). The baseline distribution in 2005 is worse, with only one small-baseline pair (15 May - 19 June), while other pairs have baselines over 200 m. Three summer-to-summer interferograms were also formed for small baselines, as can be seen on Figure 8.

I requested 9 acquisitions from descending track 195 in 2004-2005 (Figure 5). For 2004 I requested 4 scenes (31 May - 13 September) and made use of an additional scene acquired on 22 November. Only two small-baseline interferograms were possible to form from these 5 acquisitions (Figure 9). In 2005 I asked for 5 radar scenes (from 16 May to 3 October) and they resulted in a rather unfavorable distribution of baselines with only one small-baseline interferogram possible. However, I formed 12 different interferograms from these images

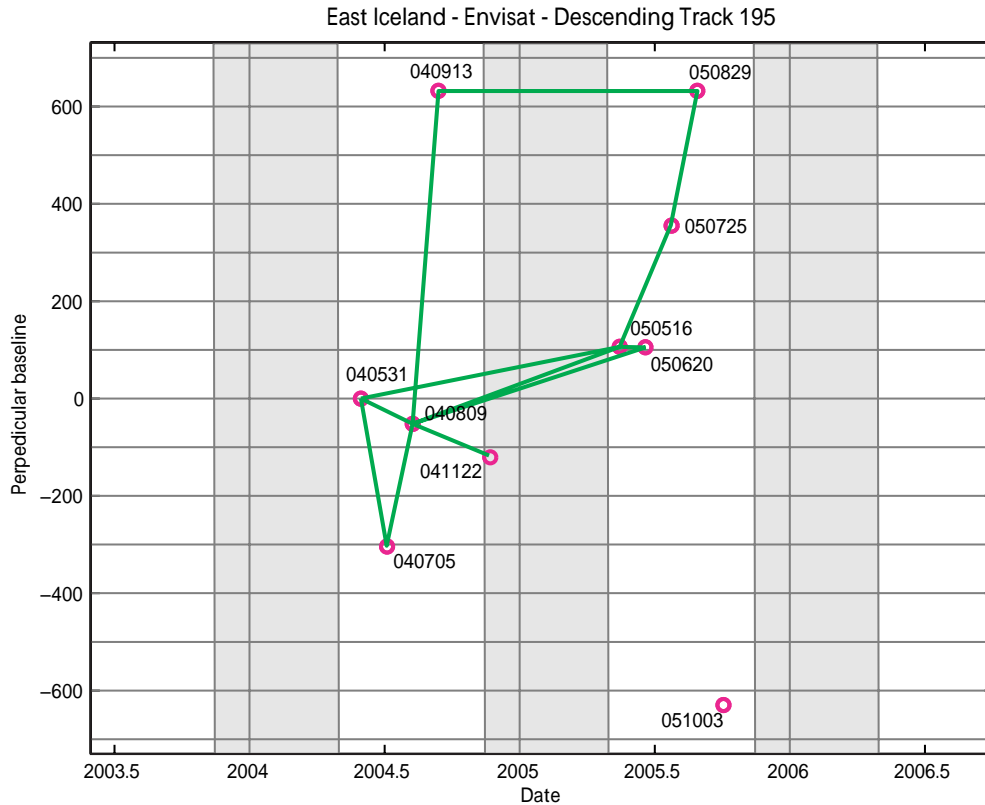


Figure 9. Same as Figure 8, except for descending track 195.

that have baselines ranging from 0 m to over 700 m, but only interferograms with baselines smaller than about 200 m turned out to be usable (Section 3.3).

2.4 Data Processing Steps

The data in this project were processed using the ROI_PAC radar interferometric software developed by the Jet Propulsion Laboratory (JPL) in Pasadena, California [Rosen *et al.*, 2004]. In my data processing I followed a typical 2-pass processing procedure using a simulated interferogram to remove the effects of topography [e.g. Massonnet and Feigl, 1998; Hanssen, 2001]. The simulation was formed using a 25 m Digital Elevation Model (DEM) of Iceland provided by the Iceland Meteorological Office.

The data processing of each interferogram consists of the following steps:

1. Directory structure is set up on a Linux computer and "zero-level RAW" radar data from ESA are uploaded from CDs. Precise satellite orbit information is downloaded from the Technical University of Delft (The Netherlands) and InSAR processing input files edited.

2. Data are now converted from the ESA RAW format to a format used by the ROI_PAC processing software. In addition the data are checked for missing lines and the Doppler centroid is calculated.
3. Single-look complex (SLC) radar images are generated from the RAW data.
4. One of two SLC images is selected as a master image and the offset of the other image (slave image) is estimated relative to the master image. The offset-field is estimated from cross-correlations of small sub-images across the images.
5. The slave image is resampled according to the offset estimation and the interferogram is calculated. The phase caused by the curving of the earth is removed resulting in a 'flattened' interferogram that contains phase signatures due to topographic heights and deformation.
6. The Digital Elevation Model (DEM) is projected into radar coordinates and a simulated back-scatter image is formed.
7. The offset-field between the simulated back-scatter image and the master amplitude image is estimated and the simulated image is resampled accordingly.
8. The DEM, in radar coordinates, is converted to simulated unwrapped phase using information about the perpendicular baseline. The topographic phase signature in the interferogram is removed by subtraction of the simulated unwrapped image from the processed interferogram. The result is a differential interferogram that only should contain phase signature to deformation (and errors).
9. Sometimes the differential interferogram contains a residual phase ramp due to a bias in the orbital information, which is removed at this stage in the processing.
10. The wrapped differential interferogram is filtered to reduce high frequency noise.
11. The unfiltered differential interferograms are visually inspected for possible landslide motion and sub-section of the interferograms are selected.
12. The sub-sections are unwrapped and geocoded, i.e. projected from the radar geometry of interferograms to geographical WGS-84 coordinates.

3 General Results

In this Chapter I discuss the general results of the project. I begin by describing the quality of the processed interferograms and list briefly where deformation is detected within them. Then I move on to discuss the coherence conditions in the area, which is one of the main limitations of InSAR. And finally I discuss the difficulties of removing the topographic phase from the interferograms due to the rather inaccurate DEM available.

3.1 General Interferogram Results

I processed a total of 44 interferograms in this project of which 23 are from descending ERS-1/2 data acquired in 1993-1999 and 21 from Envisat data acquired in 2004-2005 (12 from descending orbits and 9 from ascending orbits). The time span of the interferograms varies from one day to almost four years and the perpendicular baselines vary from 0 m to over 700 m. Information about the interferograms are listed in Tables 1-2 and the spatio-temporal baseline information is displayed graphically in Figures 7-9.

Many of the processed interferograms are of excellent quality with nearly a constant interferometric phase in non-deforming areas while exhibiting sheer details about ground movements in several places. This said, however, many other interferograms proved to be not usable due to interferometric decorrelation and due to topographical artifacts in the data. The decorrelation is primarily caused by snow or changes in the surface characteristics, e.g. due to vegetation growth or erosion; this limitation is further discussed in Section 3.2. Topographical artifacts result primarily from inaccuracies in the DEM of the area and I discuss this problem further in Section 3.3. Despite the problems of decorrelation and topographic artifacts, many short-baseline interferograms provide excellent results for the area and many details can be extracted from these interferograms.

Descending data are primarily useful to image slopes that face to the west and can therefore be used to study the previously known Þófi landslide in Seyðisfjörður. Of the 32 descending interferograms spanning time-periods of one month or more, 19 interferograms are of good enough quality to study this landslide, while the other 13 proved unusable. However, only two of those 19 interferograms exhibit measurable displacement in this area, one from 1998 and another one from 1999, the other show no signs of displacement. The results of the InSAR analysis in Seyðisfjörður are described in Section 4.1. Very active landslide creep was discovered in Vopnafjörður on a northwest-facing slopes of Smjörfjöll mountains. Displacements were seen at this location in all but two interferograms that could be used to measure deformation in the area. More interferograms were decorrelated at this location than in Seyðisfjörður and sometimes too much landslide motion may have been the problem. The Vopnafjörður results are described in detail in Section 4.3.

Many other locations were discovered in the descending interferograms that appear to have active ground movement (Table 1). These areas have not been inspected in the field but they all occur on rather steep slopes and the observed displacements are probably due to ac-

| No. | Data set | B_{\perp} (m) | Δt days | Coherence | Seyðisfjörður | Vopnafjörður | Other places |
|----------------|---------------|-----------------|-----------------|-------------------------------|---------------|--------------|------------------------------|
| ERS-1/2 | | | | | | | |
| 1 | 930725-950718 | 170 | 722 | 0.22 | No | - | No |
| 2 | 930725-970618 | 10 | 1423 | 0.29 | - | - | Lambadalur in Borgarfjörður |
| 3 | 950718-950823 | 40 | 35 | 0.28 | No | Yes, >6 cm | No |
| 4 | 950718-950926 | 90 | 70 | 0.26 (Good < ~ 200 m) | No | - | No |
| 5 | 950718-970618 | 165 | 700 | 0.22 | No | Yes | Eyvindarárdalur |
| 6 | 950823-950926 | 130 | 35 | 0.21 (Good < ~ 200 m) | No | - | No |
| 7 | 950926-950927 | 235 | 1 | 0.41 | - | - | - |
| 8 | 950927-970723 | 50 | 665 | 0.17 Poor | No | - | No |
| 9 | 951031-951101 | 65 | 1 | 0.28 | - | - | - |
| 10 | 960213-960214 | 105 | 1 | 0.20 Poor | - | - | - |
| 11 | 960911-970618 | 200 | 279 | 0.24 | No | Yes, >3 cm | Eyvindarárdalur & Suðurdalur |
| 12 | 960911-991006 | 35 | 1120 | 0.22 | - | - | Several places |
| 13 | 970618-970723 | 260 | 35 | 0.26 | No | Yes, 3 cm | No |
| 14 | 970618-971001 | 20 | 105 | 0.31 | No | Yes, 3 cm | Suðurdalur |
| 15 | 970723-971001 | 240 | 70 | 0.26 | No | No | Suðurdalur |
| 16 | 970723-990519 | 80 | 665 | 0.17 Poor everywhere | - | - | - |
| 17 | 971001-981021 | 40 | 385 | 0.15 | - | - | No |
| 18 | 980708-981125 | 45 | 140 | 0.19 | Yes | Yes, >2cm | Suðurdalur |
| 19 | 981021-990519 | 280 | 140 | 0.15 Poor everywhere | - | - | - |
| 20 | 981125-981230 | 5 | 35 | 0.15 Poor everywhere | - | - | - |
| 21 | 990414-990519 | 50 | 35 | 0.15 Poor everywhere | - | - | - |
| 22 | 990414-991110 | 30 | 210 | 0.15 Poor everywhere | - | - | - |
| 23 | 990519-991110 | 20 | 175 | 0.18 | Yes | - | Eyvindarárdalur |
| ENVISAT | | | | | | | |
| 24 | 040531-040705 | 320 | 35 | 0.35 (Good < ~ 800 m) | - | - | - |
| 25 | 040531-040809 | 60 | 70 | 0.34 | No | Yes, 1-2 cm | No |
| 26 | 040531-050516 | 100 | 350 | 0.21 (Some < ~ 800 m) | No | Yes, >3cm | No |
| 27 | 040705-040809 | 260 | 35 | 0.42 | - | - | - |
| 28 | 040809-040913 | 710 | 35 | 0.23 (Some < ~ 700 m) | - | - | - |
| 29 | 040809-041122 | 65 | 70 | 0.17 (Limited < ~ 500 m) | No | - | - |
| 30 | 040809-050516 | 165 | 280 | 0.19 (Some < ~ 500 m) | No | Yes | No |
| 31 | 040809-050620 | 165 | 315 | 0.20 | No | Yes, >3cm | No |
| 32 | 040913-050829 | 1 | 350 | 0.32 (Good < ~ 1000 m) | No | Yes, >3cm | Reykjadalur in Mjólfjörður |
| 33 | 050516-050620 | 35 | 35 | 0.26 (Good < ~ 600 m) | No | No | No |
| 34 | 050516-050725 | 260 | 70 | 0.21 | - | - | - |
| 35 | 050725-050829 | 280 | 35 | 0.35 | - | - | - |

Table 1. Information about the 23 ERS and 12 Envisat descending interferograms and detected deformation in East Iceland. The second column lists what dates were involved in each interferogram, and the next three columns show information about the perpendicular baseline B_{\perp} , the time-span Δt in days, and the interferogram coherence. The last three columns provide information about whether or not deformation was detected in Seyðisfjörður, Vopnafjörður and other places, or if no measurement was possible (denoted with a dash "-").

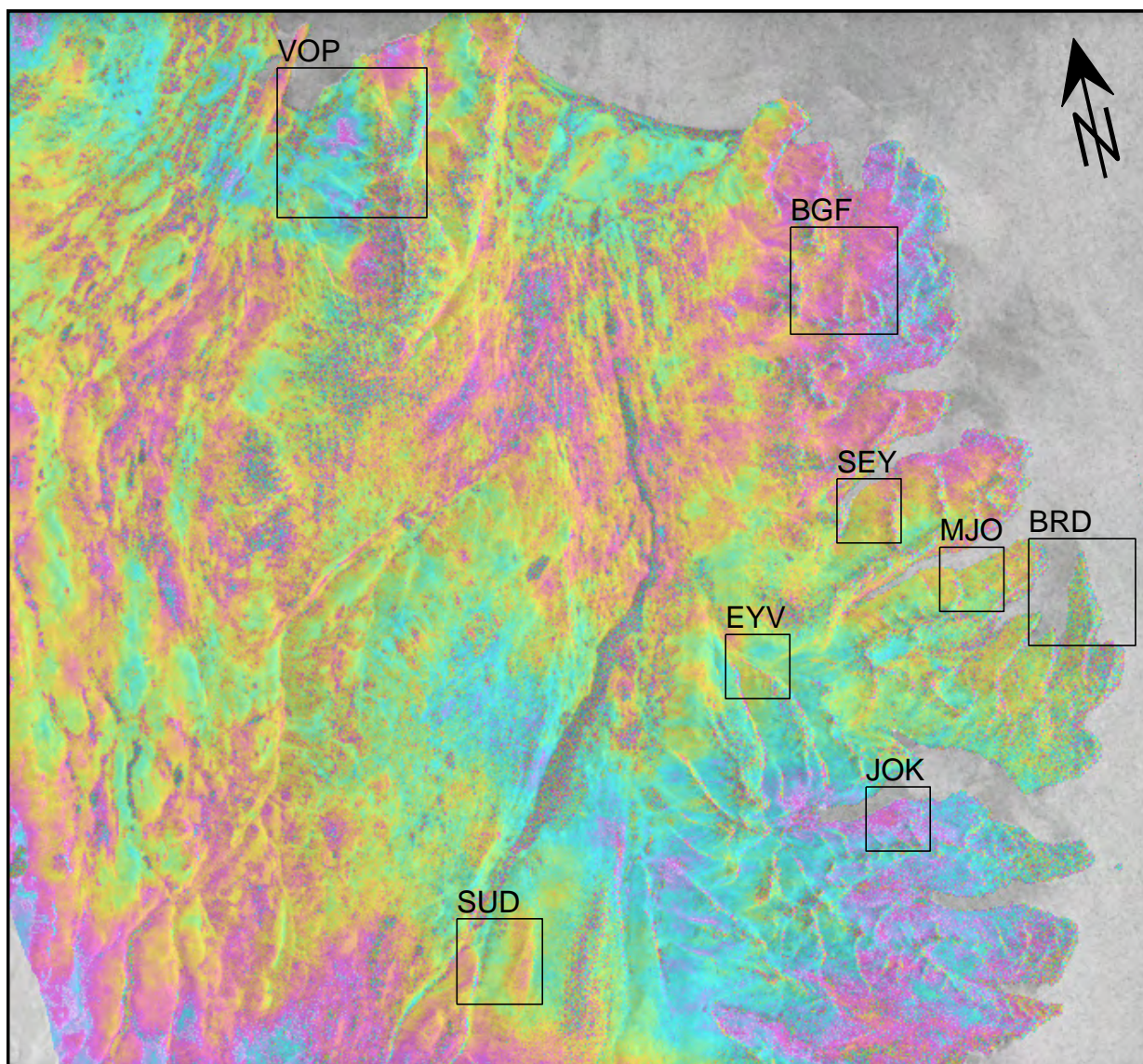


Figure 10. A descending Envisat interferogram of East Iceland (31 May - 9 August, 2004) showing locations where deformation was detected (in this and/or in other interferograms), see Chapter 4 for details. The abbreviations stand for Vopnafjörður (VOP), Borgarfjörður (BGF), Seyðisfjörður (SEY), Mjóifjörður (MJO), Barðsnes (BRD), Eyvindarárdalur (EYV), Jökulbotnar (JOK), and Suðurdalur (SUD). ©ESA.

| No. | Data set | B_{\perp} (m) | Δt days | Coherence | Loðmundarfjörður | Other places |
|-----|---------------|-----------------|-----------------|-----------|------------------|--------------------------------|
| 36 | 040530-051002 | 30 | 490 | 0.20 | Yes, 3 cm | - |
| 37 | 040704-040808 | 80 | 35 | 0.53 | No | Surtsstaðatunga |
| 38 | 040704-050724 | 40 | 375 | 0.36 | Yes, 3 cm | Several |
| 39 | 040912-040808 | 35 | -35 | 0.36 | No | Surtsstaðatunga and Breiðdalur |
| 40 | 040912-050828 | 150 | 350 | 0.31 | Yes | Surtsstaðatunga and Þingmúli |
| 41 | 050619-050515 | 60 | -35 | 0.22 | No | No |
| 42 | 050724-050515 | 340 | -70 | 0.19 | - | - |
| 43 | 050724-050619 | 280 | -35 | 0.23 | - | - |
| 44 | 050724-050828 | 310 | 35 | 0.32 | - | - |

Table 2. Same as Table 1, except for the 9 ascending Envisat interferograms.

tive landslides. Two of these areas seem to coincide with landslide locations catalogued from geomorphological and geological investigations by *Jónsson* [1976]. These are Lambadalur valley in Borgarfjörður (Section 4.4.1) and Suðurdalur near Fljótsdalur (Section 4.4.6). The other locations are not in the landslide catalogue (Figure 10), but these areas include Reykjadalur in Mjóifjörður (Section 4.4.2), Barðsnes Peninsula (Section 4.4.3), Eyvindarárdalur valley (Section 4.4.5), and Jökulbotnar in Reyðarfjörður (Section 4.4.4).

Almost no ERS data from ascending orbits exist for this area, as was discussed above. Ascending data are primarily useful to image slopes that face to the east and can therefore be used to study the previously known landslide location in Urðarbotn above the town of Neskaupstaður. I requested ascending Envisat acquisitions in 2004-2005 and from these data I generated 9 interferograms (Table 2). The limited results from the Urðarbotn landslide are described in Section 4.2. Locations where active displacements were discovered in the ascending interferograms are shown in Figure 11 and each case is described in detail in Section 4.5.

3.2 Coherence Conditions

Degradation in interferometric coherence or interferometric correlation, usually simply referred to as decorrelation [*Zebker and Villasenor, 1992*], is one of the main limitation of using InSAR to measure ground deformation. The complex coherence can be estimated using:

$$|\gamma| = \frac{|\sum_{n=1}^N y_{1,n} y_{2,n}^*|}{\sqrt{\sum_{n=1}^N |y_{1,n}|^2 \sum_{n=1}^N |y_{2,n}|^2}} \quad (1)$$

where $y_{2,n}^*$ is the complex conjugate value of the second radar scene at pixel n , and N is the number of pixels in a spatial window $N = N_{azimuth} \times N_{range}$. The coherence is bounded within the interval $[0,1]$ where a value of 1 represents perfect correspondence between the radar scenes. There are many factors that cause a loss of coherence. The most important is temporal decorrelation which results from changes in the surface scattering characteristics during the time between the two radar acquisitions. Such changes can be caused by many different processes, including vegetation growth, erosion by water and wind, agricultural activities, and snow.

To be able to compare the quality of the interferograms I extracted an area of 1000×1000

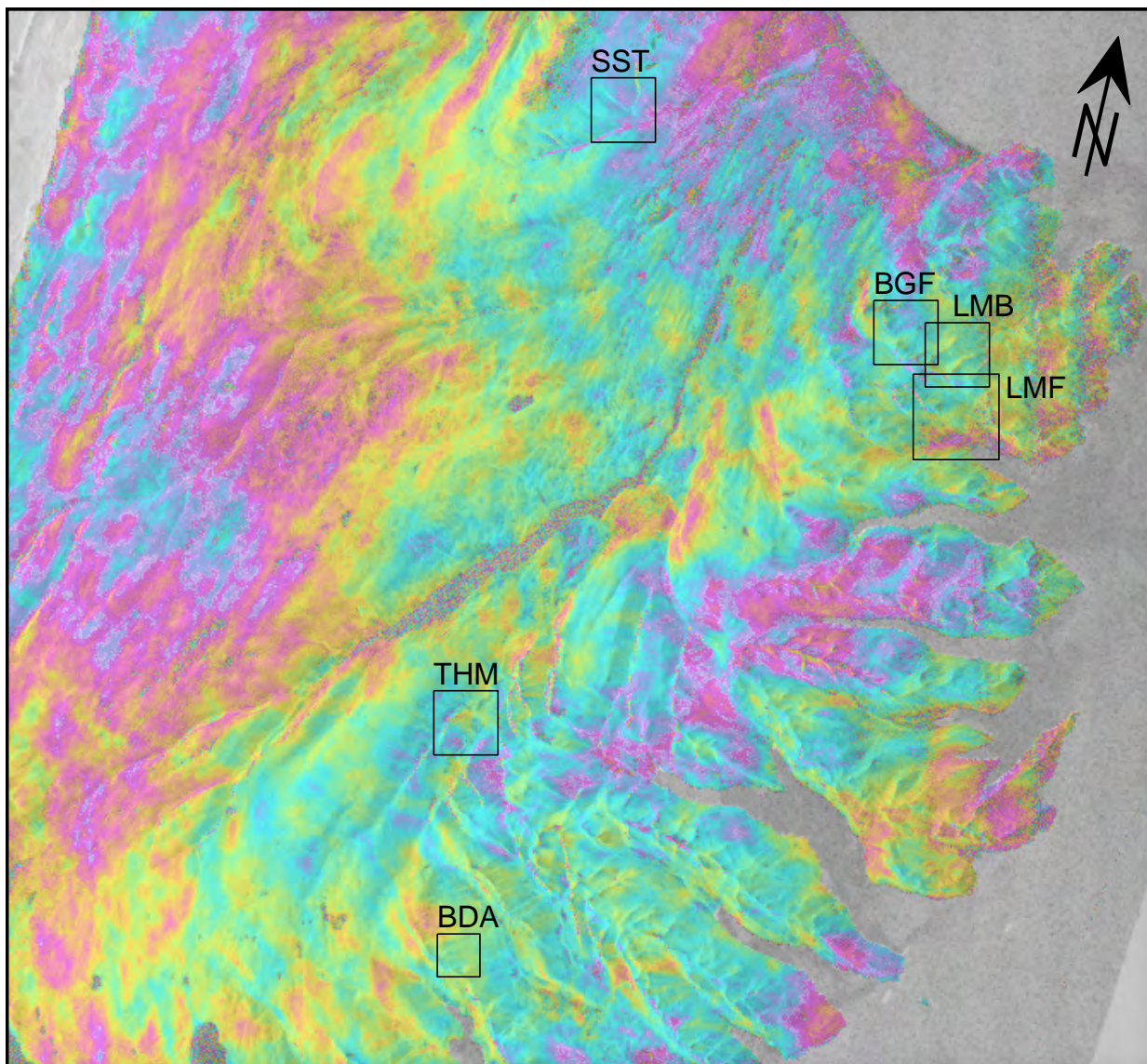


Figure 11. Ascending Envisat interferogram of East Iceland (8 August - 12 September, 2004) showing locations where deformation was detected (in this and/or in other interferograms), see Chapter 4 for details. Abbreviation stand for Surtsstaðatunga (SST), Beinageitarfjall (BGF), Lambadalur (LMB), Loðmundarfjörður (LMF), Þingmúli (THM), and Breiðdalur (BDA). ©ESA.

pixels and calculated the mean coherence within these interferogram subsets (Tables 1 and 2). The area includes both high and low elevations as well as significant slopes and layovers, but no major water surfaces. The coherence ranges from 0.15 in interferograms that appear almost completely decorrelated to 0.41 for one of the tandem interferograms. The ascending interferograms cover approximately the same area and show coherence between 0.19 and 0.53. However, the ascending coherence values cannot be directly compared with the descending values as different slopes are being imaged and different areas are hidden in layovers.

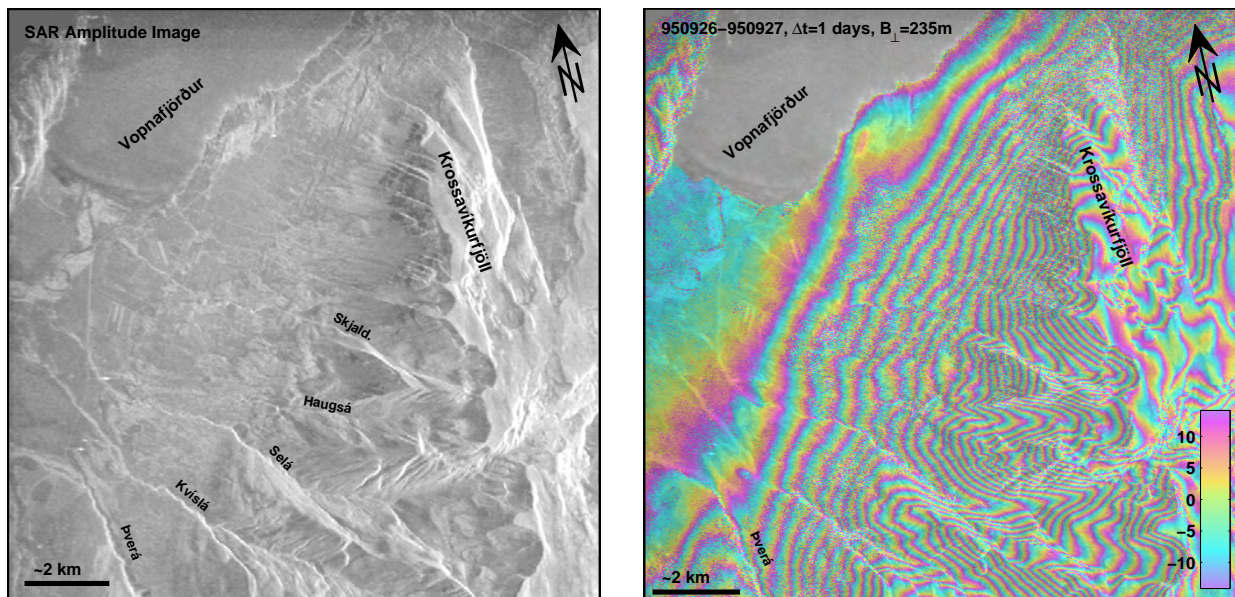


Figure 12. SAR amplitude image (left) and a 1-day tandem interferogram (right) from Vopnafjörður. The images are in radar coordinates but many geographical features can be recognized, such as the different streams. The Tandem interferogram shows topographic fringes and here one color fringe denotes about 40 m of elevation. ©ESA.

Here I take a one-day tandem interferogram from 26-27 September as an example. This interferogram shows good coherence at the lowest and highest elevations, but poor coherence in the ocean and between elevations of 200-600 m (Figure 12). The band of low correlation is not due to vegetation as a 70-day interferogram exhibits excellent correlation in these locations (Figure 13). The reason appears to be snow-melting during this day in late September 1995. Our interpretation is that during the time of the 26 September acquisition snow covered the ground down to about 200 m above sea level. Then, during 26-27 September the snow melted at low elevations while above ca. 600 m the temperatures were cold enough for the snow to remain intact. This interpretation is supported by other interferograms that share one of these images. The 70-day interferogram retains significant correlation in most areas, except above water surfaces, some low-lying areas, and at the highest elevations (Figure 13). The reason for decorrelation of the low areas is probably agricultural activity while the high decorrelation is due to snow in the May acquisition. The one-year interferogram is mostly decorrelated, except at some patchy areas in the middle of the slopes, presumably

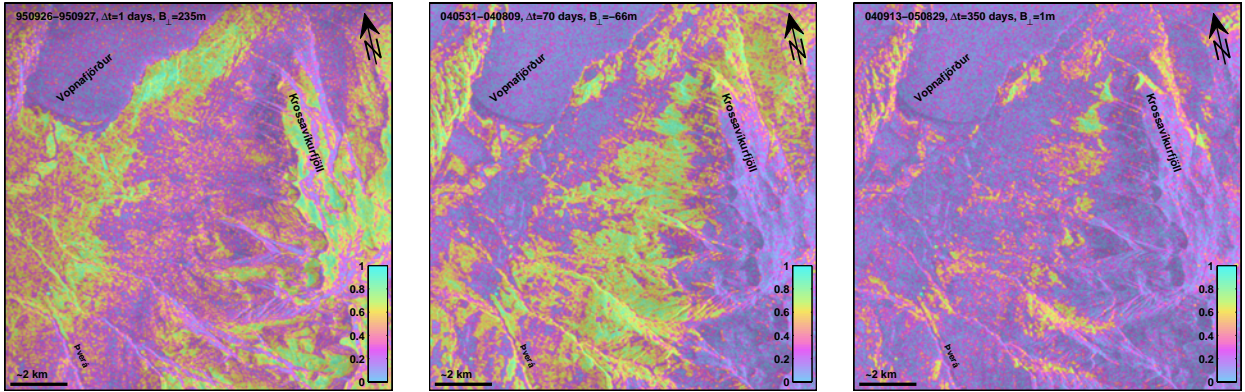


Figure 13. Examples of interferometric coherence in Vopnafjörður in a one-day (left), 70-day (interferogram), and 1-year interferograms. The filtered versions of the interferograms are shown in Figures 12 and 33. ©ESA.

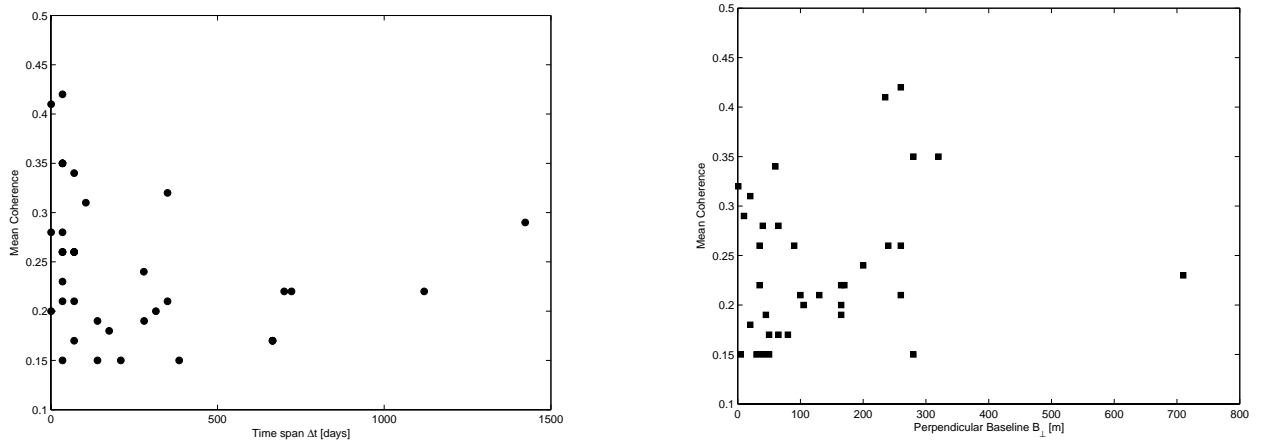


Figure 14. Mean coherence of descending interferograms as a function of the time the interferogram spans (left) and perpendicular baseline (right).

above significant vegetation.

When the interferometric correlation in our test area is displayed as a function of time-span of the interferogram, no obvious correlation is found between the two parameters (Figure 14). The only visible trend is that maximum mean coherence appears to decrease a little bit with increasing time-span. However, there are many short time-span interferogram that exhibit poor coherence and these interferograms are affected by snow. Even a less obvious pattern is seen when coherence is plotted versus perpendicular baseline (Figure 14), but a decrease in coherence is expected for longer baselines [Zebker and Villasenor, 1992]. However, this comparison is somewhat limited because some of the longer baseline interferograms span a relative short time, while some of the small-baseline ones (<100 m) span a long time (years), so temporal decorrelation may distort the pattern. Still, when both baseline and time-span are taking into account, no clear patterns emerge due to the strong dependence of snow in all interferograms.

We finish this discussion by concluding that snow-free interferograms that span less than six months can be used for detailed analysis of small landslides. Longer time-spans of up to one year or even several years can be used for measurement at some sites and on large landslides that does not require detailed pixel-to-pixel analysis.

3.3 Limitations due to the inaccurate Digital Elevation Model

Radar interferograms exhibit phase signatures due to topography that is directly proportional to perpendicular baseline B_{\perp} between the two satellite passes, i.e. the perpendicular component of the spatial distance between the two orbital trajectories. This phase signal results from the differential distance to two ground scatterers when viewing them from slightly different incidence angles. The topographic phase can be expressed as

$$\phi = \frac{4\pi}{\lambda R \sin \alpha} B_{\perp} H \quad (2)$$

where λ is the radar wavelength (~ 5.6 cm for ERS and Envisat), R is the slant distance to the satellite, α is the local incidence angle, and H is the elevation of the scatterer above some reference. This equation implies that when the two passes are exactly identical ($B_{\perp} = 0$) there is no sensitivity to topography while the longer the baseline is, the more the sensitivity is. Spatial decorrelation results from viewing distributed targets on the ground from different incidence angles and this becomes important for long baselines, until a critical baseline ($B_{\perp} \approx 1000$ m for ERS) is reached where no measurement is possible anymore [Zebker and Villasenor, 1992].

A useful quantity that is often used is the altitude of ambiguity H_a , which is the topographical height difference needed to create one fringe in an interferogram [Massonnet and Feigl, 1998]. This quantity is inversely proportional to perpendicular baseline length B_{\perp} :

$$H_a = \frac{\lambda R \sin \alpha}{2B_{\perp}}. \quad (3)$$

This means for a baseline of e.g. 200 m, a DEM error of 45 m will result in one artificial fringe in the differential interferogram, which may then be erroneously interpreted as displacement.

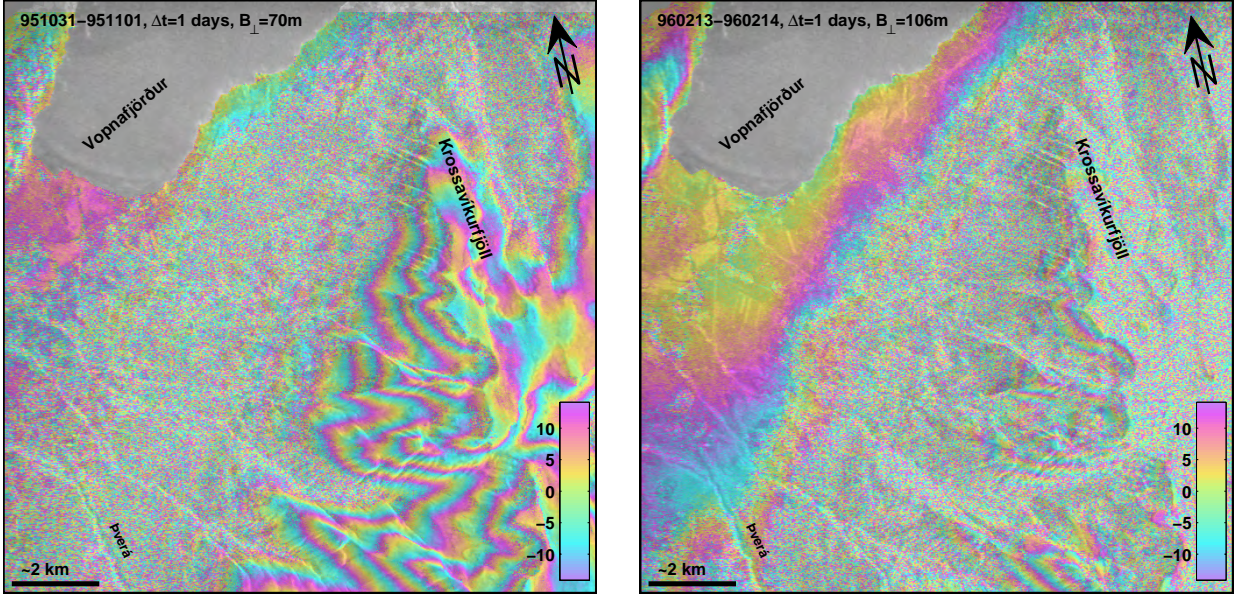


Figure 15. Two 1-day tandem interferograms of Vopnafjörður that show topographical fringes like in Figure 12. The different fringe rate is proportional to the perpendicular orbital baseline in each case. Both interferograms are heavily decorrelated due to snow. ©ESA.

When this project started the only DEM available was a 90-m DEM from the National Land Survey of Iceland, as no SRTM (Shuttle Radar Topography Mission) data exist for Iceland because of its location above 60°N. This 90 m DEM had obvious resolution limitations as full radar interferograms are usually processed to 20 m × 20 m ground pixel spacing. Therefore, a considerable effort was spent in the early phase of this project to create a DEM from 1-day tandem interferograms assuming no deformation occurred during that day. These interferograms can then be unwrapped and the absolute phase translated into topographic height, which then can be scaled and used to remove the topographic signature from deformation interferograms to form differential interferogram containing ideally only deformation-phase signatures. This method is usually referred to as the four-pass method (or three-pass if one of the two tandem scenes is used in the deformation interferogram). Five 1-day tandem pairs exist for this area, but two of them have short baselines that means they provide limited information about the topography (Figure 7). The other three tandem pairs were ordered and processed. These interferograms are from 26-27 September 1995 ($B_{\perp} = 235$ m), 31 October-1 November 1995 ($B_{\perp} = 65$ m), and 13-14 February 1996 ($B_{\perp} = 105$ m). The main problem with these interferograms is snow as they are all from Fall

or Winter months. The September pair is the best set, but it has decorrelation problems between 200-600 m as was discussed above. The other two pairs are heavily decorrelated due to 1-day changes in snow properties (Figure 15). Therefore, despite considerable efforts, no suitable DEM could be generated from the tandem interferograms, although parts of the September interferogram were unwrapped locally and used in the beginning.

A much better DEM became available for this project in 2005. This DEM has a resolution of $25\text{ m} \times 25\text{ m}$ and was generated by interpolating digitized 20 m contours of 1:50000 maps from the National Land Survey of Iceland. This DEM proved to be much better than the 90 m DEM and eased and improved the differential interferogram analysis significantly. However, this DEM also has its limitations and it is not very accurate. Differential interferometric analysis revealed significant topographic residuals in the interferograms when the baselines were longer than about 300 m (Figure 16). A 30 m DEM error will result in a 1-fringe error in a 300 m baseline interferogram and although one would expect better accuracy from interpolating 20-m contour lines one needs to bear in mind that the contour lines themselves also contain errors. Therefore, I concluded that interferograms with baselines exceeding 200 m include too many topographical artifacts to be reliable for deformation measurements. This is a pity, because this excludes almost 1/3 of the processed interferograms, many of which may include valuable information if the topography could be correctly removed. But until a better DEM becomes available, this will remain a problem.

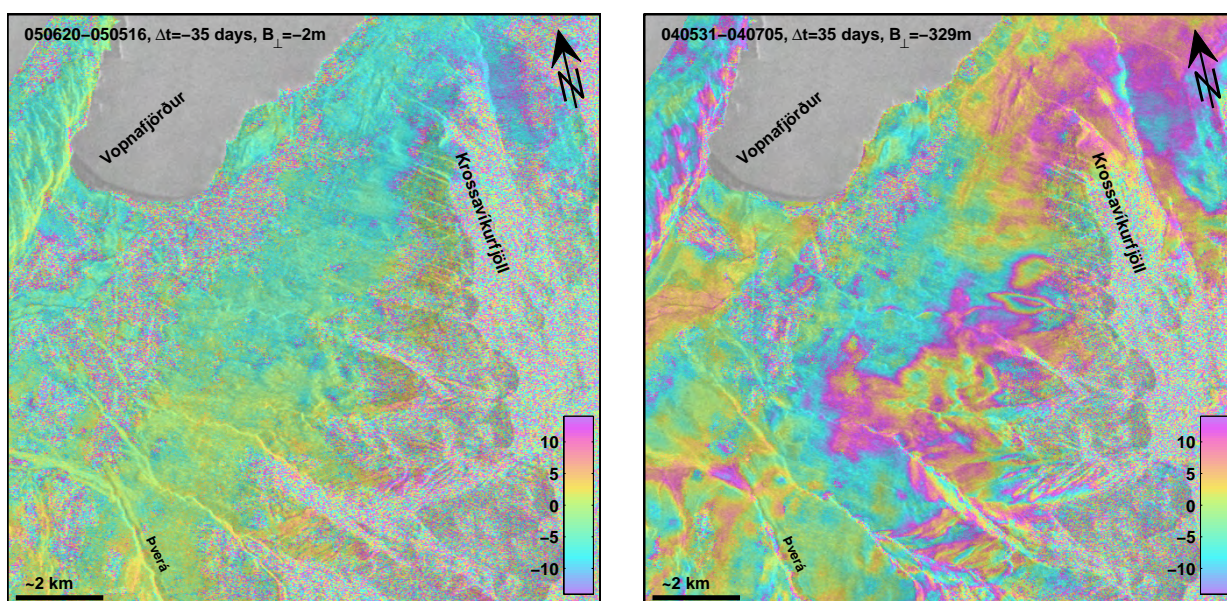


Figure 16. Two Envisat interferograms from Vopnafjörður, one spanning 35 days in 2005 (left) and the other spanning 35 days in 2004 (right). The 2004 interferogram has a perpendicular baseline of 320 m and shows obvious artifacts due to the inaccurate DEM. Therefore, this interferogram can not be used for a reliable deformation measurement. The 2005 interferogram is more reliable as its baseline is only 2 m, but it exhibits no signs of landslide displacement. ©ESA.

4 Observed Landslide Motion at Various Locations

In this Chapter I describe the observed deformation at the various locations in East Iceland. I begin by reporting my findings at the two previously known landslide locations near the towns of Seyðisfjörður and Neskaupstaður. Then I will move on to describe my results at other locations, first in Vopnafjörður, then in other areas where displacements were detected in ERS-1/2 and Envisat data acquired from descending orbits, and finally, I will detail my results retrieved from ascending Envisat data.

Only small subsets of the full interferograms are presented, focussed in each case on the area of interest, as it is impossible to display in this report format all the details of the full resolution interferograms that typically are about 6000×6000 pixels in size. Therefore, each interferogram was carefully examined using a high resolution monitor and any detected evidence for displacement was documented (Table 1 and the Appendix). Then I extracted interferogram subsets with the focus on known landslide areas, such as Seyðisfjörður, and on other areas where I detected displacements.

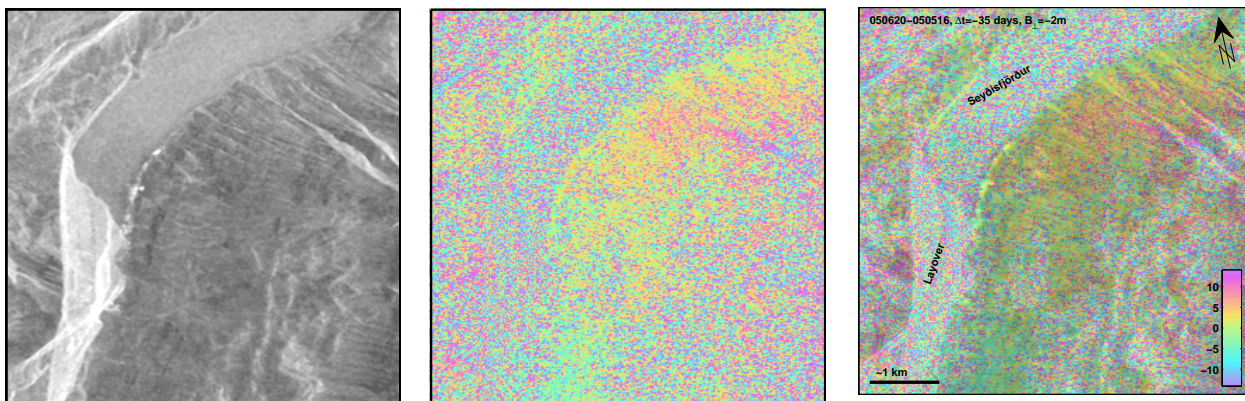


Figure 17. A display example of an interferogram from Seyðisfjörður. The displayed image includes a SAR amplitude images (left) as a background shading for the interferometric phase observation (middle) and the result is a shaded interferogram (right). ©ESA.

The results in the subsequent sections are mostly displayed in their original radar geometry (or radar coordinates) rather than in geographical coordinates. This is to keep the data as original as possible and to avoid losing signal details when the data are projected into geographical coordinates (geocoding), as it results in significant modifications of the data. To locate the observed signals the interferometric phase is overlain on a SAR amplitude image that shows strength of the radar returns, which is primarily a function of the surface roughness and the local slope. The resulting interferogram is a shaded color phase-image, where the shading helps to put a reference to where displacements are taking place (Figure 17). Although I like to keep the data as original as possible, most of the subset interferograms displayed in the following sections have been somewhat post-processed. The post-processing involved adaptive filtering to reduce high-frequency noise in the interferograms as well as masking of ocean areas and sometimes other areas that were interferometrically completely

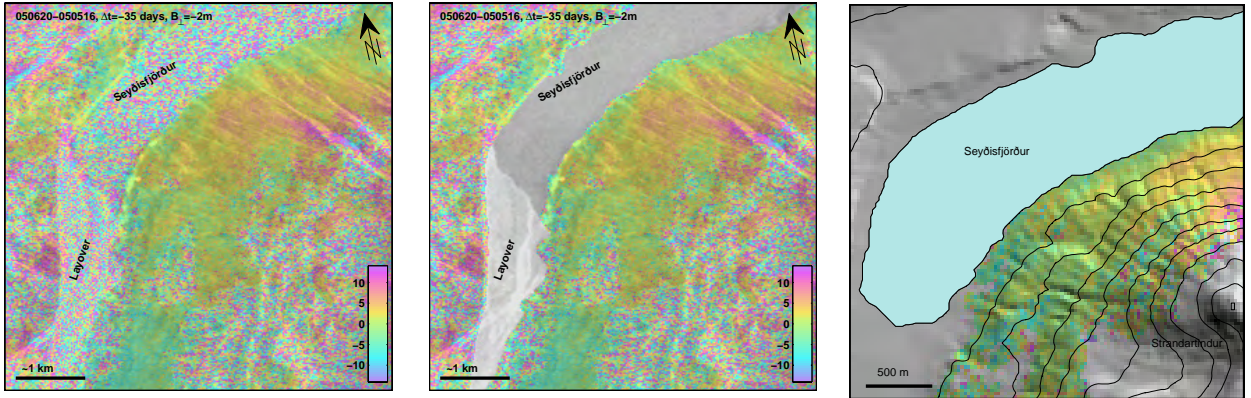


Figure 18. An example of the postprocessing of an interferogram from Seyðisfjörður: Filtered interferogram (left), masked interferogram (middle), and a geocoded interferogram (right). ©ESA.

decorrelated. Also, in some cases I geocode the interferograms to pin down the exact location of the detected deformation. Figure 18 shows an example from Seyðisfjörður (300×300 pixels) of the post-processing of an interferogram subset that is first filtered, then masked, and finally geocoded. The geocoding projection of radar data from radar coordinates to geographical coordinates (Latitude/Longitude or UTM) involves significant interpolations and modifications of the radar data, especially in areas that are topographically rough like eastern Iceland. In cases where I geocoded subsets of interferograms I began by unwrapping the subsets, i.e. by integrating the modulo 2π interferometric phase [e.g. Zebker and Lu, 1998], and then geocoded the unwrapped interferograms. Many unwrapping algorithms exist to carry out the two-dimensional integration and here I use a rather conservative one that only unwraps areas where the phase shows high degree of correlation. This results in a few unwrapping errors but does leave gaps in the images. The geocoded images are displayed by overlaying them on a shaded relief map. However, most of the InSAR results in the following sections were not geocoded, but displayed as filtered and masked interferogram subsets in the original radar coordinates, i.e. like the middle image in Figure 18.

The differential interferograms in this report are displayed wrapped with phase values in the range $[-\pi, \pi]$. This means for a half-wavelength of $56.6/2=28.3$ mm (ERS/Envisat) the corresponding LOS displacement range is $[-14, 14]$ mm, which is the colorscale I use in most of the figures. The scale is defined as LOS displacement, rather than range change, meaning that a positive trend (green-red-blue) represents movement of the ground towards the radar (range decrease), i.e. uplift towards the radar, and a negative trend (green-blue-red) represents LOS displacement away from the satellite (range increase). In most of my interferograms the master scene is the image acquired on the earlier date, while the slave image is from a later date, and therefore the wrapped phase showing e.g. positive LOS displacement represents positive LOS displacement with time. In the few cases where the slave image is the older scene, I flipped the sign of the interferograms to ensure the time-evolution consistency between all the interferograms.

4.1 The Þófi Landslide in Seyðisfjörður

Seyðisfjörður is one of the Eastern Fjords and a town carrying the same name is located at the bottom of the fjord. To the west and east of the town are steep mountains, Bjölfur and Strandartindur, which both are over 1000 m high (Figure 19). The Strandartindur side has problems related to landslide creep, active debris flows, water flooding, and rockfall [Jensen and Sönser, 2002]. One of the problem areas is related to a shelf or a step on the Strandartindur slope that is called Þófi. This shelf is located at an elevation of 1-200 m above sea level, directly above large fish-factory buildings that line the coast. The Þófi shelf has developed due to intersections of WNW-ESE and NNE-SSW fractures and it is now mostly covered by till [Sæmundsson and Pétursson, 1999a; Jensen and Sönser, 2002]. An indication of recent mass movements in the Þófi area was detected in the field in 2000 when fresh and open ground cracks were found [Jensen and Jóhannesson, 2002]. This discovery was followed by an installation of 25 GPS stations in Fall of 2001 to monitor the movement and the first full reoccupation of the network was carried out in Fall of 2002 [Jensen, 2001; Jensen and Jóhannesson, 2002]. During the first year the measurements showed systematic displacement rates of up to 33 cm/year in the southwestern part of the Þófi area and the size of the moving area was found to be larger than expected, or at least $400 \times 250 \text{ m}^2$, and thus the network was expanded in 2002 [Jensen and Jóhannesson, 2002]. The 2002-3 measurements show continuing fast movements in Þófi while later measurements in 2003-4 and 2004-5 indicate little or no displacements [Tómas Jóhannesson, pers. comm., 2007].

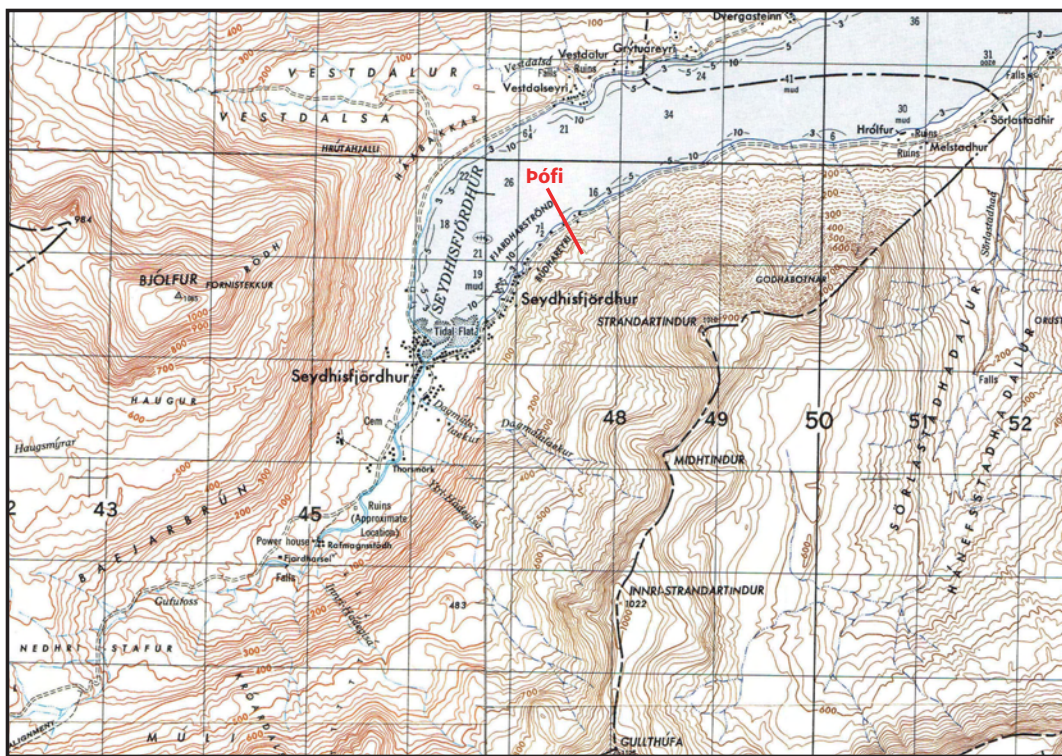


Figure 19. A Map of the town of Seyðisfjörður and surroundings. ©NLSI.

The location of the Þófi landslide on the steep northwestern slopes of Strandartindur mountain means that it can only be imaged by descending radars that look towards the WNW, while ascending data result in a layover. The surface conditions and the rather low altitude of 1-200 m make observation at this site relatively favorable and the area retains some degree of coherence for long time periods of up to a couple of years. We have a prior knowledge about the extent of the Þófi landslide from the GPS measurements, which indicate that the creeping area is only about 400 m broad. This poses a challenge for InSAR as the resolution of the radar is only about $4 \times 20 \text{ m}^2$ on the ground and usually approximately square pixels of $20 \times 20 \text{ m}^2$ are used. This means that the expected size of the Þófi landslide is only a couple of tens of pixels, which requires a careful analysis and does not allow much image filtering. While interferograms in East Iceland retain a significant amount of interferometric correlation over a period of several years, filtering of the interferograms is usually needed to obtain useful information from longer time-span interferograms. Therefore, due to the small extent of the Þófi landslide, only interferograms spanning less than about 6 months proved to be useful in this area.

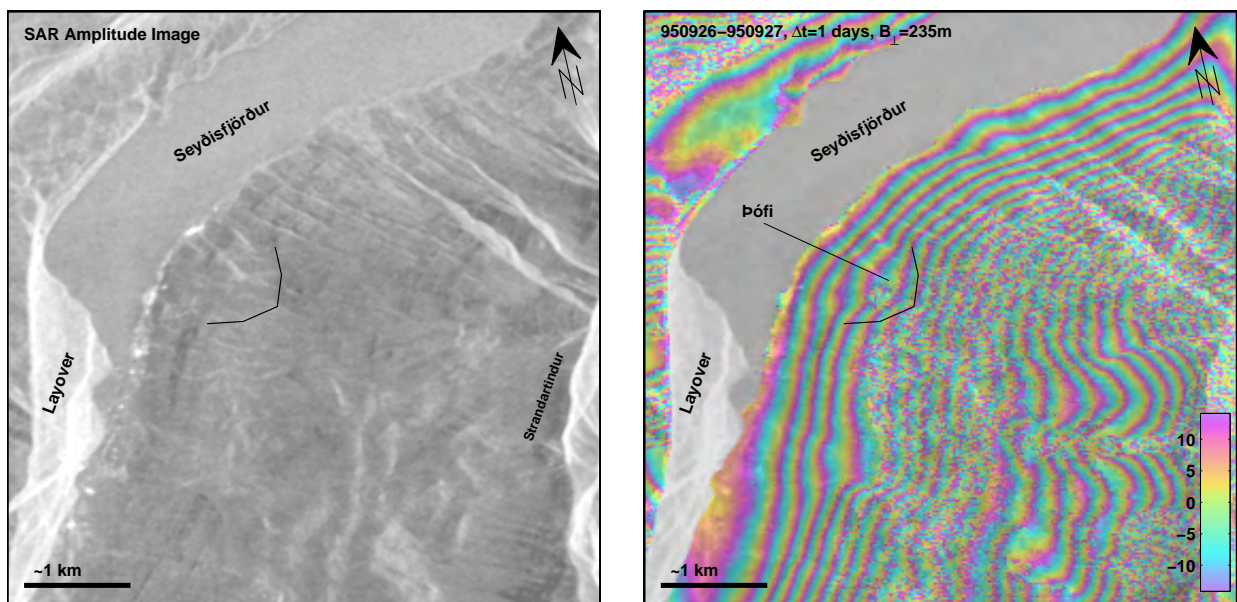


Figure 20. SAR amplitude image (left) and a 1-day tandem interferogram (right) from Seyðisfjörður. The images are in radar coordinates and the upper edge of the Þófi shelf is shown by a black thin line. The amplitude image shows bright returns from factory buildings along the coast. A large layover from Bjólfur mountain to the west covers most of the town of Seyðisfjörður. The Tandem interferogram shows topographic fringes and here one color fringe denotes about 40 m of elevation. The Þófi landslide is visible as a step in the topography. ©ESA.

The Þófi landslide is not clearly identifiable in a SAR amplitude image of the area (Figure 20), but bright reflections are seen from the fish factory buildings near the coast. A large layover from the steep Bjölfur mountain to the west covers most of the Seyðisfjörður town such that almost no reflections from houses in the town can be seen. A one-day tandem interferogram of the area shows phase values that are proportional to topographic height and the color fringes can be viewed as elevation contours of the area in radar coordinates (Figure 20). The Þófi area appears as a step in the topography between about 100 and 300 m above sea level. This interferogram shows a band of decorrelation between elevations 300-500 m which probably indicates snow-melting below 500 m and no snow-cover below 300 m during this day in September 1995.

Interferograms from before 1998 indicate no movement of the Þófi landslide (Table 1). Two interferograms that both span approximately 2 years, one from July 1993 to July 1995 and the other from July 1995 to June 1997, exhibit significant amount of high-frequency noise due to decorrelation and demonstrate the problem of using multi-year interferometry at this location (Figure 21). In these interferograms there is no sign of deformation on the Þófi landslide, although decorrelation prevents reliable measurement. Three 1-2 month interferograms from the summer of 1995 are of much better quality but they clearly show that no movement took place in the Þófi area during the time these interferograms span (Figure 22, Table 1). Two interferograms, one spanning one year 1996-1997 and another spanning 3.5 months in 1997 do not either hint at any displacement in Þófi (Figure 22). Two other interferograms that span 1996-1999 and 1997-1999 are too noisy to provide any information about the landslide motion during these time intervals (Table 1).

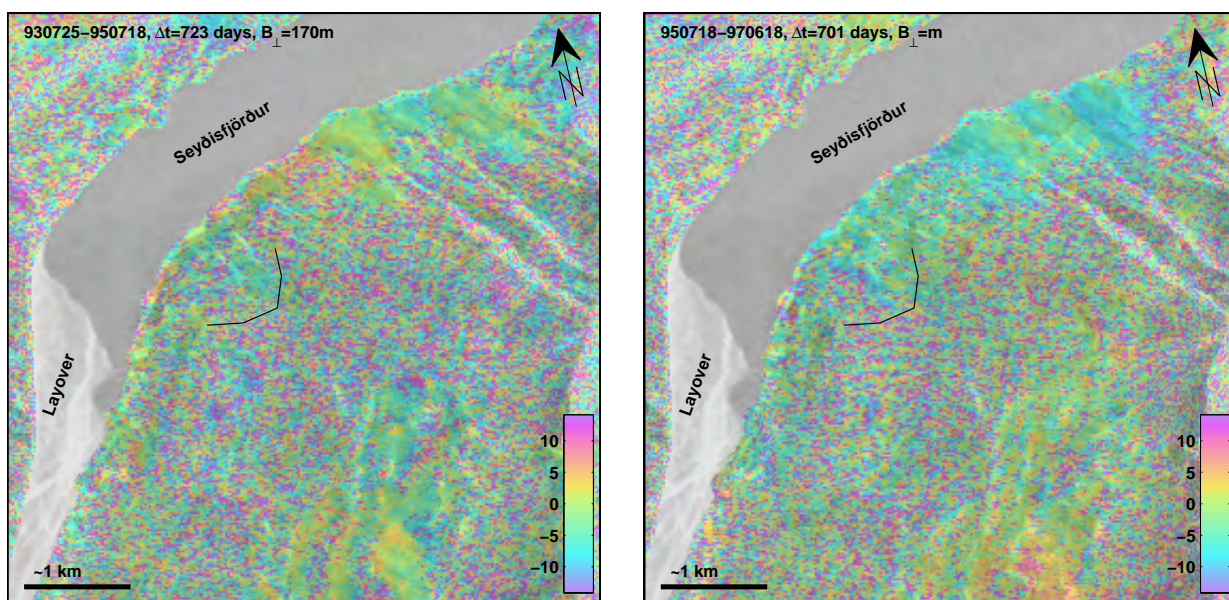


Figure 21. Two-year interferograms spanning 1993-1995 (left) and 1995-1997 (right). The interferograms are mostly decorrelated, which inhibits reliable measurement on the Þófi landslide. ©ESA.

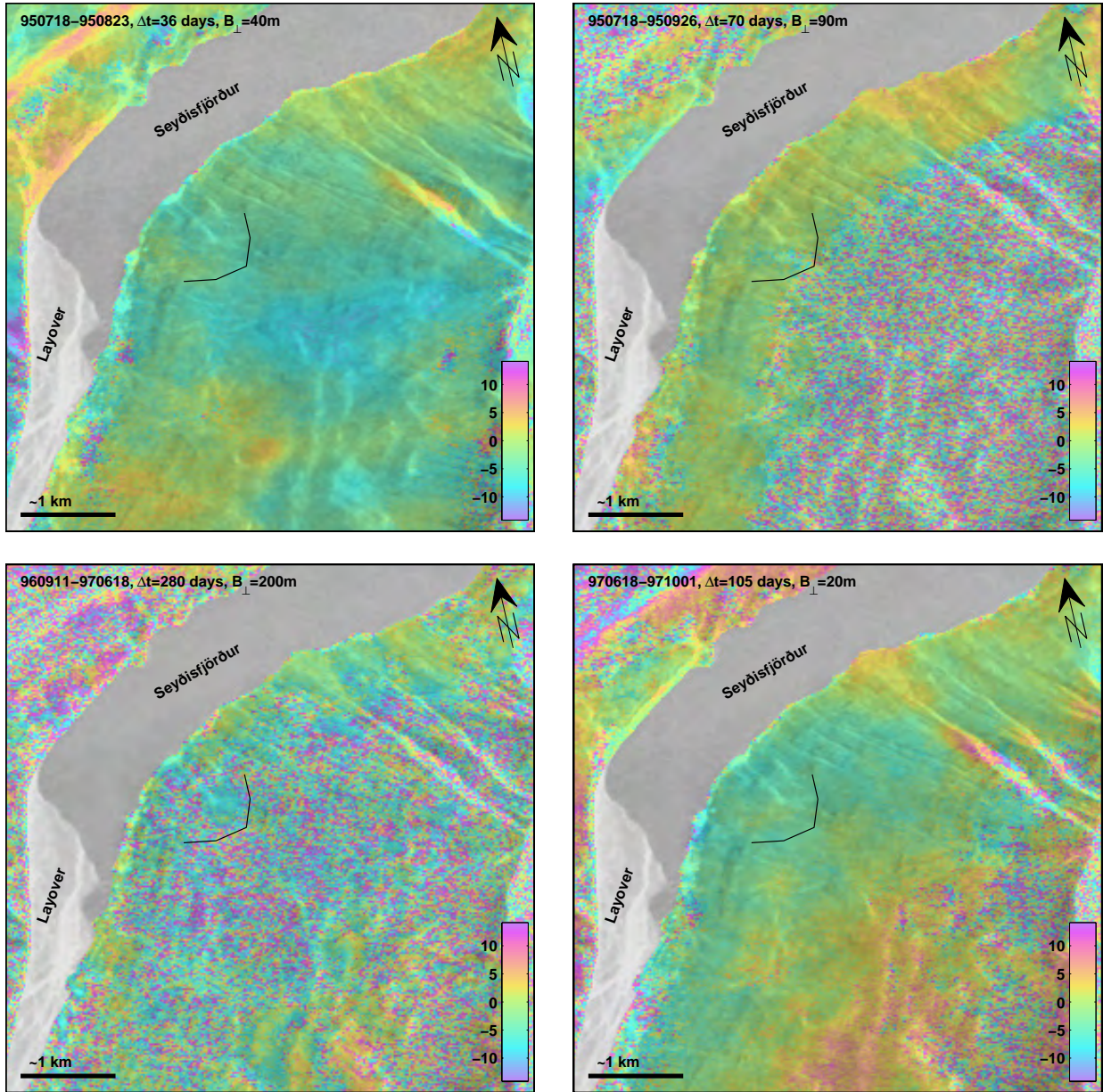


Figure 22. *Two Seyðisfjörður interferograms from 1995 spanning 35 days and 70 days (top), and two interferograms spanning Sept. 96 - June 97 and June 97 - Oct. 97 (bottom). The interferograms from 1995 and 1997 show no signs of movement on the Þófi landslides, while the 1996-1997 interferogram is mostly decorrelated and provides limited information. ©ESA.*

An interferogram from 1998 spanning 4.5 months from 8 July to 25 November demonstrates the problem of decorrelation when the interferogram time-span becomes several months (Figure 23). Most of the Seyðisfjörður area appears here noisy and the interferogram is completely decorrelated at elevations above ~ 400 m, presumably due to snow during the November acquisition. However, although the interferogram is noisy, its filtered version exhibits a rather coherent phase along the coast. What is significant here is the abrupt and consistent change in interferometric phase values that can be seen in the Þófi area. My interpretation is that this signal represents ground movement, although the area that appears moving is rather small, only about 2-300 m broad, and might have gone unnoticed, if I had not specifically inspected this area. The noisy images make it difficult to determine how strong the signal is, but it appears to amount to at least 1-2 cm of range increase or displacement of the ground down away from the satellite look direction. A large area located along the coast to the northeast also shows consistent interferometric phase value shift of similar magnitude. However, the smooth appearance of this signal and its single appearance in this interferogram strongly suggest that it is of atmospheric origin, but not due to ground displacement.

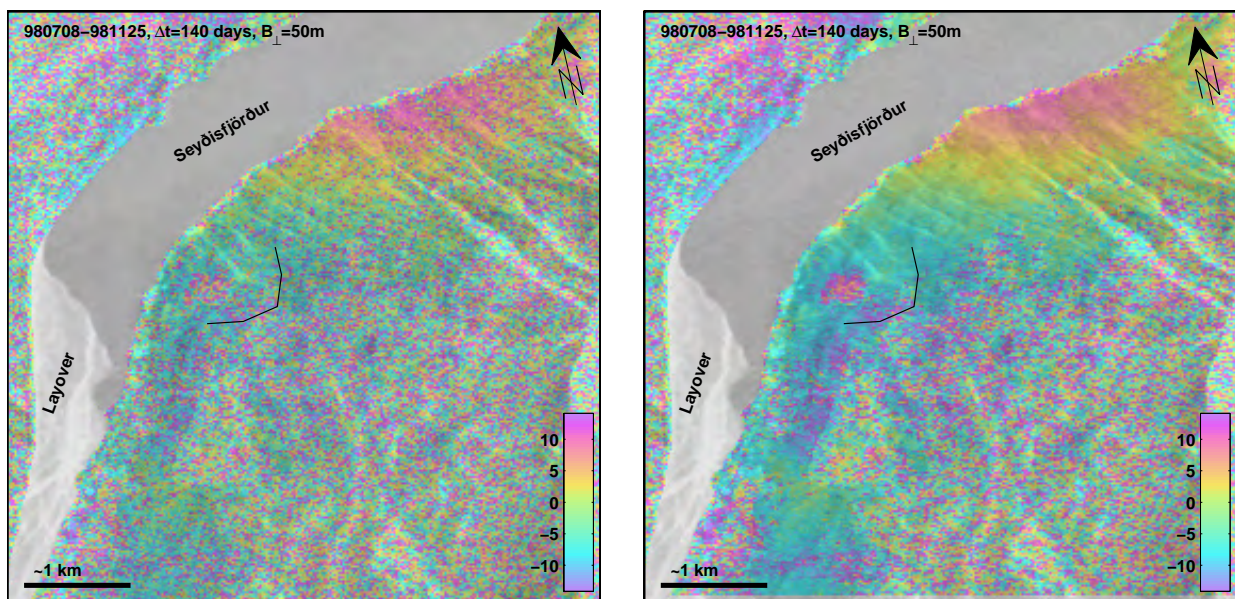


Figure 23. An interferogram Seyðisfjörður spanning July to November 1998 shown both unfiltered (left) and filtered (right). This interferogram shows an abrupt change in interferometric phase values on the Þófi landslide amounting to at least 20 mm range increase or LOS subsidence. The area that is moving appears to be about 2-300 m broad. ©ESA.

The location of the small moving area coincides well with the area in the southwest-half of the Þófi site that had been found moving from the GPS measurements [Jensen and Jóhannesson, 2002]. I geocoded this interferogram to better assess where the moving region is located (Figure 24). This involves a projection of the unwrapped interferogram from its radar geometry coordinates to geographical coordinates. The projection requires interpolation onto

a very different grid and does therefore modify the observed data significantly. The geocoded version of the interferogram has the same 25 m posting as the DEM used in this process and is therefore somewhat coarser than the original interferogram. The resulting image shows the location of the moving area to be on the southwestern side of the Þófi area and mostly located just above 100 m elevation (Figure 24). It should be mentioned here that neither the DEM nor the geocoding procedure is fully reliable, so the location of the moving area in the interferogram should be regarded as only an approximation. However, this location corresponds well with the area that was found to be moving from GPS measurements 2001-2 [Jensen and Jóhannesson, 2002] and therefore shows that the Þófi landslide became active well before the first GPS measurements were carried out.

Profiles across the moving area show better that the moving area is only 200 m broad and has LOS displacement of up to 2 cm (Figure 24), while up-slope profiles indicate that the moving area is 100-150 m above sea level. The local topographic slope of the landslide in Þófi is around 14° and the local incidence angle is therefore 37° (Figure 24). This implies that $2/\sin(37) = 3.3$ cm of surface parallel down-slope motion is needed to explain the observed 2 cm LOS displacement, or an average velocity of 9 cm/year during the 4.5 months the interferograms spans.

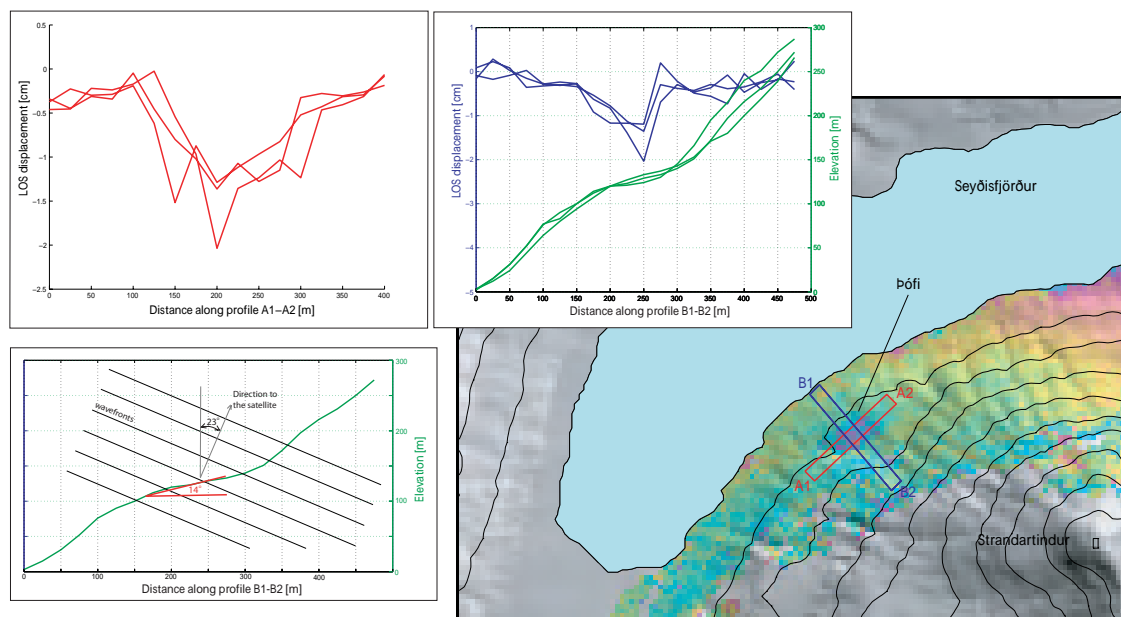


Figure 24. Geocoded version of the interferogram shown in Figure 23 showing the location of the moving area in Þófi. The map shows 100 m elevation contour lines and most of the deformation appears to be on the southwest part of the Þófi area. The top-left inset shows three parallel profiles A1-A2 across the landslide indicating that the moving area is 200 m wide with up to 2 cm of LOS displacement. The top-right inset shows up-slope profiles B1-B2 in comparison with topographic profiles that show the moving area between 100-150 m above sea level. The bottom inset shows that the local slope is around 14° so about 3 cm of surface parallel down-slope movement is needed to produce the observed signal. ©ESA.

Interferograms from 1999 show a similar pattern. The best interferogram spans six months from May to November 1999 and although it is noisy, it clearly shows signs of consistent phase change on the Þófi landslide (Figure 25). In this case the deformation appears to be slightly stronger than in the 1998 interferogram and the area that is moving is larger. The center of the 1998 area in this image appears decorrelated, possibly due to too much displacement, but the amount of LOS range increase during these six months exceeds 2-3 cm (7-10 cm/year creep velocity assuming surface parallel motion).

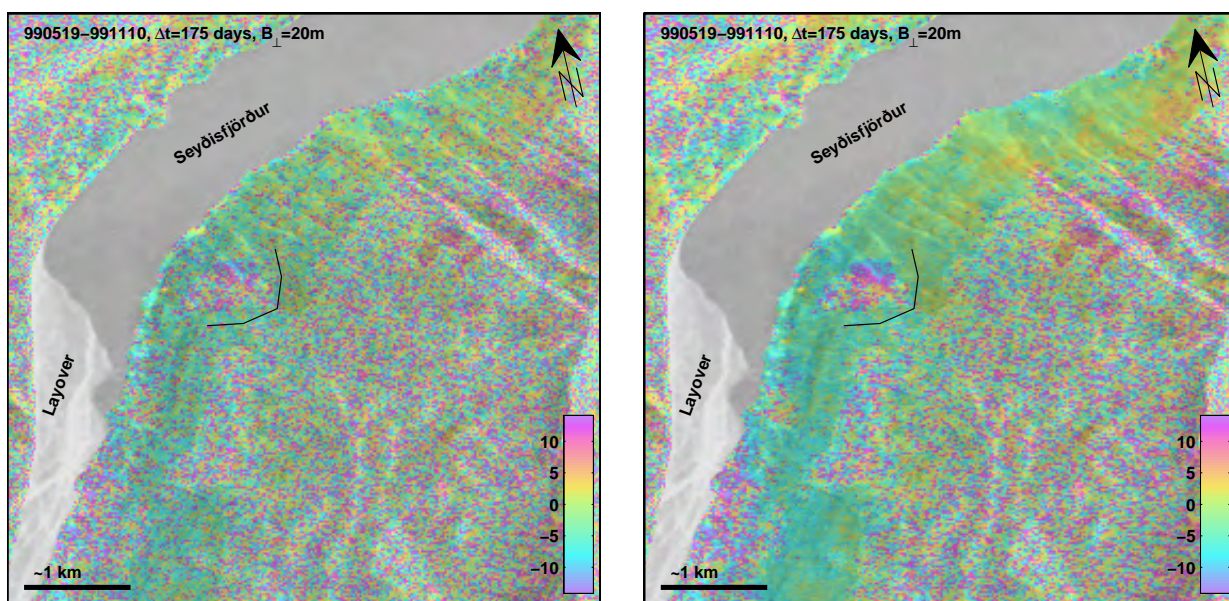


Figure 25. An interferogram of the Þófi landslide spanning May to November 1999 shown both unfiltered (left) and filtered (right). This interferogram shows a similar signal as the 1998 interferogram (Figure 23), except here the moving area appears somewhat more extensive. © ESA.

No data exist from the year 2000 from this track and in early 2001 the ERS-2 satellite started malfunctioning, severely limiting the use of data for interferometry. Therefore, I do not have any data of the Þófi landslide that coincides with the GPS observations made in 2001-2. However, I requested Envisat radar data in 2004 and 2005 and several interferograms were formed using the descending track data, although many of baselines turned out to be too long for a useful measurement (Figure 9). Here I show examples from four interferograms spanning time periods from 35 days to one year in 2004-2005 (Figure 26). Although the one-year interferogram is somewhat noisy, it is clear that none of these interferograms exhibit obvious signs of displacement on the Þófi landslide. The same is true for other interferograms from 2004 and 2005 (Table 1). These InSAR results agree with GPS observations that show no systematic displacements of measurement points during 2004-5 [Tómas Jóhannesson, *pers. comm.*, 2007].

To summarize my findings in Seyðisfjörður I can state that interferograms from summers

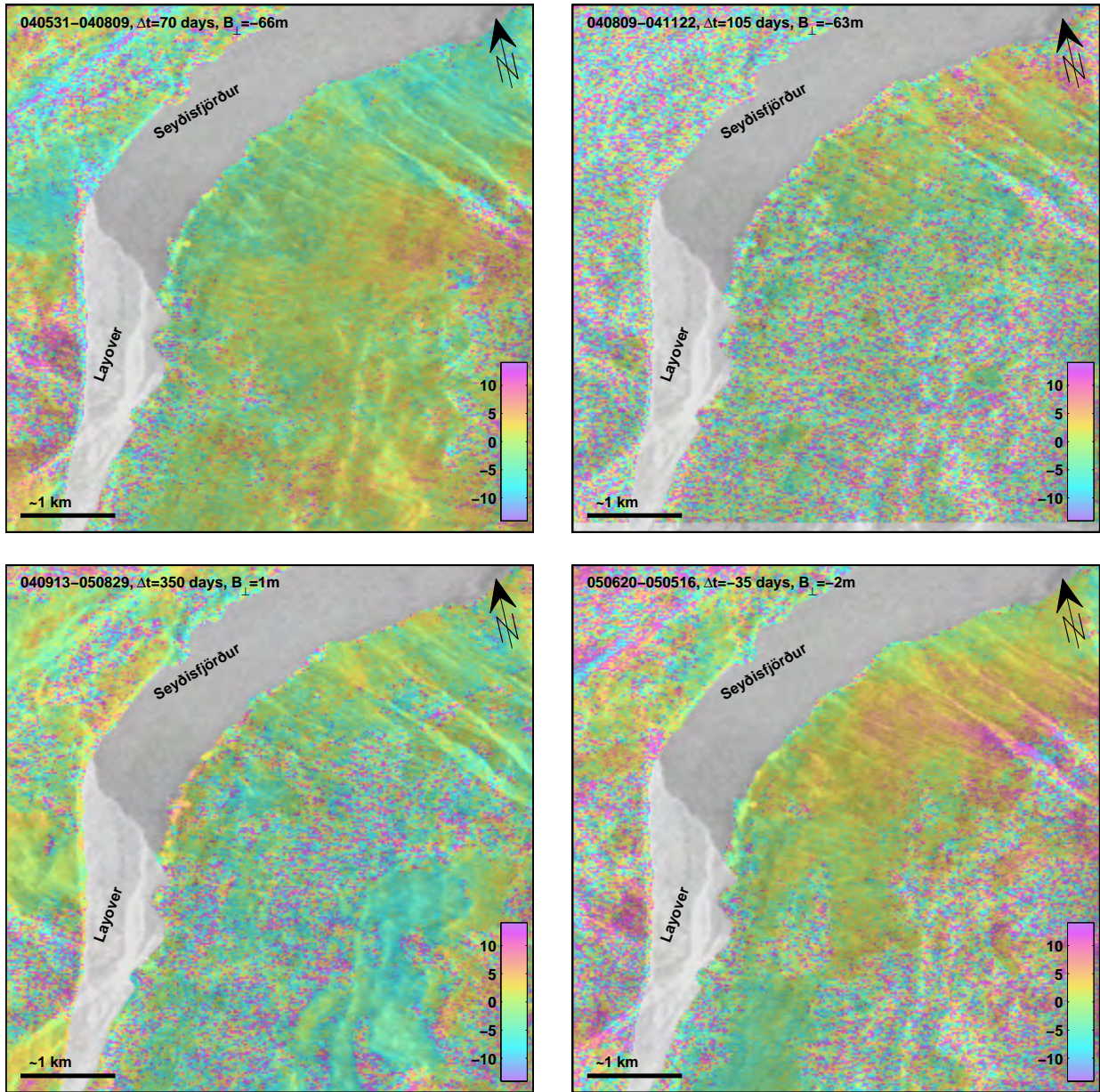


Figure 26. *Descending Envisat interferograms from 2004-5 showing no signs of deformation on the Þófi landslide. ©ESA.*

of 1998 and 1999 show a small sign of deformation on the Pófi landslide that amounts to a few centimeters in each case and the deforming area is bound to the southwestern part of the Pófi area, which is consistent ground observations. Data from 1993-1997 and from 2004-2005 on the other hand indicate that no deformation took place at this location. No useful interferograms could be formed during 2000-2003 due to lack of data and due to problems with the ERS-2 satellite. The Pófi landslide is a rather small area that complicates our analysis as one needs be careful when applying filtering to the data, which then in turn makes it difficult to analyze noisy data that span more than one year.

4.2 The Urðarbotn Landslide above Neskaupstaður

Neskaupstaður is one of the main fishing towns in East Iceland and it has a population of about 1400. North of the town are 8-900 m high mountains and the town itself stretches 2.5 km along the shore below the steep southward facing mountain slopes. Cliffs dominate the uppermost 3-400 m of the mountain side and below them are steep vegetated slopes [Sæmundsson and Pétursson, 1999b]. An unstable landslide is located 600-700 m above the town at a location called Urðarbotn. During the past decades, several debris flows have originated at this location following heavy rainfall, causing damage in the town [Jensen and Hjartarson, 2001]. GPS measurements during 1991-2001 indicate non-steady motion of the landslide from year to year with one benchmark showing displacement of 138 cm during 1992-1993, but only 11 cm during 1994-1996 [Jensen and Hjartarson, 2001]. The Urðarbotn landslide is located on a SSE-facing slope and cannot be imaged from descending orbits, as it is hidden in a layover (Figure 27). No suitable ERS data from ascending orbits exist in the ESA archives, so the only usable ascending data are the Envisat data I requested in 2004-2005. Although imaging from ascending orbits is possible, it is challenging due to the steep slopes and cliffs at this location, but most of the Urðarbotn landslide is probably visible (Figure 27).

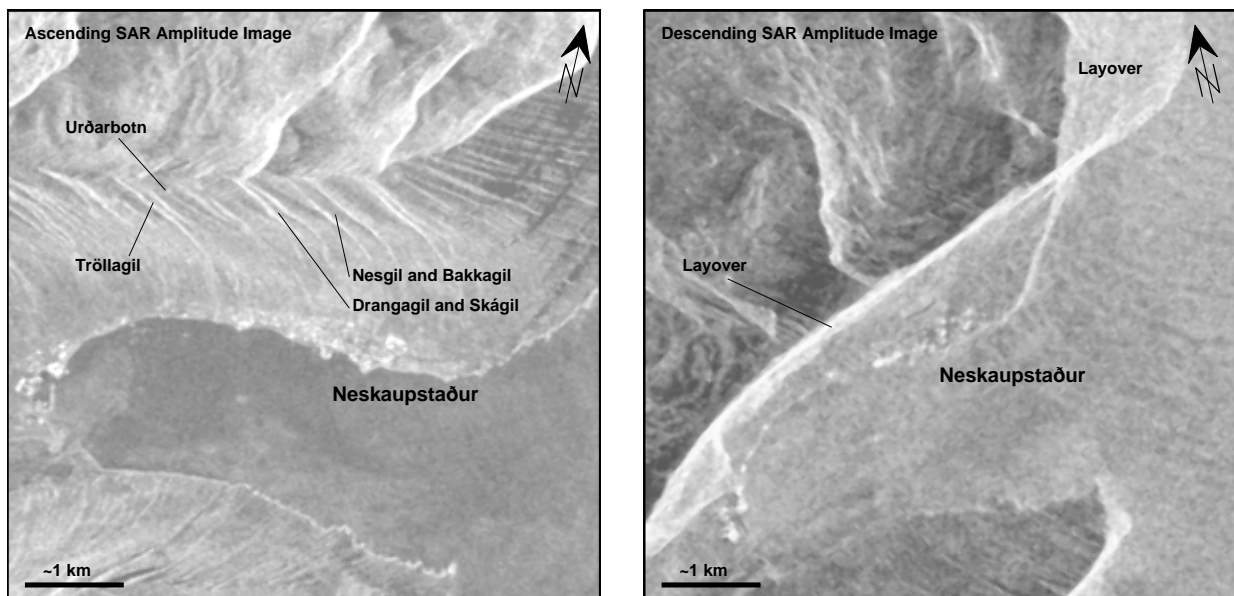


Figure 27. Ascending and descending amplitude images in radar coordinates of the town of Neskaupstaður and surroundings. The dramatic topography skews both images significantly and the entire slope above the town is hidden in a layover in the descending image, as was predicted in Figure 2. Locations high on the slope above Neskaupstaður, including the Urðarbotn landslide, appear further to the west in the ascending radar geometry than when displayed in a proper map projection. ©ESA.

No displacements are observed on the Urðarbotn landslide in the ascending Envisat interferograms I processed. Three one-month interferograms exhibit a reasonable degree of interferometric coherence high on the slopes above the town of Neskaupstaður, but none of them show any sign of displacement at the Urðarbotn site. These interferograms span 4 July - 8 August (Figure 28) and 8 August - 12 September 2004, and 15 May - 19 June, 2005. One interferogram that spans about one year 2004-5 shows similar results (Figure 28).

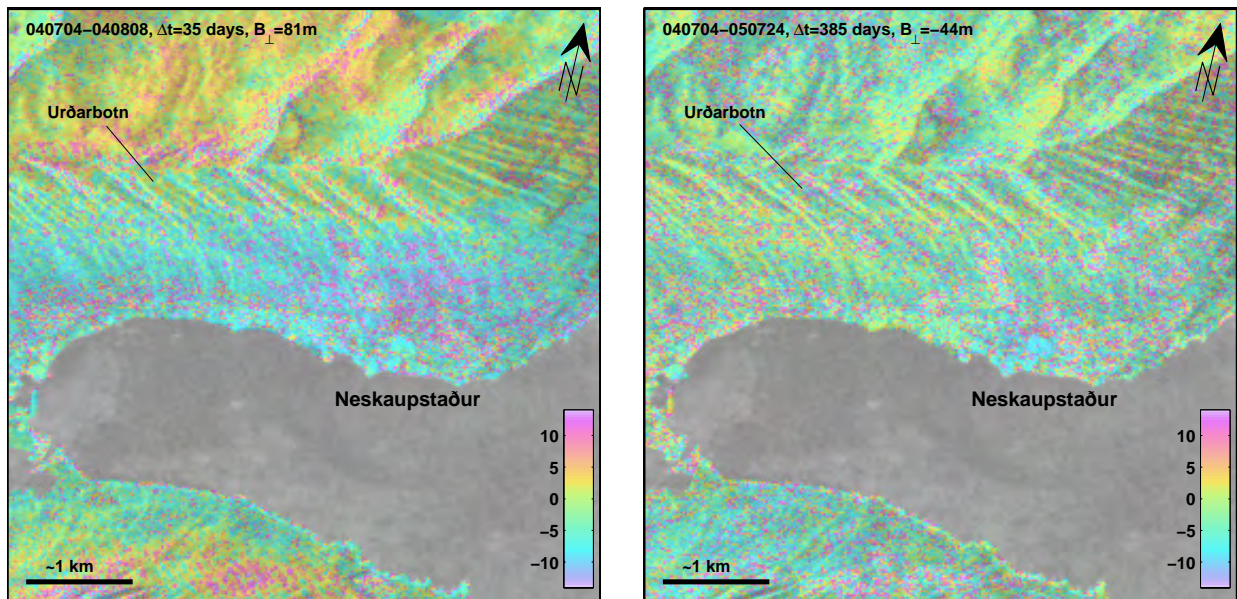


Figure 28. Two ascending interferograms of Neskaupstaður, spanning 35 days in 2004 (left) and about one year 2004-5 (right). Both interferograms are displayed unfiltered and in radar coordinates to minimize data processing artifacts. Neither of the interferograms shows signs of displacement on the Urðarbotn landslide. ©ESA.

We explore three possible reasons for the lack of observed displacement on the Urðarbotn landslide. First are limitations of the imaging geometry, as the ascending look direction is not optimal for south facing slopes. However, the Urðarbotn landslide is located in a small bowl that faces more towards the east than the slopes generally do above the town of Neskaupstaður. Therefore, the landslide should be even better suited for ascending-orbit imaging than the main slope, so limitations in the imaging geometry remain an unlikely cause. The second possible reason is the limited extent of the landslide creep. *Jensen and Hjartarson* [2001] state that the width of the Urðarbotn bowl is around 200 m at its base and that it extends uphill by only 80 m. This poses a challenge for the ca. 20 m resolution of InSAR. However, if the entire landslide was moving it would probably result in an observable signal in the one-month interferograms, but possibly not in the noisy one-year interferograms. But, if only a small portion of the landslide was moving, then the displacement might go undetected, even in the one-month interferograms. The third possible reason is simply that no displacement took place during 2004-5 at the Urðarbotn site.

4.3 The Vopnafjörður Area

Vopnafjörður is a fjord and a town in northeastern Iceland. The town is located near the shore and it has a population of 600. A broad valley extends inland from the fjord to the southwest with Smjörfjöll mountains on the southeastern side that are over 1200 m high while the hills to the northwest of it are less than 200 m high (Figure 29). The flat valley-floor is a home to several farms, particularly on the southeastern side of the valley.

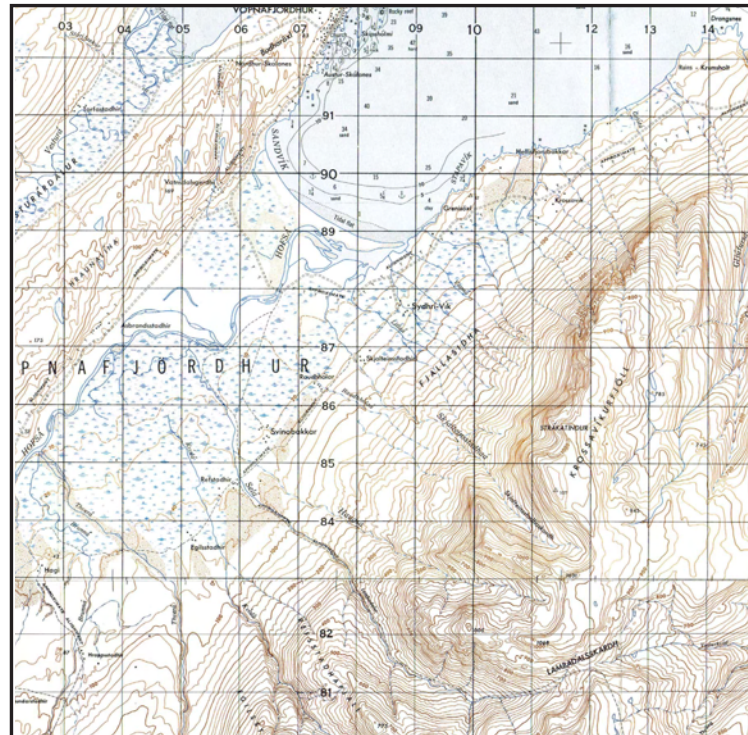


Figure 29. *Map of Vopnafjörður.* ©NLSI.

The steep northwest-facing Smjörfjöll mountain slopes are well imaged with descending radars looking down to the earth towards the WNW. The main limitation for observing this area with InSAR seems to be decorrelation due to snow, as the snow melts late in the spring and arrives early on these high mountains.

An interferogram of Vopnafjörður spanning 35 days during the summer of 1995 shows clearly movement of a landslide on the northwestern slopes of Smjörfjöll (Figure 30). This area was not known to be active before it was here detected by InSAR. This landslide is over 1 km broad near its top (where the image becomes decorrelated due to snow), but somewhat narrower further down-slope. Its southern margin is very sharp as indicated by discontinuities in the interferogram. The displacement amounts to at least 6 cm of LOS range increase indicating downward displacement of the landslide. The pattern of displacement is, however, rather complicated and includes some internal discontinuities, which seems to indicate that it is not a one solid landslide that is moving. Geocoding of this interferogram pinpoints the location of it between the rivers of Skjaldþingsstaðaá and Haugsá, above the

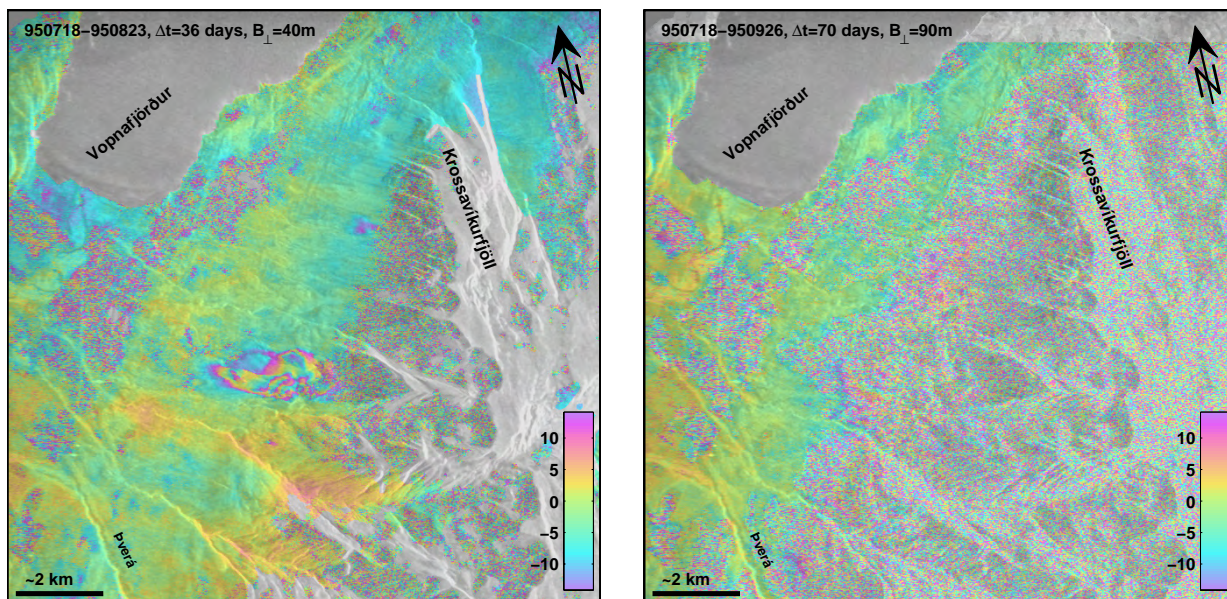


Figure 30. Two interferograms spanning 35 days (left) and 70 days (right) in 1995. The 35-day interferogram shows clear landslide movement while the 70 day interferogram is decorrelated at elevations above ca. 200 m. ©ESA.

farm of Svínabakkar (Figure 31). This image also shows that most of the movement takes place between 200 m and 500 m above sea level. Two displacement profiles across the landslide are shown in Figure 31 and they show that its southwestern edge is sharp with up to 3 cm LOS displacement in the lower half of the landslide but more LOS displacement at a higher elevation. The third profile is along the landslide, from the bottom to the top and shows gradually increasing displacement from the lower edge towards the center where the unwrapped image is troubled by discontinuities.

Movement of this landslide is also clearly visible in an interferogram that spans 9 months from September 1996 to June 1997 (Figure 32). The displacement pattern here is also similar, although this interferogram is a bit noisier due to the longer time interval it spans and it has artifacts resulting from the 200 m long perpendicular baseline. Another interferogram spanning three years from 1996 to 1999 is somewhat correlated around the landslide site, but completely decorrelated on the landslide, which indicates that the movement of the landslide was probably too large during these three year to be measured by InSAR (Figure 32).

Due to the high deformation rate of this Vopnafjörður landslide, interferograms that have short time spans provide more information. Figure 32 shows two interferograms that span 3.5 months and 5 months in 1997 and 1998, respectively. Both show clear signs of landslide movement, but the observed displacements are small. The 5-month interferogram is somewhat decorrelated, which could be due to high displacements on some parts of the landslide, but the 3.5 month interferogram exhibits clearly a maximum displacement of only about 2 cm and that the lower part of the landslide does not move at all. Comparison with

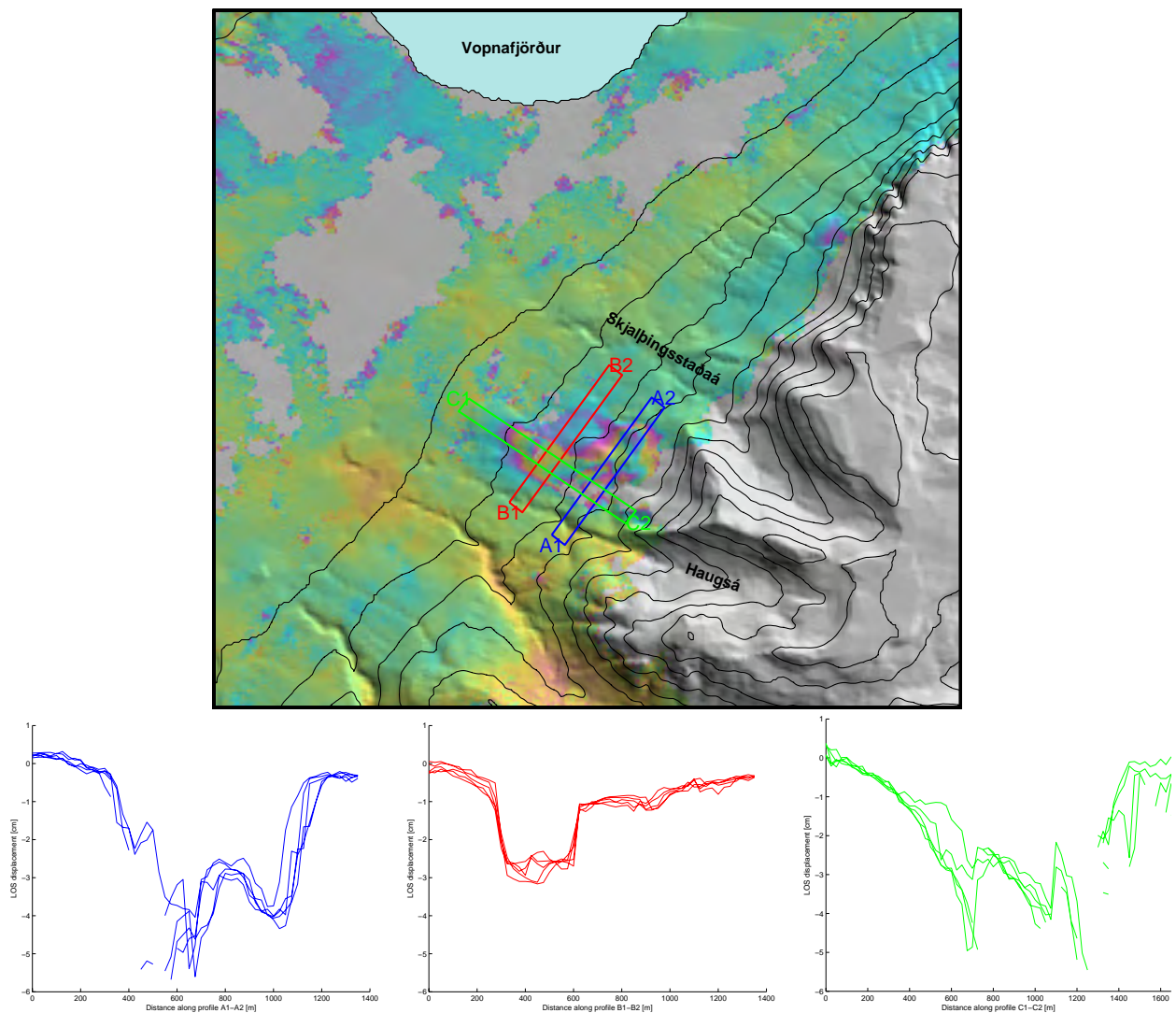


Figure 31. Geocoded version of the interferogram in Figure 30. The moving landslide is between the Haugsá and Skjalþingsstaðaá rivers, above the Svínabakkar farm. Two LOS displacement profiles across the landslide (bottom, left and middle) and one along the landslide (bottom right) show the movement of the landslide. ©ESA.

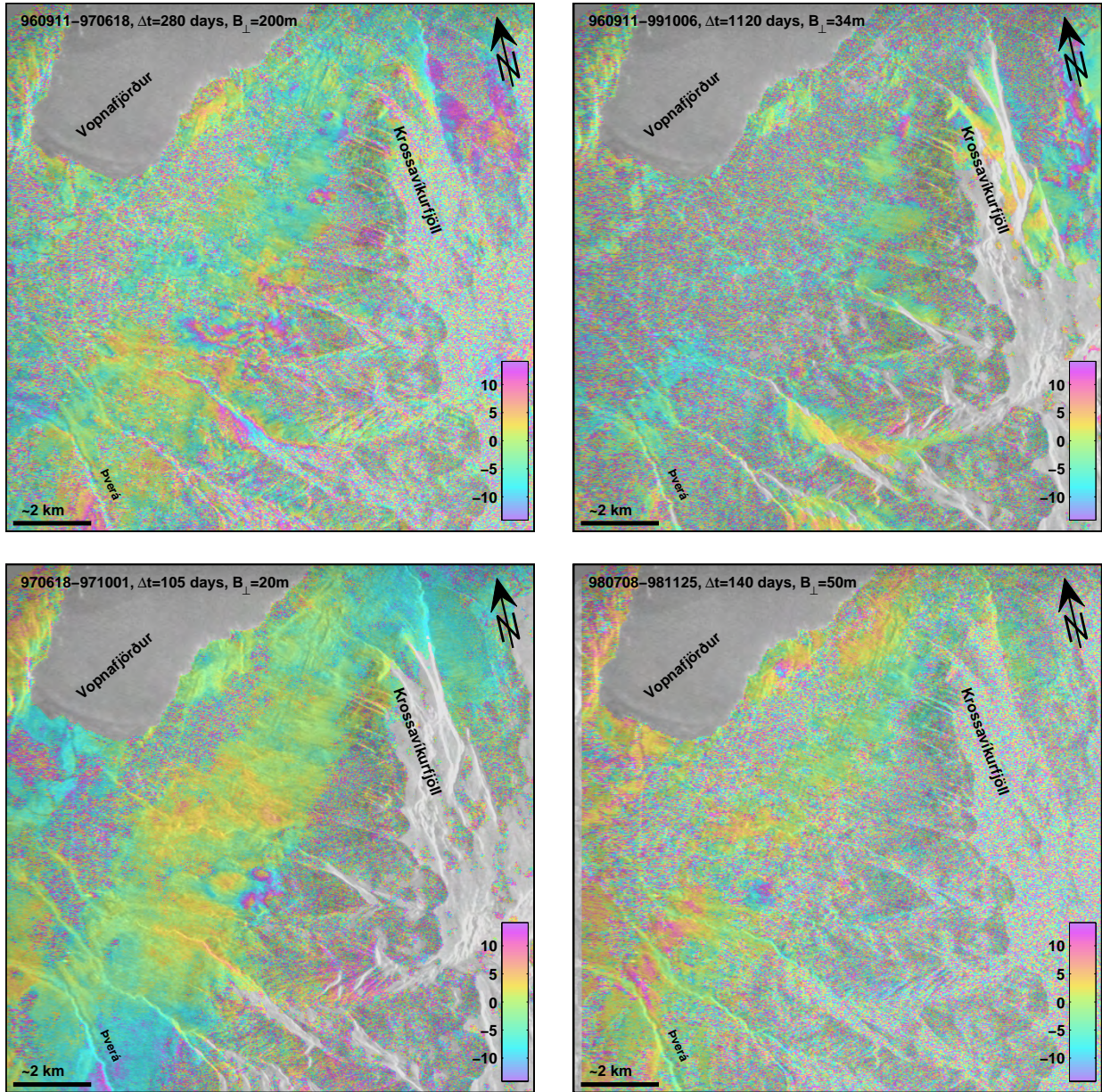


Figure 32. Two interferograms spanning nine months from 1996-1997 and three years from 1996 to 1999 (top), and another two interferogram spanning 3.5 months in 1997 and 5 months in 1998 (bottom). The 9-month interferogram shows a clear movement of the landslide while the three-year interferogram is mostly decorrelated. The 3.5 and 5 month interferogram clearly indicate landslide movement. ©ESA.

the 35-day interferogram from 1995 (Figure 30) therefore demonstrates that the landslide motion at this site is far from being steady in time. Envisat interferograms from 2004 and 2005 show similar results. Interferograms that span 70 and 35 days in 2004 and 2005, respectively, show only very small displacements, if any (Figures 33). A one-year 2004-5 interferogram, on the other hand, clearly indicates several cm of displacements where the pattern appears to agree well with the observed pattern in 1995 (Figure 33).

The landslide creep above the farm of Svínabakkar in Vopnafjörður has clearly been very active during the last decade as clear displacements are observed in almost all the interferograms that were not decorrelated in this region. In some cases the reason for the local decorrelation may have simply be due to too much displacement. Another issue about this landslide is that the motion appears non-steady, if not episodic. This is demonstrated by strong displacements observed in a 35-day interferogram from 1995, while a 105-day and 35-day interferograms from 1997 and 2005 show little or no displacements. Some hints for movement can be found at other locations further north along this slope, e.g. in Figure 32, but these locations are not very prominent.

I studied precipitation data from Vopnafjörður to inspect if observed variations in displacement rate on the landslide can be correlated to variations in precipitation. Monthly precipitation at Skjaldbingsstaðir in Vopnafjörður vary from around zero to a maximum of over 500 mm during October 1995. Low pass filtering of the monthly values shows clearly annual precipitation fluctuations peaking in the Fall (Figure 34). I plot the maximum LOS displacement value in the different interferograms as a function of both the mean precipitation rate and accumulated precipitation during the time the different interferogram span. However, in neither case can clear correlations be seen (Figure 34). A better temporal resolution of both the deformation data and the precipitation data is probably needed to make this comparison more meaningful.

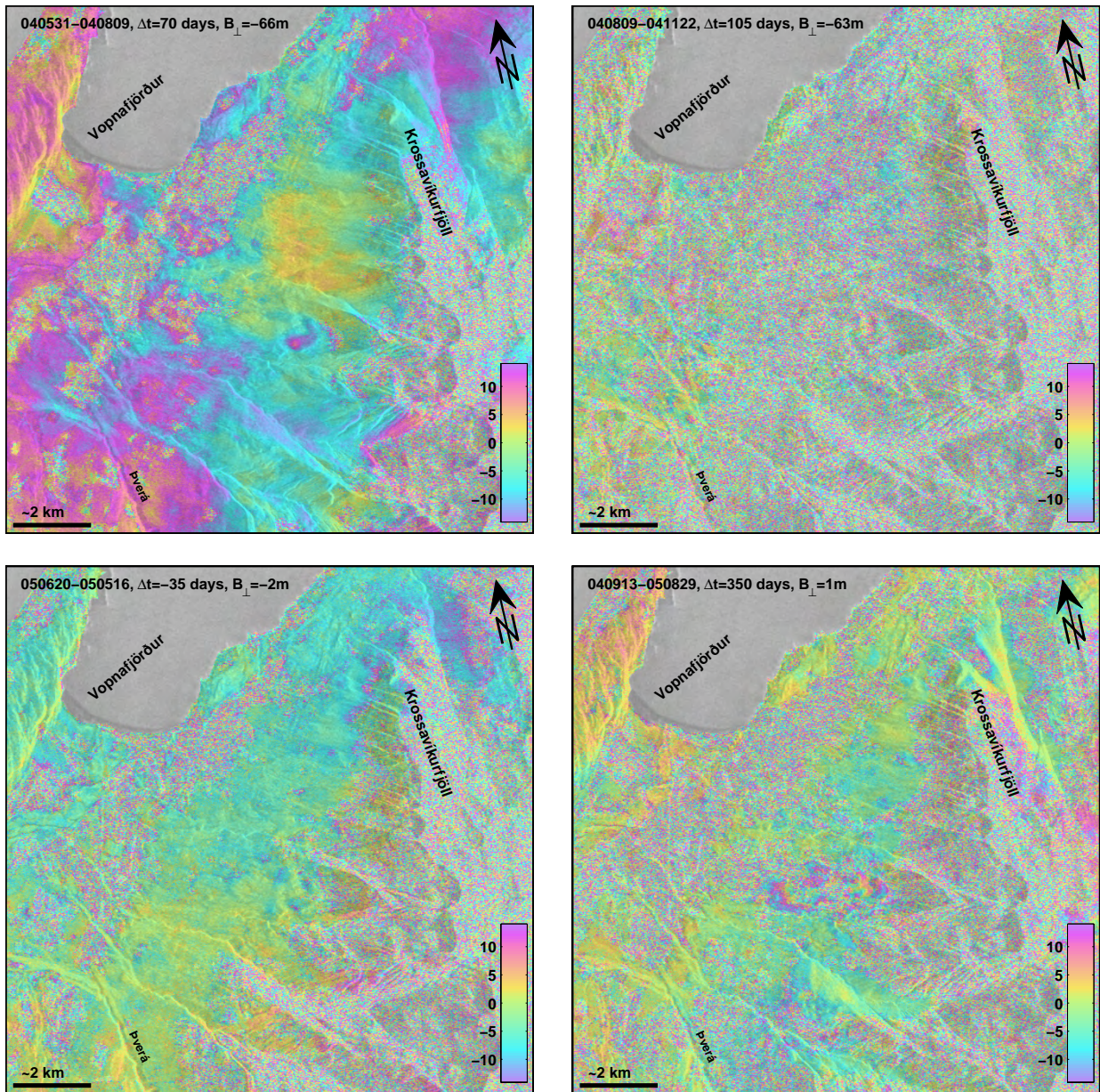


Figure 33. Four Envisat interferograms of the Vopnafjörður landslide from 2004-5. ©ESA.

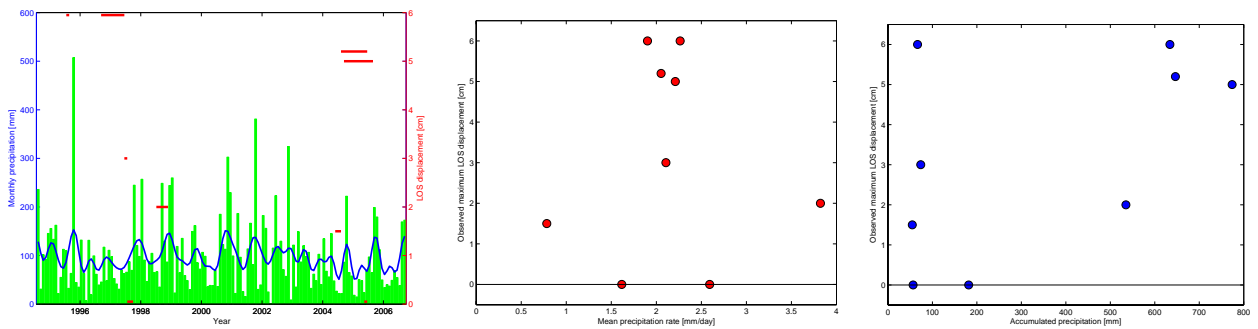


Figure 34. Comparison between precipitation and landslide movement in Vopnafjörður. A histogram of monthly precipitation from 1995 to 2006 at Skjaldbingsstaðir in Vopnafjörður (left) with low-pass filtered values showing precipitation maxima in Autumn (blue curve). Observed maximum LOS displacement in the various interferograms is shown in red and the bar length corresponds to the time period each interferogram spans. Maximum LOS displacement versus the mean precipitation rate (middle) shows no clear correlation, nor does maximum LOS displacement versus the accumulated precipitation (right) during each interferogram time-span.

4.4 Other Locations in Descending Interferograms

In this section I discuss other areas where displacements were detected in descending ERS-1/2 and Envisat InSAR data from 1993-1999 and 2004-2005, respectively. The radars look down from the ESE when descending and slopes that face ESE can therefore not be imaged during these passes. Then, I will discuss the results from ascending orbits in a separate section that follows this section.

4.4.1 Ytri-Þverhryggir in Lambadalur, Borgarfjörður

A clear signal of 1-1.5 circular fringes can be seen the Lambadalur valley, which is a small tributary valley to the Borgarfjörður valley (Figure 35). This signal is seen in a four-year interferogram 1993-1997 and cannot be a topographical artifact as this interferogram has almost zero perpendicular baseline, and is therefore insensitive to any topography. Also, the signal is found in another interferogram that spans the three years 1996-1999, although there its magnitude is somewhat smaller than in the four-year interferogram. What is interesting about this deformation signal is that it shows range decrease or LOS displacement up towards the satellite. The maximum LOS displacement is about 4 cm. This could be either caused by uplift of the ground or by horizontal motion towards the east.

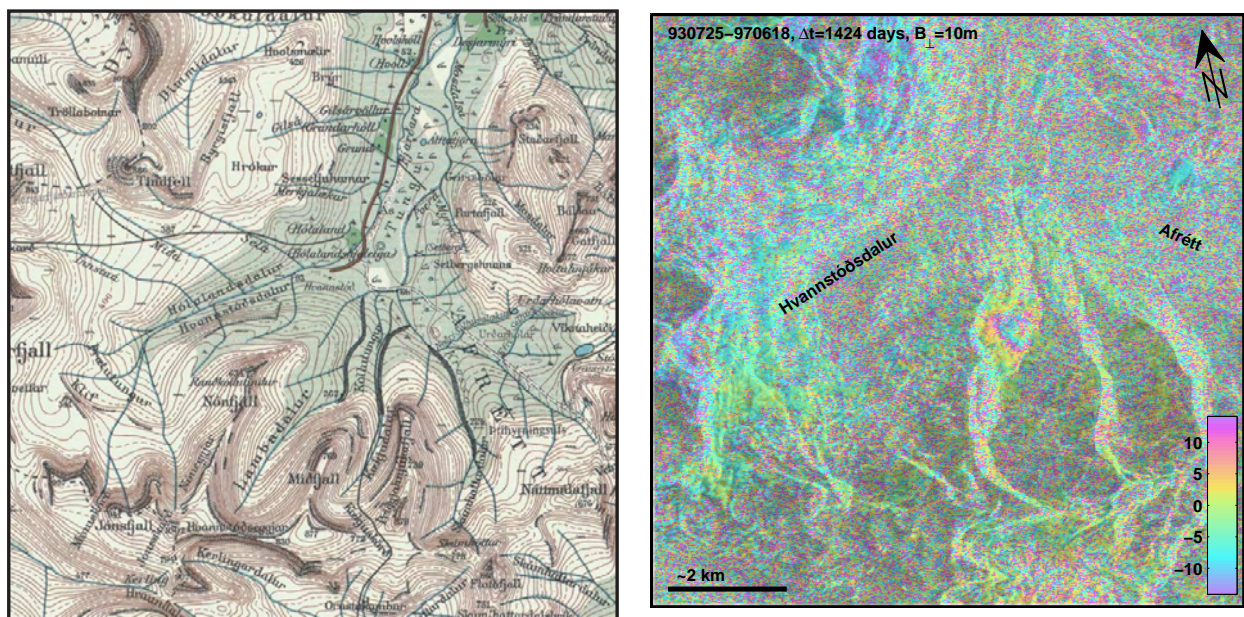


Figure 35. A map and a four-year interferogram of the Borgarfjörður area. Deformation is observed on the western side of the Lambadalur valley. ©NLSI and ©ESA.

Jónsson [1976] catalogues two landslides in Lambadalur valley which are called the inner and outer Þverhryggir landslides (Innri-Þverhryggir and Ytri-Þverhryggir). Both landslides are located on the west side of the valley on the slopes that face east. While the inner

western part of the valley appears to be lost to a layover in the interferogram, the outer part is not, and that is the location of where the signal is observed. *Jónsson* [1976] states that the Lambadalur landslide is about 1 km broad but he does not provide a map of the landslide location, but the observed signal seems to approximately coincide with the outer Þverhryggir landslide.

If the location of the deforming area coincides with the known outer Þverhryggir landslide, then the displacement is likely due to displacement that is primarily horizontal towards the east. This would be somewhat surprising as landslides usually move downhill resulting in both a horizontal and vertical component of displacement. Location of Lambadalur is approximately at the center of the radar swath, which means that the radar incidence angle at this location is 23 degrees from vertical and therefore the radar is more sensitive to vertical displacements than to horizontal displacements. However, this landslide is located on a gentle slope of only 9-10° [*Jónsson*, 1976] and therefore, if the landslide moves down parallel to the slope towards the east or ESE (i.e. the down-slope azimuth), then it would primarily cause range decrease, as is what is observed. The landslide would need to move up to 17 cm down the slope to result in the observed maximum LOS range decrease of 4 cm. Another but hypothetical explanation is that groundwater level increased within the landslide for some reason, e.g. due to precipitation increase during the period the interferogram spans, leading to poro-elastic rebound of the surface as has been observed south Iceland due to post-earthquake pore-pressure changes [*Jónsson et al.*, 2003]. However, this explanation is highly speculative and would need to be supported by analysis of precipitation data in the region, so I clearly favor the first explanation.

4.4.2 Reykjadalur in Mjóifjörður

Reykjadalur is a small valley on the south side of Mjóifjörður, between the Reykjasúla and Gilsártindur mountains (Figure 36). A localized deformation signal is observed in two interferograms on the east side of the valley. These interferograms are a three-year interferogram 1996-9 and a one-year interferogram 2004-5 (Figure 36). The magnitude of the signal is 2-3 cm of LOS range increase, indicating a downward mass movement, and the moving area seems to be about 3-400 m wide. However, despite the small extent and magnitude of the signal, it has the same spatial pattern in both interferograms, which strongly suggests that the signal is due to real displacement. Also, the one-year interferogram has nearly a zero perpendicular baseline, which eliminates the possibility that the signal is due to a DEM error or some other topographic artifact. The exact location of this signal is on the steep slope just northwest of the summit of the Gilsártindur mountain.

4.4.3 Barðsnes

Barðsnes is a peninsula to the east of Neskaupstaður town and just north of Gerpir, the easternmost point of Iceland (Figure 37). Barðsnes peninsula reaches an elevation of 650 m and is bounded by cliffs on its eastern side and steep slopes on its western side. Nobody

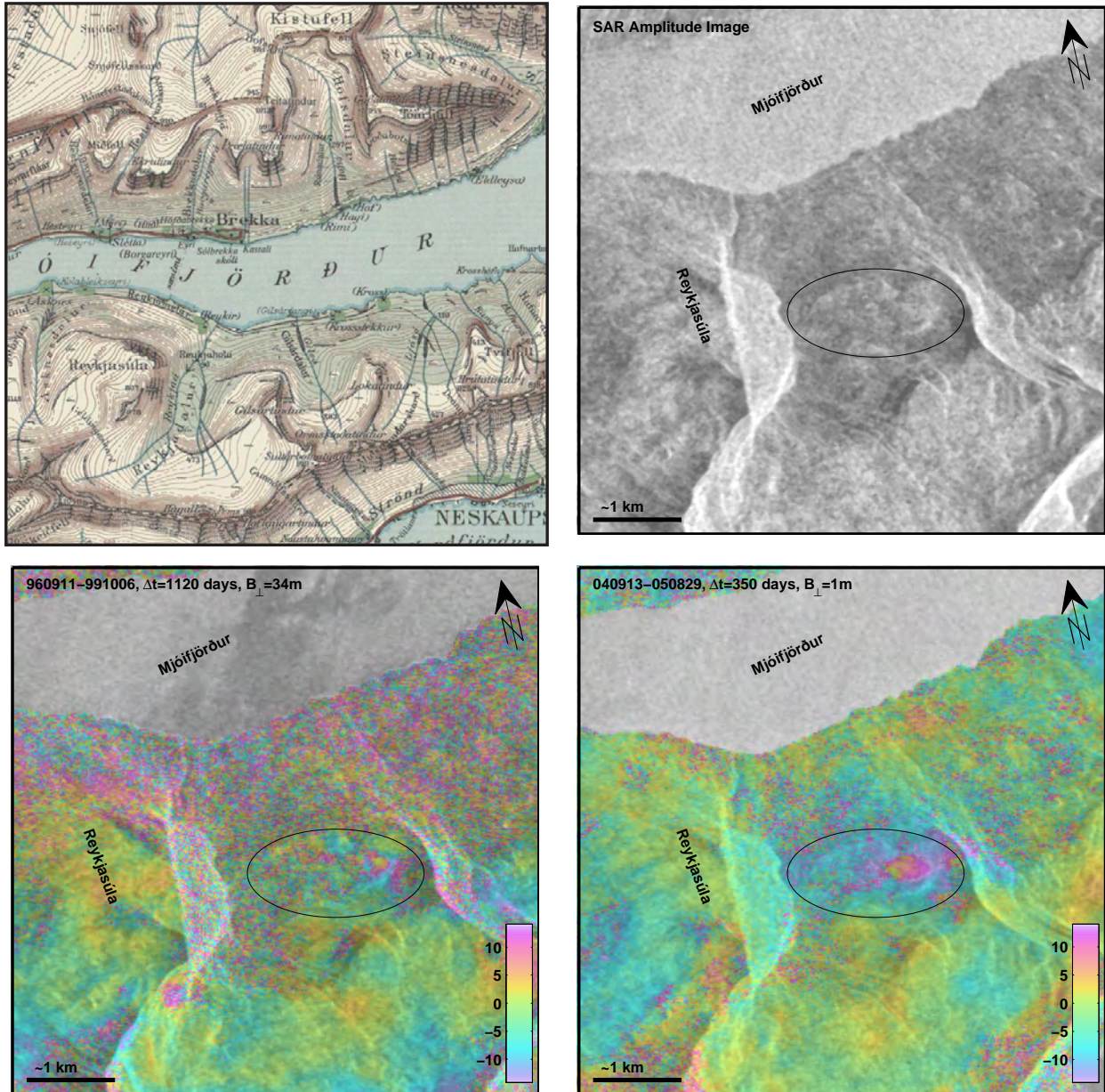


Figure 36. A map from Mjóifjörður and a SAR amplitude image showing part of the area in radar coordinates (top). Two interferograms spanning the time periods 1996-99 (bottom left) and 2004-05 (bottom right) show a small amount of deformation in Reykjadalur valley, which is on the south side of Mjóifjörður. ©NLSI and ©ESA.

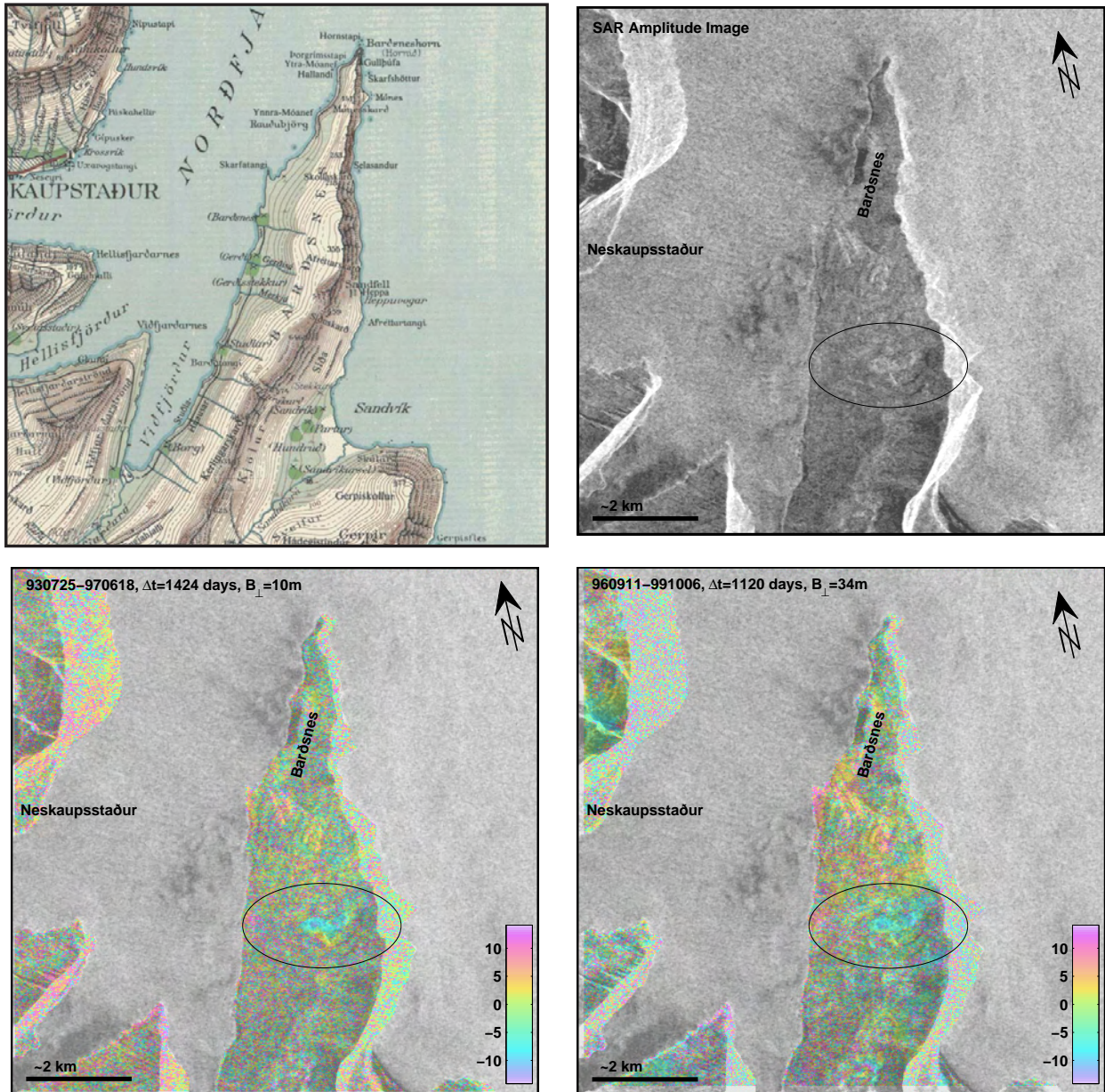


Figure 37. A map and a SAR amplitude image of the Barðsnes Peninsula (top). Two interferograms spanning 1993-1997 (bottom left) and 1996-1999 (bottom right) show possible deformation signals. ©NLSI and ©ESA.

lives on this peninsula anymore, but a few farms were once inhabited on the west side of the peninsula and in Sandvík on the eastern side. A minor but consistent signal is observed on Barðsnes in at least two longer-term radar interferograms, spanning 1993-7 and 1996-9 (Figure 37). The amplitude of the signal in both cases is small (<1 cm) but the shape and location of the area is exactly the same, which implies that this is a real signal. The affected area is 3-400 m wide and seems to be located above an abandoned farm named Gerðisstekkur.

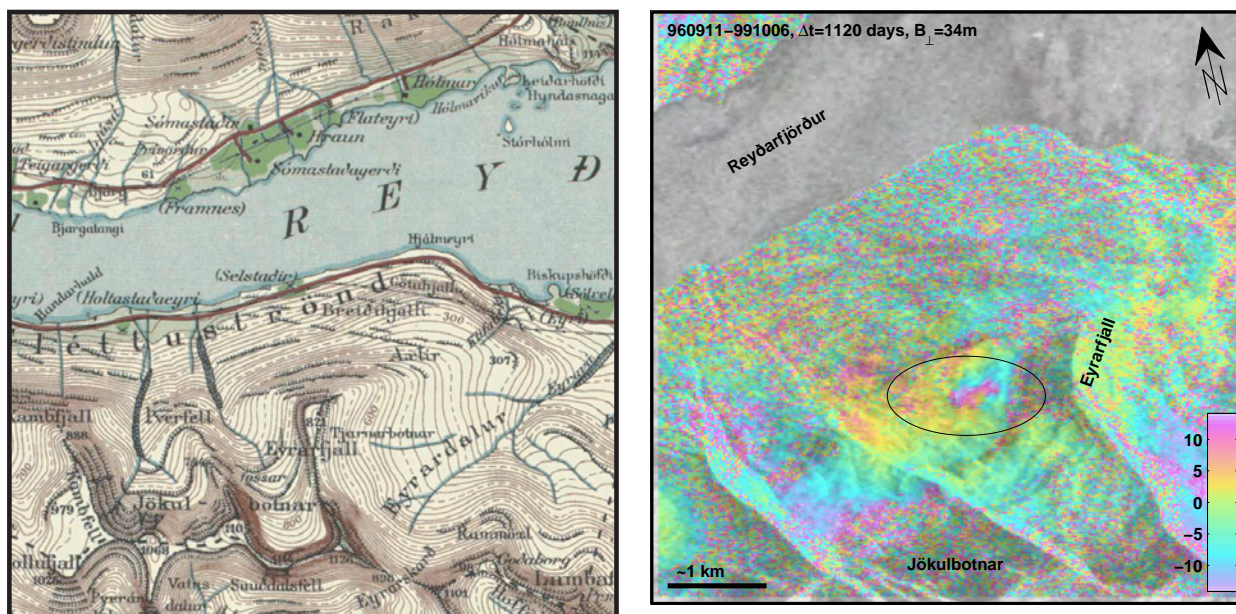


Figure 38. A map and an interferogram spanning 1996-99 of Jökulbotnar in Reyðarfjörður. ©NLSI and ©ESA.

4.4.4 Jökulbotnar in Reyðarfjörður

Jökulbotnar are two small hanging valleys above the Sléttuströnd coast, on the south side of Reyðarfjörður (Figure 38). The mountains to the south of these valleys are over 1100 m high. One interferogram exhibits a small deformation-like signal in the eastern Jökulbotnar valley, just west of the Eyrarfjall mountain. The interferogram spans three years from September 1996 to October 1999 and shows better correlation at high altitudes than most other interferograms, indicating near snow-free conditions at the time of the two acquisitions. This may explain why this deformation signal is only seen in one interferogram, as the deforming area is relatively high at 5-600 m above sea-level. However, as it is small in amplitude and aerial extent, and because it is only seen in one interferogram, the observed displacements are here categorized as speculative.

4.4.5 Eyvindarárdalur

Eyvindarárdalur is a valley about 10 km southeast of the town of Egilsstaðir. The road to Mjóifjörður runs along this valley. The valley floor is 1-200 m above sea level and it is surrounded by mountains that are 800-1000 m high. Several interferograms show deformation at a localized area on the southwest facing slope of the valley, between the rivers Ýtri-Grjótá and Innri-Grjótá (Figures 39). The observed deformation is usually small and only amounts to 1-2 cm, but it is consistently LOS range increase and consistently at the same location in the interferograms, which indicates that the signals represent real ground displacement. LOS range increase in Eyvindarárdalur is detected in several interferograms that span various different time periods during 1995-1999 but no deformation is observed at this location in 2004-2005 (Table 1).

4.4.6 Suðurdalur

Suðurdalur is a tributary valley to the larger Fljótsdalur valley southwest of Egilsstaðir town. The valley floor is flat and only at about 30 m above sea level, but surrounded by steep sides that reach 600-700 m. To the east are Gerðisbjarg and Víðivallaháls and to the west is Múli that divides Suðurdalur and Fljótsdalur valleys (Figure 40). Deformation is observed on the southeastern slopes of Suðurdalur in more than one interferogram, e.g. in a 6-month interferogram from 1998 (Figure 40). The deformation appears to be above an abandoned farm named Klúka.

Jónsson [1976] documented a landslide above the Klúka farm which is called Urðir and with a source from an area named Sóleyjarbotnar. Again, the exact location of the Urðir landslide is not clear because of the lack of maps.

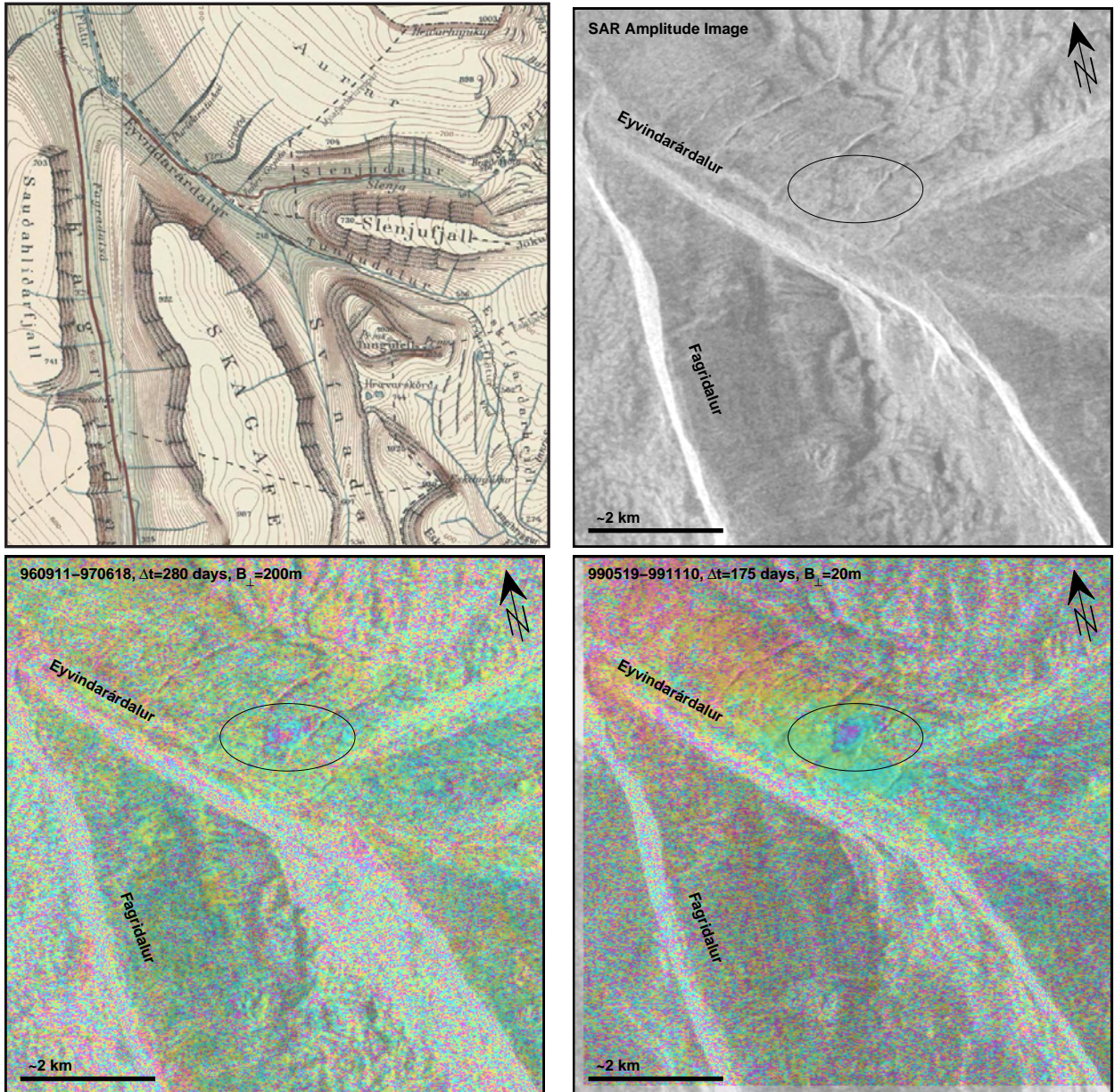


Figure 39. A map and a SAR amplitude image of Eyvindarárdalur (top). A 9-month interferogram from 11 September 1996 to 18 June 1997 a 6-month interferogram from 1999 show deformation in Eyvindarárdalur (bottom). ©NLSI and ©ESA.

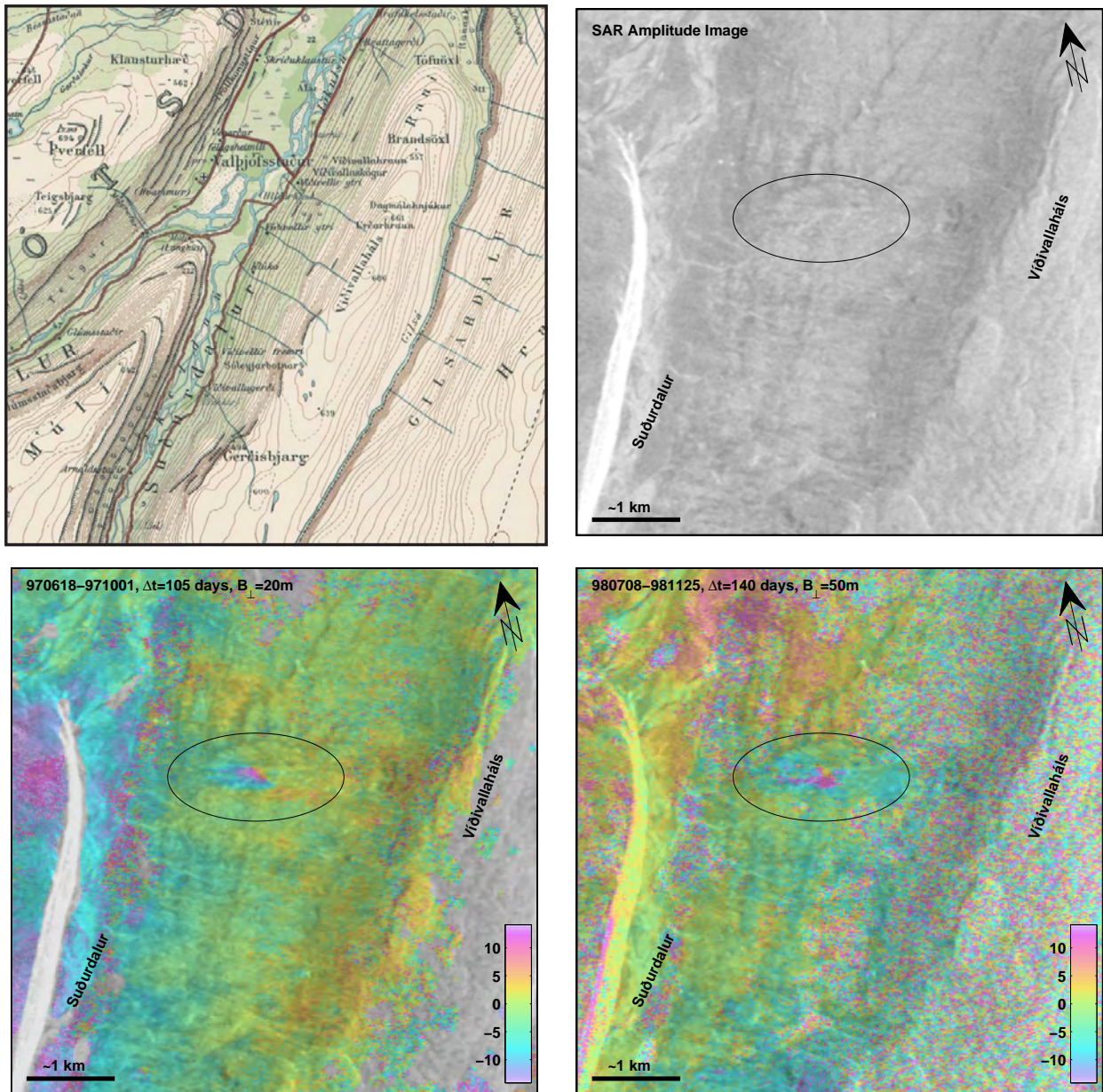


Figure 40. A map and a SAR amplitude image of Suðurdalur valley, a tributary valley to Fljótsdalur valley (top). Two interferograms from 1997 and 1998 show localized deformation on the east side of the valley (bottom). ©NLSI and ©ESA.

4.5 Detected Deformation in Ascending Interferograms

In this section I describe where displacements were detected in data from ascending satellite orbits. No suitable ascending data exists of this area from the ERS-1/2 satellites, so nearly the only available data comes from Envisat, following my request for ascending acquisitions in 2004-2005.

4.5.1 Loðmundarfjörður

Loðmundarfjörður is one of the Eastern Fjords and used to be a small farming community, but no permanent settlement has been in this fjord since 1973. In Loðmundarfjörður is one of the largest landslides in Iceland, which is usually called Loðmundarskriður or Stakkahlíðarhraun (Figure 41). *Jónsson* [1976] describes this landslide and its extension in detail. He states that it comes from the Flatafjall and Bungufell mountains and extends southwards to the fjord bottom, bounded to the west by the slopes of Karlfell mountain. It even appears to extend all the way across the fjord valley to the slopes on the southern side. He estimates that the landslides covers an area of 7-8 km². This landslide appears young and is probably 600-1600 years old, based on information from tephra layers and radiocarbon dating [*Jónsson*, 1976].

We detect clear signs of displacement in Loðmundarfjörður in one-year interferograms spanning 2004-2005 (Figure 41). The area that is moving is extensive, over 1 km wide, and during this year the maximum displacement is about 3 cm. The detected movement, however, does not take place on the large landslide described by *Jónsson* [1976], but on the eastern slopes of Karlfell mountain, under its high cliffs, somewhat above the Hrauná river (Figure 41), and appears to coincide with a location of an older landslide [*Hjartarson*, 1997]. The well known Loðmundarskriður landslide, on the other hand, shows no signs of any displacement during this time period. This is very well seen in the interferogram spanning 4 July 2004 to 24 July 2005 that shows coherent and constant phase values on the entire landslide, clearly demonstrating that it did not move during this time period.

We can not resolve precisely when the movement under Karlfell mountain took place. No displacement is detected in 1-month interferograms from summers of 2004 and 2005, but it is seen in all interferograms that span the time from summer 2004 to summer 2005 (Table 2 and Figures 41-42). Therefore, the movement was either slow and steady, i.e. too slow to be detected in the 1-month interferograms, or it was sudden and took place sometime between 12 September 2004 and 15 May 2005.

4.5.2 Surtstaðatunga in Kaldárgil, Jökulsárhlíð

Kaldárgil is small valley that extends to the southwest from the Jökulsárhlíð area in East Iceland (Figure 43). No farms are in this valley as it is very narrow and is mostly at elevations above 300 m. To the northwest of the valley are several gullies, i.e. Merargil, Litlaþvergil, and Ásdalur. Small deformation signals are observed in several interferograms in the area

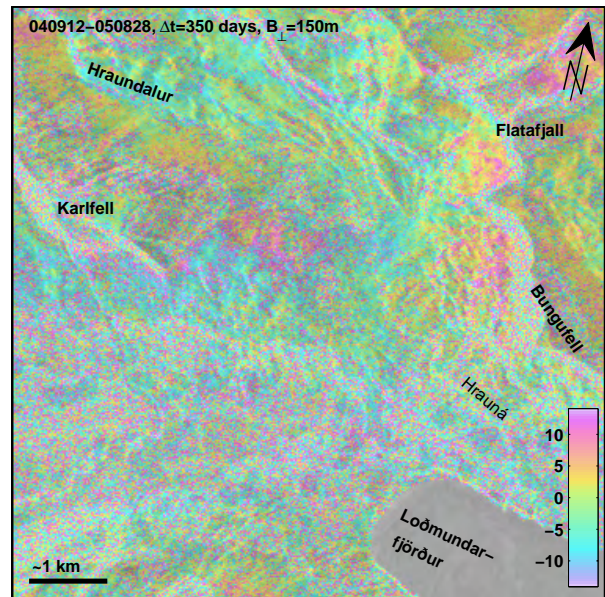
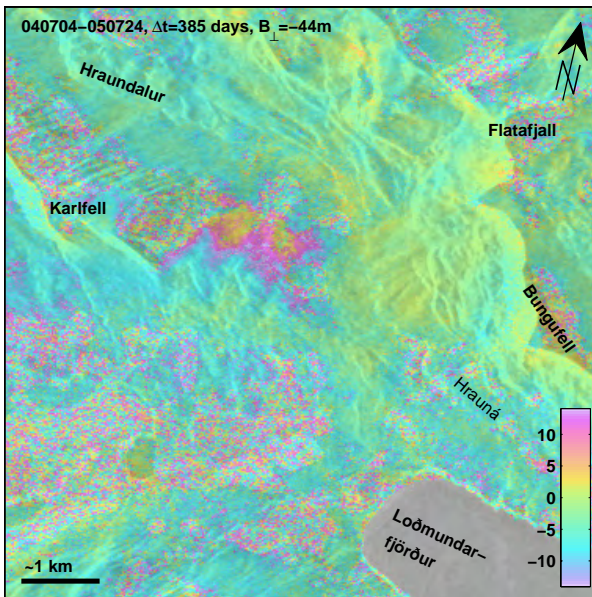
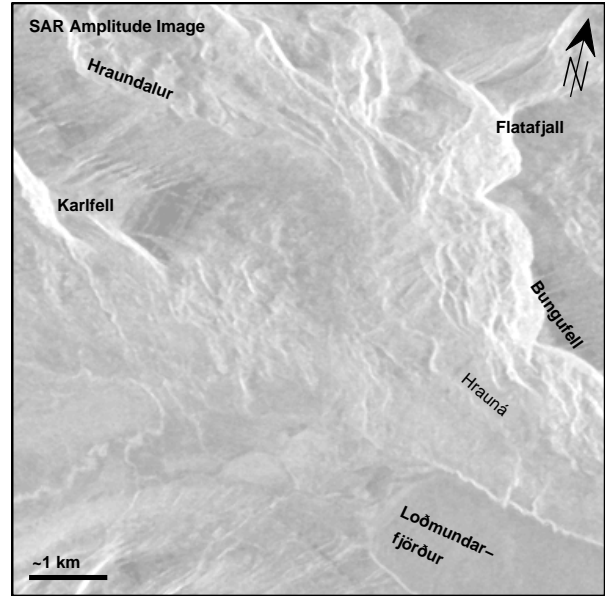
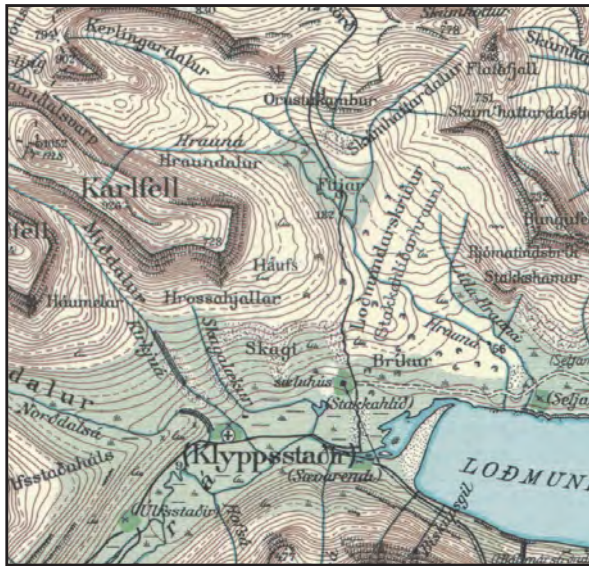


Figure 41. A map of Loðmundarfjörður and an SAR amplitude image in radar coordinates, showing the main geographical features (top). Two 1-year interferograms showing clear displacement east of Karlfell mountain (bottom). ©NLSI and ©ESA.

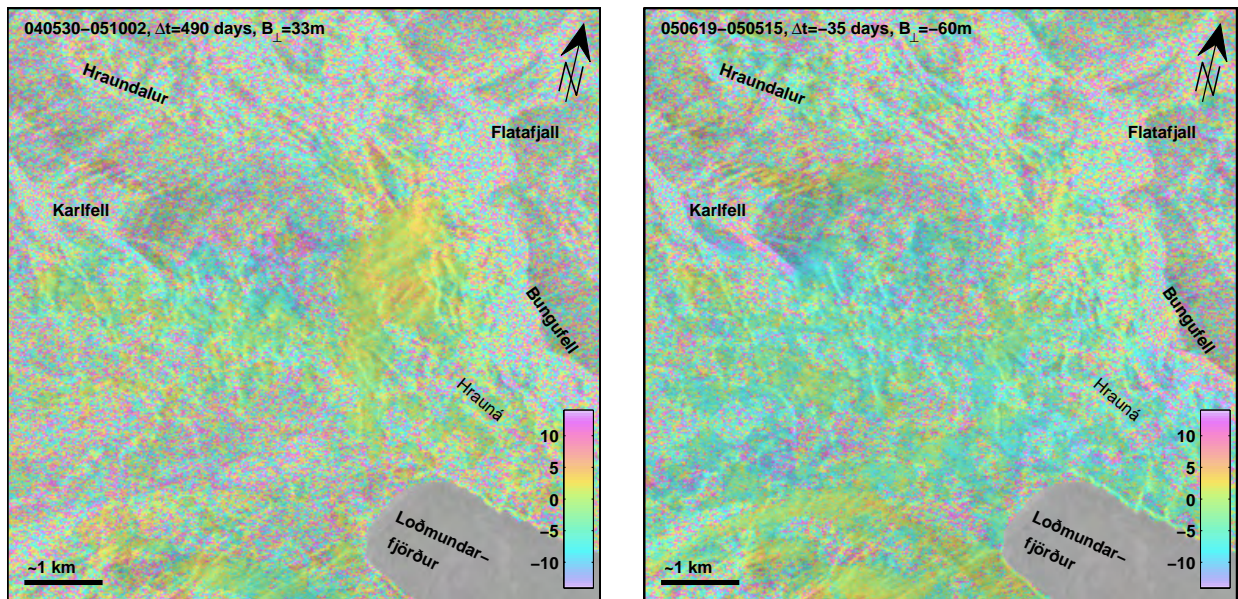


Figure 42. *Two interferograms from Loðmundarfjörður. The 16-month interferogram (left) is noisy, but indicates similar displacement pattern as observed in Figure 41, but the 35-day interferogram (right) has no observable deformation. ©ESA.*

between the Merargil and Litlaþvergil gullies, which is called Surtsstaðatunga. Two 35-day interferograms from 2004 show a small localized deformation on the southwestern slopes of the Litlaþvergil gully (Figure 44). The quality of these interferograms is relatively good and they are here displayed unfiltered. The interferograms share the same slave image and one might think that this signal is related to some artefact in that image. However, although the signals is similar, the phase values in the latter image are multiplied by -1 (because the slave image date is earlier than the date of the master image), so the two interferograms indicate uniform time progression of this signal. Blowups of these signals show that they are indeed very similar and are co-located (Figure 46). The area that is moving is only about 200 m wide and has sharp boundaries at all sides except below it to the northeast. The maximum LOS displacement is around 2 cm and it occurs on the upper portion of this localized area in both cases. Comparison with a 35-day interferogram from early summer 2005 indicates that no movement took place at this location during that time.

A one-year interferogram spanning 4 July 2004 to 24 July 2005 is decorrelated on the slopes in Litlaþvergil gully, but this interferogram exhibits a small moving area at another location in the Surtsstaðatunga area (Figure 45). This signal is not an artifact, as it can be seen in the other one-year interferograms of the area. The sense motion is away from the satellite (i.e. downslope movement) and the magnitude is just less than 1 fringe, or about 2 cm.

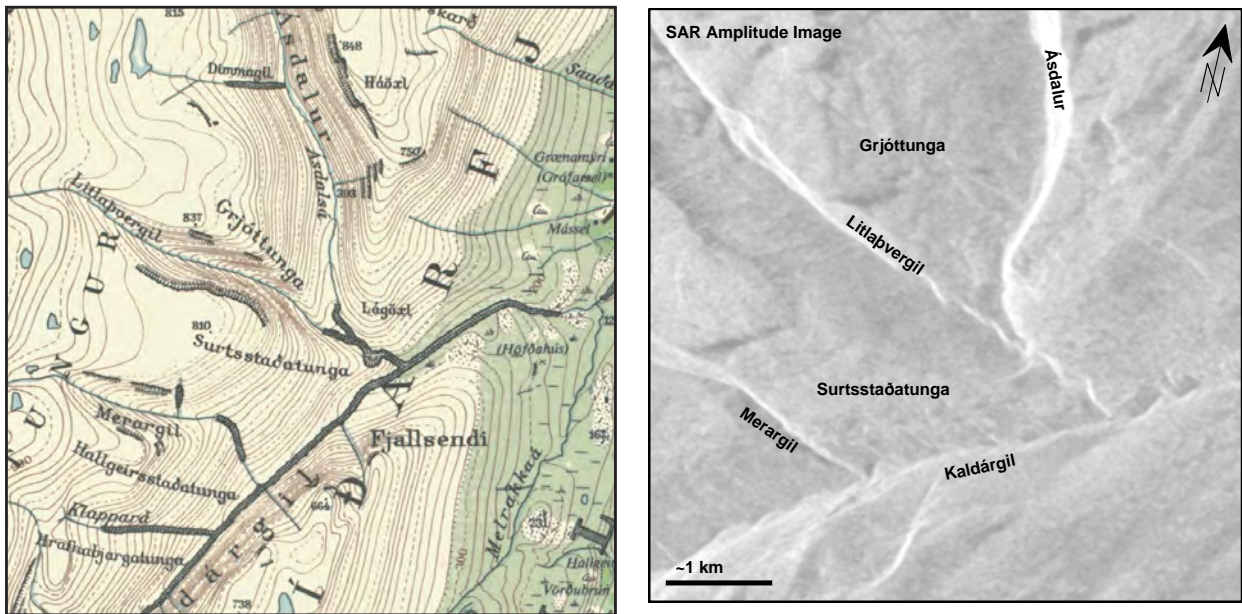


Figure 43. A map of Kaldárgil valley in Jökulsárhlíð and a SAR amplitude image in radar coordinates of the same area with labels to identify the main geographical features. ©NLSI and ©ESA.

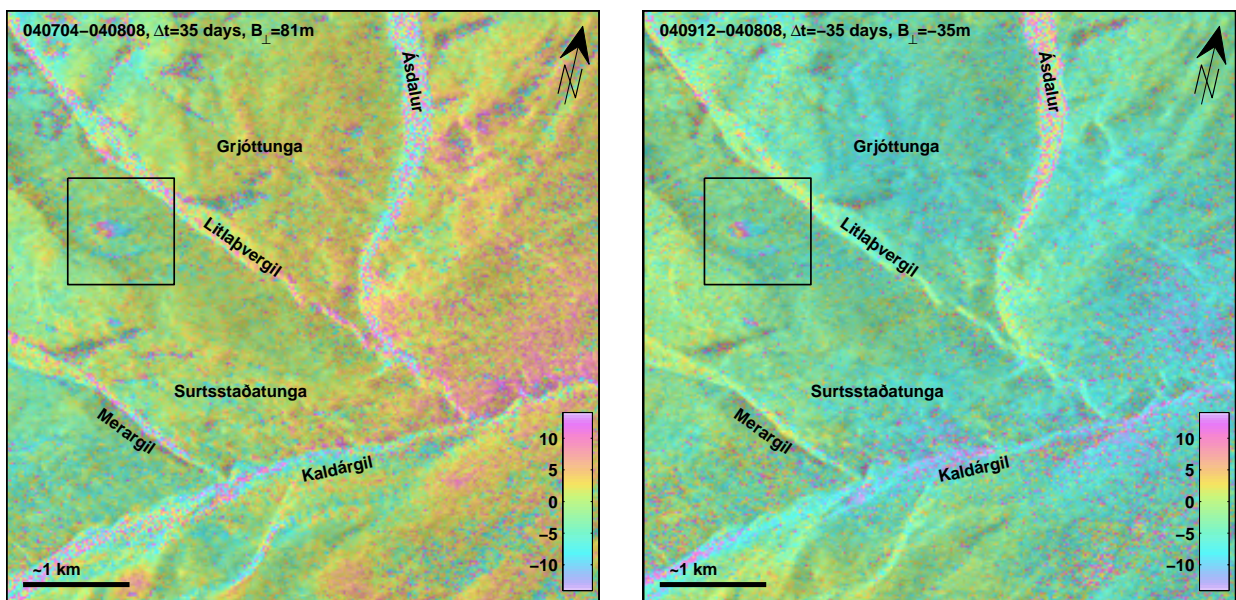


Figure 44. Two interferograms from Kaldárgil in Jökulsárhlíð each spanning 35 days in 2004. Both show a clear localized movement at the same location in the gully of Litlabergil. ©ESA.

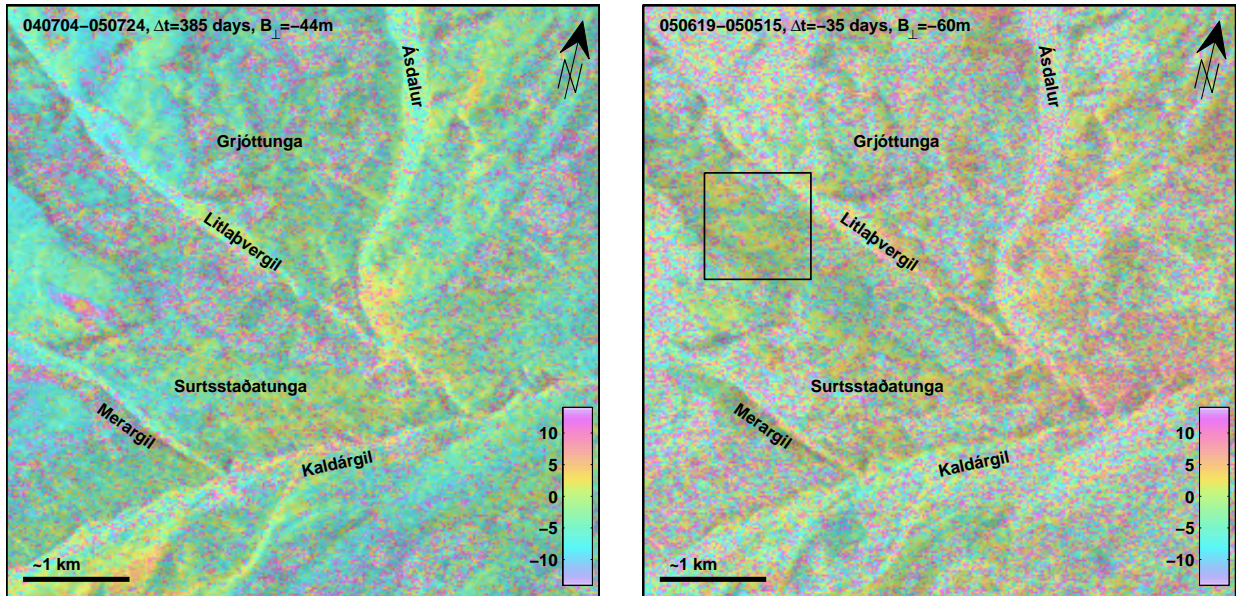


Figure 45. Two interferograms from Kaldárgil, one spanning about one year from July 2004 to July 2005 (left) and the other 35 days in May-June 2005 (right). The one-year interferogram indicates localized movement in Surtssstaðatunga, but at a different location than in the interferograms in Figure 44. ©ESA.

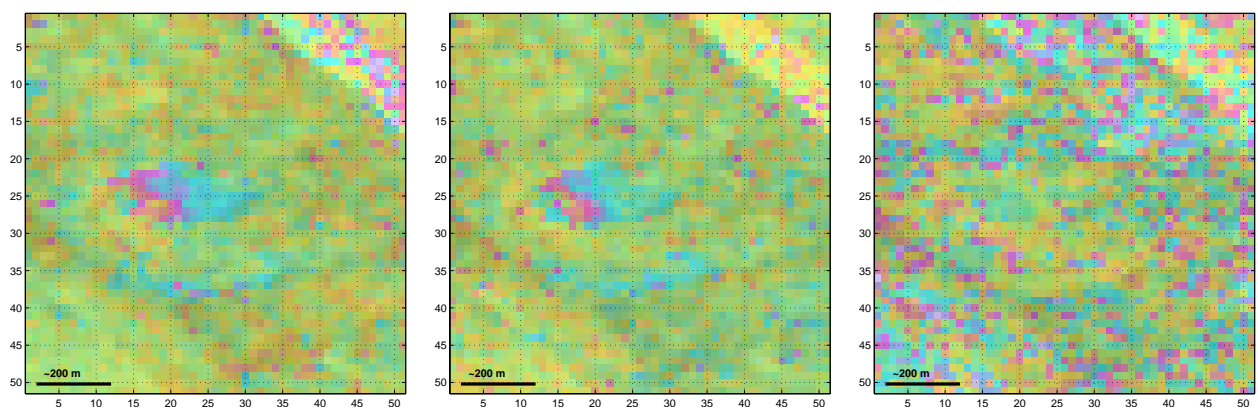


Figure 46. Blowups of the three one-month interferograms in Figures 44 and 45 showing the southwestern slopes of Litlabergil gully. ©ESA.

4.5.3 Þingmúli in Skriðdalur

In Skriðdalur valley, south of Egilsstaðir town, is a ridge called Þingmúli that divides the valley into two tributary valleys, Norðurdalur and Suðurdalur (Figure 47). On the eastern slopes of the ridge, close to its northern terminus, is an old landslide called Múlastekkshraun [Jónsson, 1976]. This large landslide extends from high on the ridge all the way down to the valley river and an abandoned farm called Múlastekkur is located on top of it near the river. The eastern slopes of the ridge are well imaged by ascending radars while the steep western slopes are lost in layovers. This location is rather noisy in one-year interferograms, but an anomaly was detected in one of the interferograms and the location appears to correspond well with the documented Múlastekkshraun landslide (Figure 47). The interferogram shows about 2 cm LOS displacement away from the satellite indicating downslope movement and the pattern seems to suggest movement of two separate tongues, although decorrelation makes it difficult to point out details of the movement pattern. As the interferogram exhibits a relatively low coherence at this location and as movement here was not detected in other interferograms, mostly because of their higher noise level, I classify this movement as somewhat speculative. However, its co-location with the old landslide deposits is encouraging.

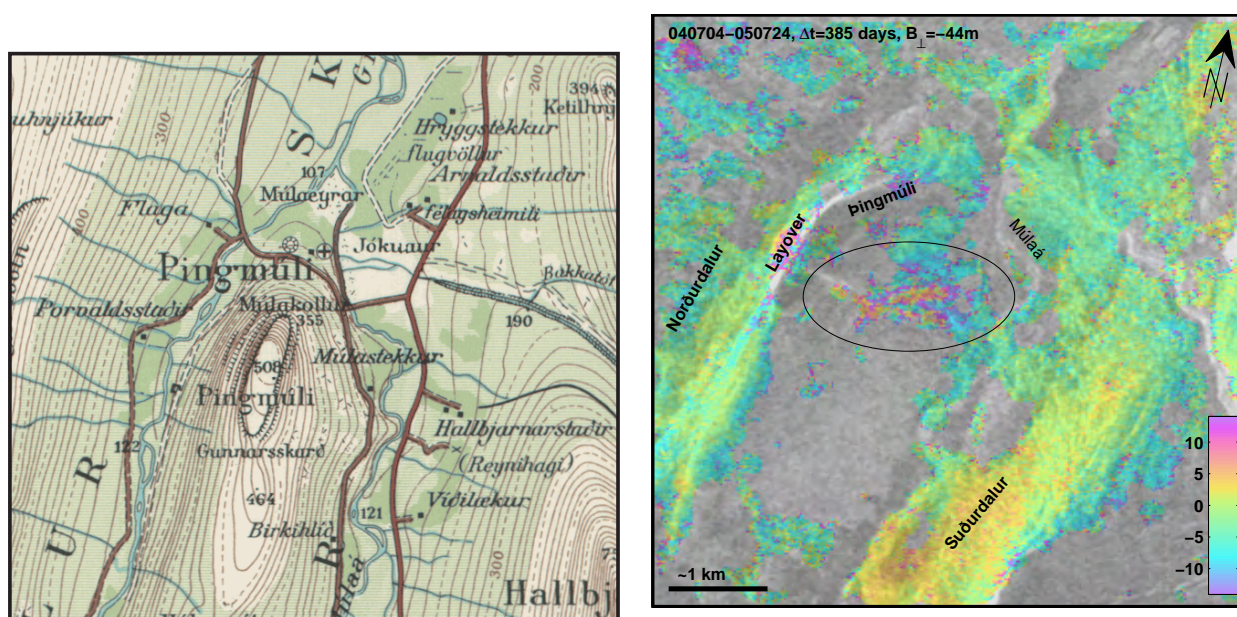


Figure 47. A map and a one-year interferogram showing possible deformation on eastern slopes of the Þingmúli ridge. ©NLSI and ©ESA.

4.5.4 Lambadalur and Beinageitarfjall

Deformation in Lambadalur valley in Borgarfjörður was already discussed in Section 4.4.1, where I described observed movement in a four-year descending interferogram (1993-7) that corresponds with the location of Ytri-Þverhryggir landslide. Here in a one-year ascending interferogram from 2004-5, deformation in this valley is again observed and now at two locations (Figure 48). First is a subtle signal on the western side of the valley, near its northeastern end, which appears to be at the same location as the deformation detected in the four-year interferogram (Figure 35). However, the more prominent deformation signal in the 2004-5 interferogram is further south and also the western side of the valley. The location of this one-fringe signal seems to correspond to another documented old landslide that is called Innri-Þverhryggir [Jónsson, 1976]. Despite the interferogram decorrelation at this location, the deformed area is relatively large or almost 1 km broad.

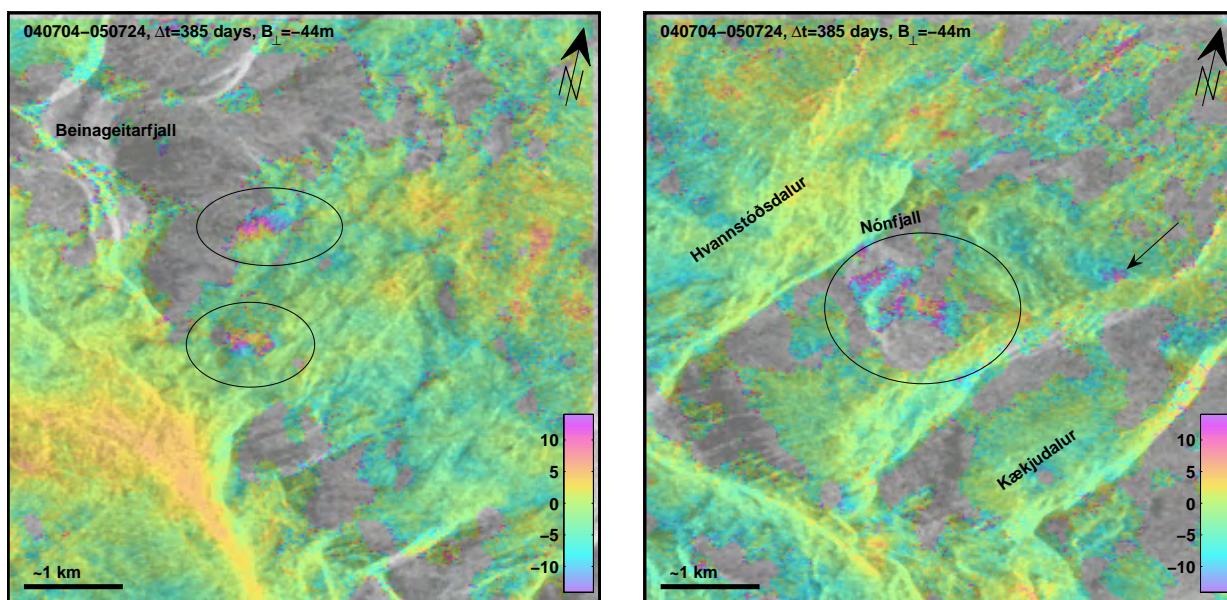


Figure 48. *Two locations in a one-year interferogram showing two small areas near Beinageitarfjall mountain (left) and another two in Lambadalur valley (right). The Lambadalur signals appear to correspond with the documented Innri- and Ytri-Þverhryggir landslides. ©ESA.*

The same interferogram indicates some ground movement in the nearby Hvannstöðsdalur, just under the Beinageitarfjall mountain. These signals are only observed in this interferogram and are here classified as speculative, although both indicate downslope movement. Jónsson [1976] documents one old landslide in Hvannstöðsdalur valley but that landslide is not close to where these two signals are observed.

4.5.5 Breiðdalur

Breiðdalur is a large valley in the southern part of the Eastern Fjords that is bounded by mountains that reach over 1000 m on both sides. A possible deformation signal is observed on the southern side of the innermost part of the valley in a 35-day interferogram from 2004 (Figure 49). The quality of the interferogram at this location is relatively good allowing to detect small anomalies in the phase. The subtle signal is near the Innri-Ljósá river, high on the southern slopes, and its maximum amplitude corresponds to about 1.5 cm downslope LOS displacement. Higher on the slope the signal is much smaller, but the outline of the displaced area can still be traced here, owing to the good quality of the interferogram. This signal is only observed in this 35-day interferogram, but most other interferograms were decorrelated at this location. However, in a noisy 1-year interferogram there is a patch of coherent phase that appears to have been displaced and its location corresponds with the upper part of the area seen moving in the 35-day interferogram (Figure 49). There is another location of possible movement seen in the 35-day interferogram (see arrow in Figure 49), although this signal is somewhat speculative due to the noisy surrounding and its limited spatial extent.

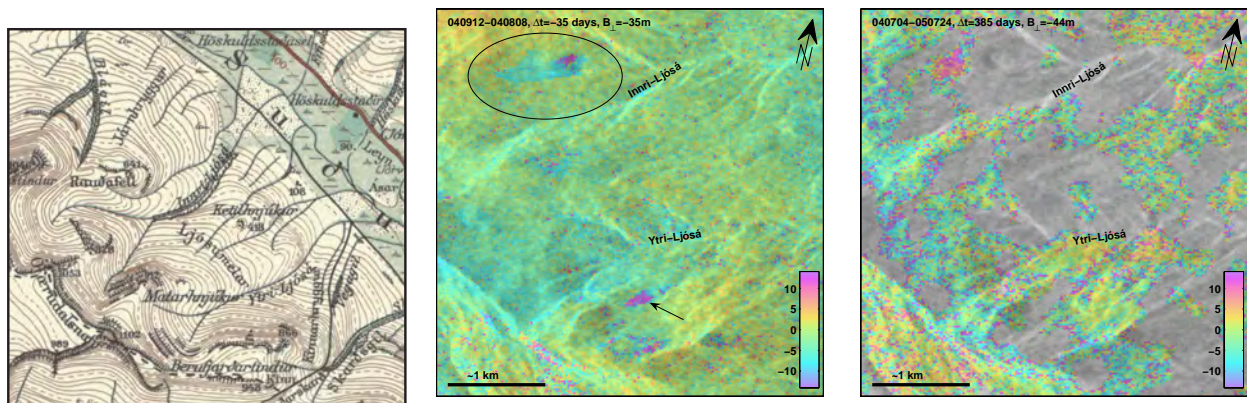


Figure 49. A map of a portion of the Breiðdalur valley and two interferograms showing a sign of subtle ground displacement. ©NLSI and ©ESA.

5 Discussion

The detection of displacements in InSAR data of the Þófi landslide up to two years before cracks were discovered in the field demonstrates the monitoring potential of this technique in eastern Iceland. Deformation on this landslide can be seen in InSAR data from 1998 and 1999, i.e. well before fresh surface cracks were discovered in the field in 2000. GPS measurements show displacement rates of up to 33 cm/year during 2001-2, but unfortunately, no suitable ERS radar data exist from this time period to compare to the GPS measurements, because ERS-2 started malfunctioning in early 2001 and data after that time are of limited use for radar interferometry. The Envisat InSAR data and GPS observations from 2004-2005 both show that little or no displacements occurred on the Þófi landslide during this time period. While the Þófi results may demonstrate the monitoring potential of InSAR, the Urðarbotn observations expose one of its limitations, i.e. that InSAR can not be used to image landslides that are small in extent (<200 m), which is probably the case for many unstable slopes in Iceland. However, the Þófi case and the discovery of a number of other sites that are actively creeping show that this technique can be useful in monitoring landslides at many locations and in detecting sites where landslide creep is active.

In this project I concentrated on ERS-1 and ERS-2 data from 1993-1999, which all are from a single frame on descending track 424, and on data from recent ascending and descending Envisat acquisitions in 2004-2005. More ERS data from track 424 exist that could be used for a more complete InSAR analysis for the time period 1992-1999 and some of the data from after 2001 may also prove to be usable. In addition, data from descending tracks 195 and 152 were not used in this project (Figure 6), but they can potentially provide additional information. Furthermore, data of this area from other satellites exist, mainly from Radarsat-1 and JERS-1, but the data availability in the archives of these satellites was not investigated. The Canadian Radarsat-1 satellite was launched in 1995 and is still in orbit. It operates on a similar wavelength as the European ERS and Envisat satellites and does probably not provide much extra information about the landslide deformation during time periods when good ERS and Envisat data exist. However, there may be useful data from 2000-2004 in the Radarsat-1 archives and there may exist more ascending data than in the ERS/Envisat archives. The Japanese JERS-1 satellite was in orbit during 1992-1998 and operated on L-band wavelength of 23.5 cm, which is much longer than the C-band wavelength (5.6 cm) used by the other satellites. The advantage of this longer wavelength is that temporal decorrelation due to surface changes and snow is less prominent, so longer-term interferograms of eastern Iceland using data from this satellite, i.e. spanning several years, would likely prove to be useful. However, JERS-1 radar data of Iceland have never been actively used for interferometry, despite undoubtedly rich data archives.

The results from Seyðisfjörður and Vopnafjörður show that movement of landslides in eastern Iceland is episodic, with periods where they do not move at all, while during other periods they may move by many cm. This episodic behavior demonstrates the importance of continuous monitoring of Icelandic landslides, as slow-moving landslides may suddenly accelerate or dormant landslides may be reactivated. Such monitoring is possible to certain

extent with the current radar satellites such as Envisat and Radarsat-1, i.e. in a similar way as was done within this project using 2004-2005 Envisat data. However, it is important to realize that data above many regions are not routinely acquired unless users request data acquisitions.

Along with Envisat and its successor (Sentinel-1, anticipated launch in 2011) there are other recent and forthcoming radar missions such as the Japanese ALOS mission, the Canadian Radarsat-2 mission, and the German TerraSAR-X mission. Data from all these missions can potentially be used to measure and monitor landslide motion in Iceland in the future. The ALOS satellite operates on a similarly long wavelength as the older JERS-1 satellite, which can be beneficial to study motion over multiple years. The Radarsat-2 mission is similar to the Radarsat-1 and ERS/Envisat missions in many ways and will operate on C-band wavelength like these satellites. The TerraSAR-X satellite will use a shorter X-band wavelength (3.1 cm) which poses a challenge for interferometry because of temporal decorrelation. However, this satellite can be operated in modes that have higher resolution than the other satellites and it will have shorter repeat time, so it can potentially be used to monitor small fast-moving landslides.

The results of this project show that InSAR is a useful technique to both search for and monitor landslides in eastern Iceland that are larger than 1-200 m in aerial extent. Radar data acquisitions of eastern Iceland are neither regular nor frequent and the 2004-2005 data exist only because of my request to European Space Agency. Therefore, a monitoring policy and an observation plan for eastern Iceland is needed to secure future data acquisitions.

6 Conclusions

In this project I processed 44 radar interferograms to investigate the capabilities of this technique for landslide-creep detection and monitoring in eastern Iceland by studying previously known landslides and by surveying large areas in search for active landslide creep. The radar data that I used were ERS data from 1993-1999 and Envisat data from 2004-2005. The conclusions of the project can be summarized by the following points:

1. The coherence of C-band radar interferometry is generally good enough for single- and multi-month observations during summers in eastern Iceland. Inter-annual and multi-year observations can also provide useful information on larger landslides, but not on the smaller landslides as some filtering is generally required, which prevents small-scale analysis. The main InSAR measurement problems in eastern Iceland are first, the lack of a digital elevation model of adequate quality, which prevents analysis of long-baseline interferograms, and second, the frequent high-elevation snow cover, which often limits the use of spring and autumn images.
2. Deformation was detected on the known Þófi landslide near Seyðisfjörður in InSAR data from 2 years before 2000, when surface cracks were discovered in the field. Interferograms spanning several months in summers of 1998 and 1999 show 2-3 cm of LOS displacement that may represent surface parallel velocities of 7-10 cm/year. This rate is lower than the maximum observed GPS velocities during 2001-2002 (up to 33 cm/year), but no suitable InSAR data exist from that time period to compare with the GPS data. No deformation was detected in InSAR images 1995-1997 or 2004-2005 on the Þófi landslide, indicating that the landslide creeps episodically.
3. Radar imaging of the Urðarbotn landslide above Neskaupstaður town is only possible from ascending orbits and almost no ascending data exist in the European Space Agency's archives. However, newly collected ascending radar data from 2004-5 do not show any movement of the landslide, either because it did not creep during this time period, or that the spatial extent of the moving area was only very small.
4. More than 10 locations of previously unknown landslide creep were discovered in eastern Iceland in the processed interferograms. In some cases the locations of observed creep corresponded to landslides that have been geomorphologically documented. The most prominent landslide motion was detected in Vopnafjörður and in Loðmundarfjörður. The Vopnafjörður landslide creep shows variations in both displacement rate and aerial extent during the observation period, which further demonstrates the episodic behavior of landslides in eastern Iceland.

Acknowledgements

I thank Kristján Ágústsson at the Icelandic Meteorological Office (IMO) for his support and discussions throughout this project. I also thank the various scientists who attended several project meetings at the IMO for their comments and advise. This project was supported by the Icelandic Avalanche Fund and all satellite data were provided by the European Space Agency through Category-1 project #2424.

References

- Hanssen, R. *Radar interferometry - data interpretation and error analysis*, Kluwer Academic Press, Dordrecht, The Netherlands, 308 pp, 2001.
- Hjartarson, Á., Loðmundarskriður (in Icelandic), *Náttúrufræðingurinn*, 67, 97-103, 1997.
- Jóhannesson, T., and Th. Arnalds, Accidents and economic damage due to snow avalanches and landslides in Iceland, *Jökull*, 50, 81-94, 2001.
- Jensen, E. H., *Hætta á skyndilegu jarðskriði úr brún Þófans á Seyðifirði*, IMO document ÚR-EHJ-2001-01, 5pp, 2001.
- Jensen, E. H., and T. Jóhannesson, *Assessment of landslide risk in Seyðisfjörður, eastern Iceland: first measurement results (in Icelandic)*, IMO document ÚR-EHJ-2002-03, 10pp, 2002.
- Jensen, E. H., and T. Sönsér, *Process oriented landslide hazard assessment for the south side of Seyðisfjörður*, IMO report VÍ-ÚR02, 45pp, 2002.
- Jensen, E. H., and A. Hjartarson, *Field investigation of the 27 June 2002, Neskaupstaður landslide (in Icelandic)*, IMO document ÚR-EHJ-2002-02, 11pp, 2002.
- Jónsson, Ó., *Landslides (in Icelandic)*, Ræktunarfélag Norðurlands, Akureyri, 623pp, 1976.
- Jónsson, S., and K. Ágústsson, Landslides in Iceland studied using SAR interferometry, *Proc. to the Envisat Conference*, European Space Agency, Salzburg, 2004.
- Jónsson, S., P. Segall, R. Pedersen, and G. Björnsson, Post-earthquake ground movements correlated to pore-pressure transients, *Nature*, 424, 179-183, 2003.
- Massonnet, D., and K. L. Feigl, Radar interferometry and its application to changes in the earth's surface, *Rev. Geophys.*, 34, 441-500, 1998.
- Pedersen, R., S. Jónsson, T. Árnadóttir, F. Sigmundsson, and K. Feigl, Fault slip distribution of two June 2000 Mw6.5 earthquakes in south Iceland estimated from joint inversion of InSAR and GPS measurements, *Earth and Planet. Sci. Lett.*, 213, 487-502, 2003.
- Rosen, P. A., S. Henley, G. Peltzer, and M. Simons, Update repeat orbit interferometry package released, *EOS Trans. AGU*, 85, p47, 2004.
- Scharroo, R., and P. N. A. M. Visser, Precise orbit determination and gravity field improvement for the ERS satellites, *J. Geophys. Res.*, 103, C4, 8113-8127, 1998.
- Sigmundsson, F., H. Vadon, and D. Massonnet, Readjustment of the Krafla spreading segment to crustal rifting measured by satellite radar interferometry, *Geophys. Res. Lett.*, 24, 1843-1846, 1997.
- Sæmundsson, Þ., and H. G. Pétursson, *Evaluation of the debris-flow and rock-fall hazard near the town of Seyðisfjörður (in Icelandic)*, IMO report VÍ-99033, 1999a.
- Sæmundsson, Þ., and H. G. Pétursson, *Debris Flow Hazard in Neskaupstaður (in Icelandic)*, IMO Document VÍ-G99026-ÚR16, 1999b.

- Vadon H., and F. Sigmundsson, Crustal deformation from 1992-1995 at the Mid-Atlantic Ridge, SW Iceland, mapped by satellite radar interferometry, *Science*, *275*, 193-197, 1997.
- Zebker, H. A., and J. Villasenor, Decorrelation in interferometric radar echoes, *IEEE Geosci. Remote Sensing*, *30*, 950-959, 1992.
- Zebker, H. A., and Y. Lu, Phase unwrapping algorithms for radar interferometry: residue-cut, least-squares, and synthesis algorithms, *J. Opt. Soc. Am.*, *15*, 586-598, 1998.

A Appendix

A.1 Descending interferograms from ERS-1/2 data 1993-1999

Here I provide information about the different ERS-1/2 differential interferogram and what can be seen in them:

930725-950718

This 2-year interferogram has a baseline of 170 m and has a relatively good correlation considering the time it spans. However, the interferogram is quite noisy, which prevents detailed small-scale inspection, as well as having almost 200 m baseline. The Vopnafjörður landslide is completely decorrelated in this interferogram, in contrast to the slopes just north-east of it, which might mean too much landslide displacement during this 2-year period. The Seyðisfjörður landslide is noisy, but there is no sign of movement there, nor are any other obvious signs of displacement in the whole interferogram.

930725-970618

This 4-year interferogram has almost a zero-perpendicular baseline and it results in a rather good correlation. There is an observable deformation signal in one of the valleys in East-Borgarfjörður. This valley is called Lambadalur. On the west side of valley, below a peak called Rauðkollutindur (Nónfjall), is a signal amounting to 1.5 fringes, representing LOS movement of about 4 cm and the area is about 1 km in diameter. This signal is almost certainly real, as this interferogram has almost zero baseline, and no atmospheric disturbances of this scale can be seen in the entire interferogram. Another likely signal is found on Barðsnes peninsula, above and east of abandoned farm Gerðisstekkur. The signal here amounts to only 1-2 cm of LOS displacement and it has an opposite sign to what is seen in Lambadalur. Another possible, but speculative, localized signals are found above the town of Eskifjörður, just under the peaks of Sauðatindur and Andri. However, it is hard to verify the nature of these signals.

950718-950823

This 35-day interferogram has only about 40 m baseline and is of outstanding quality. The correlation is very good almost everywhere and there is almost no signs of atmospheric disturbances, nor artifacts due to the topographic removal. There is a very clear signal in Vopnafjörður, amounting to some 2-3 fringes, at least, representing at least 6 cm of LOS displacement. There is also a hint of movement further northeast, east of the farm Syðri-Vík, but there the displacement is less than 1.5 cm. Despite the quality of this interferogram, no other deformation signals can be found in Seyðisfjörður or anywhere else in East Iceland.

950718-950926 and 950823-950926

These 70 and 35-day interferograms share the same slave scene and have 90 m and 130 m perpendicular baselines, respectively. The results for these two interferograms are identical. Both show good correlation at low altitudes (<200 m) while higher areas are completely decorrelated, almost certainly due to snow cover on 26 September 1995. The Vopnafjörður landslide is not visible here as it is at higher altitude, but the Seyðisfjörður landslide is visible and there is no detectable movement at this site. No deformation signals are found in these interferograms.

950718-970618

This two 2-year interferogram has a perpendicular baseline of 165 m and the correlation is not too bad. The main landslide in Vopnafjörður looks very noisy and it is hard to draw any conclusions from there in this interferogram. However, there is a small hint of a displacement further northeast in Vopnafjörður, a bit northeast of what was found in interferogram 950718-950823, it amounts to a 1/2 a fringe. The Seyðisfjörður area is also noisy and no clear movement can be detected there in this interferogram. The only other place where there is a hint of deformation is in Eyvindarárdalur, a signal that is better seen in interferogram 960911-970618.

950926-950927, 951031-951101, and 960213-060214

These three 1-day tandem interferograms were initially ordered because of the poor DEM. They have perpendicular baselines of 235 m, 65 m, and 105 m, respectively. The September tandem is of excellent quality, but has almost too many topographic fringes on steep slopes for reliable unwrapping. The October tandem has a shorter baseline and therefore fewer topographical fringes, but it quite decorrelated in places due to changes in snow properties during this one-day time interval the interferogram spans. The February tandem is even poorer than the October interferogram, due to the same snow changes reasons.

950927-970723

This almost two-year interferogram has a small perpendicular baseline of about 50 m, but it is still severely decorrelated. There is no measurement possible in Vopnafjörður and many other places, although the Seyðisfjörður landslide is somewhat correlated, but no movement is detected there in this interferogram. The reason for the decorrelation is probably snow cover on 950927. This is interesting, as the tandem 950926-950927 has a very good correlation, and this means that there was probably snow on the ground during 950926-950927 but the properties of the snow did not change much.

960911-970618

This Interferogram spans nine months and has a rather long perpendicular baseline of 200 m. However, the correlation is fairly good in places. There are clear signs of deformation in Vopnafjörður at two locations, but the interferogram is too noisy to quantify how much deformation there is. A possible deformation signal is seen in Eyvindarárdalur between the Ytri-Grjótá and Innri-Grjótá rivers. This signal amounts to less than one fringe but appears to be real. Another possible deformation signal is found in the Víðivallaháls mountain in Suðurdalur, approximately above the farm of Klúka. This signal is rather narrow and maybe amounts to about 1 fringe.

960911-991006

This three-year interferogram has a baseline of 35 m and has reasonable coherence but strong long-wavelength atmospheric disturbances. The Vopnafjörður landslide is decorrelated, but the surrounding regions areas are not, which probably means that the displacements were too great during these 3-years to measure the movement on this landslide. The "uplift"-signal in Lambadalur in Borgarfjörður is visible in this interferogram, just like in the 930725-970618 image. The patterns are similar, but the signal amplitude is somewhat smaller in this image, so part of the deformation must have taken place before 960911. The Seyðisfjörður landslide and the areas nearby are mostly decorrelated in this long-term interferogram, making a measurement there close to impossible. However, there are number of small localized deformation signals in this image that are not seen in many or any other interferograms and they appear to be 1/2 fringe signals that could correlate with existing old landslides in many places. These places include two subsidence signals on the east side of the valley Fa-gridalur, Eyvindarárdalur (the usual location), Reykjadalur in Mjóifjörður, in Jökulbotnar near Eyrarfjall mountain south of Reyðarfjörður.

970618-971001 (and 970618-970723 and 970723-971001)

This 3.5 month interferogram has a small baseline of only 20 m (the 1-month 970618-970723 and 2-month 970723-971001 have 260 m and 240 m baselines, respectively). The correlation is good everywhere below some 400 m or so (probably due to snow in October), but the interferogram has significant long-wavelength atmospheric artifacts, which can be clearly seen in flat areas like near Héraðsflói Bay. Most of the atmospheric disturbances are from 971001, as they do not appear in the 970618-970723 interferogram. Vopnafjörður has a clear deformation signal in this interferogram and it amounts to three localized lobes of 2 cm LOS displacement each. The pattern looks different than in other interferogram, and this displacement appears to have taken place during 970618-970723 as the 970723-971001 interferogram is almost deformation-free in Vopnafjörður. Again, there is no sign of deformation in Seyðisfjörður, in any of the three interferograms. However, there is again hint of deformation above Klúka farm in Suðurdalur, just like was found in the 960911-970618 interferogram, here also amounting to 1/2 fringe, or so. This does not appear to be related to

the common scene 970618, as the deformation shows the same sign in the two interferograms and the pattern looks different, i.e. it is a bit more extensive in the former time period. Also, this deformation is not seen in 970618-970723, but is again seen in 970723-971001, so it took place during the second part of the summer, in contrast to the Vopnafjörður deformation.

970723-990519

This 80 m baseline interferogram has very little coherence in most places and is of little use.

971001-981021

This 1-year interferogram has a baseline that is only 40 m but it almost completely decorrelated, presumably due to snow-cover on 981021. Only isolated patches near the coast and some inland valleys remain coherent. No measurement is possible in Vopnafjörður nor in Seyðisfjörður due to decorrelation.

980708-981125

This 5-month interferogram has a baseline of 45 m, but it is rather noisy. However, a clear sign of deformation can be seen on the Vopnafjörður landslide, although it is difficult to quantify the deformation. A localized change in phase values can be seen in Seyðisfjörður as well, it is maybe a few hundred meter broad area that seems to correspond with the deformation detected by GPS in Þófi above the factory. Deformation can also be seen above Klúka farm in Suðurdalur.

981021-990519 and 981125-981230

These 210 and 35-day interferograms have 260 m and 5 m baselines, respectively, but both are almost completely decorrelated due to snow. No deformation measurements are therefore possible in these interferograms.

990519-991110 (990414-990519 and 990414-991110)

This 175-day interferogram spans the summer months of 1999 and has a small baseline of only 20 m. However, the correlation is poor in most places, presumably due to snow in November. No measurement is possible in Vopnafjörður due to decorrelation, but there is clear indication of movement on the Seyðisfjörður landslide and the movement is more extensive than in the 980708-981125 interferogram. The area that is moving is about 400 m wide and the movement is about 2-3 cm. Small area is also seen moving in Eyvindarárdalur, at the same location as in interferogram 960911-970618.

A.2 Descending interferograms from Envisat data 2004-2005

Here I provide information about the different Envisat differential interferogram and what can be seen in them:

040531-040705

This 35-day interferogram has a baseline of 320 m and has a good correlation everywhere, except on the highest mountains, probably due to late-spring snow in May. However, the problem is the long baseline that results in a number of artifacts that are introduced due to inaccurate DEM. This limitation hinders any serious deformation analysis of this pair. Running a local analysis and DEM removal of Vopnafjörður improve things only slightly and similar artifacts remain.

040531-040809

This 70-day interferogram has a baseline of 60 m and is of very good quality. The coherence is very good except at the highest elevations. The topographic signal is reasonably well removed leaving a fairly clean differential interferogram. There is a small hint of localized motion on the Vopnafjörður landslide; approximately circular feature, in the upper half of the landslide. The signal is maybe 1/2 fringe or 1-2 cm LOS displacement. The Seyðisfjörður landslide shows no movement and no other area appears to be moving during these two months.

040531-050516

This 1-year interferogram has a baseline of 100 m and has a reasonable degree of correlation at low altitudes, but is clearly affected by snow cover at higher altitudes. There is a clear signal of movement in Vopnafjörður and it looks identical to the signature seen in 040913-050829, but is noisier than in the late summer interferogram. There are no other visible movements.

040705-040809

This 35-day interferogram has a baseline of 260 m and has good correlation almost everywhere. The problem here is also the long baseline, similar to the 040531-040705, which hinders any good analysis.

040809-040913

This 35-day interferogram has a baseline of 710 m, which is way too long for accurate topographic signature removal. Correlation is good at low altitudes, but poor at high altitudes,

probably due to early snow in September.

040809-041122

This 70-day interferogram has a baseline of 65 m and only has some correlation at the lowest altitudes, approximately below 100-200 m. Above this altitude there is no correlation due to winter snow. The decorrelation hinders analysis in Vopnafjörður, but the interferogram is somewhat coherent on the Seyðisfjörður landslide, although no movement is detectable there.

040809-050620

This one-year interferogram has a 165 m baseline and reasonable coherence, especially in the western part of the scene. For some reasons the offset estimation did not work well for the fjords, an unknown problem related to the 050620 scene. Displacement on the Vopnafjörður landslide can clearly be seen and it looks similar as in the clearer 040913-050829 interferogram. No displacement is to be found on the Seyðisfjörður landslide and no other places can be detected. There are small artifacts near Vopnafjörður due to the long baseline.

040809-050516

Also a one-year interferogram with 165 m baseline and very similar to the 040809-050620, but noisier, probably due to snow above ca. 500 m in the slave image. Vopnafjörður landslide is visible like in the other summer-to-summer interferogram, but it is not very clear here.

040913-050829

This one-year interferogram has almost 0 m baseline and exhibits a very good correlation at elevations below 1000 m or so. Displacements are very easily detectable, as the phase is more or less constant across the scene and almost no atmospheric disturbances noticeable. The Vopnafjörður landslide is clear in this image, showing a large area moving above Svínabakkar farm and the displacement exceeds one fringe. There are also small signals to be seen in the neighboring Böðvarsdalur, on the east slopes, but it is disputable. High on the southern side of Mjóifjörður there appears to be a LOS displacement of about 2-3 cm. The pattern is approximately circular and is located in a small valley (Reykjadalur) east of Reykjasúla mountain. The signal appears to be high up in the valley on the eastern side. There are no other clear signals to be seen, even though the interferogram is of unusually good quality and spans a full year.

050516-050620

This is a good quality 35-day interferogram with a very small baseline and relatively little atmospheric noise. The interferogram is decorrelated above 5-600 m in most places due to snow on the earlier date. There are no signs of deforming landslides during this month.

050516-050725

This 70-day interferogram has a baseline of 260 m and is not usable. The baseline is too long, and on top of that there appear to be strong atmospheric artifacts, visible on the flat area near Héraðsflói Bay.

050725-050829

This 280 m interferogram spans only 35 days and the coherence is very good. However, the baseline is very long and some strong atmospheric artifacts are visible, probably related to the July date. No reliable deformation detection or measurements are possible.

A.3 Ascending interferograms from Envisat data 2004-2005

Here I provide information about the different Envisat differential interferogram and what can be seen in them:

040530-051002

This interferogram has a small perpendicular baseline of 30 m but a long time-span of almost 1.5 years. The long time-span and the different seasons in which the two radar scenes were acquired result in rather low degree of correlation. Most areas above 200-300 m are found to be completely decorrelated, presumably due to snow cover during the time of one of the acquisitions. However, some low-land areas are somewhat correlated and about 3 cm of range increase can be seen in Loðmundarfjörður. It is the same signal as is seen more clearly in interferogram 040704-050724.

040704-040808

This 35-day and 80 m baseline interferogram exhibits excellent coherence that is measured much higher on the average than in any other image I processed in eastern Iceland. However, here I had some unresolved problems with removing the topography and the image has topographic artifacts that make analysis difficult. However, I clearly see that no movement occurs in Loðmundarfjörður during this one month in 2004. The only sign of motion that can be seen is in above Litlaþverárgil in Surtsstaðatunga, a clear but small displacement.

040704-050724

This interferogram has a small baseline of 40 m and spans in time just over one year, from early July 2004 to late July 2005. The quality of this interferogram is excellent; it exhibits the best inter-annual correlation of any of the processed interferograms, it is correlated from the coast up to the highest elevations, and it has almost no atmospheric disturbances nor topographic artifacts. Several deformation signals can be seen in this image. The most striking one is around 3 cm LOS increase seen in Loðmundarfjörður. The area that is moving is large, or about 1 km wide and appears to have two maxima of 3 cm displacement. Another area is a small but clear 1-fringe displacement in Kaldárgil in Jökulsárhlið. It is high on the slope between two gullies called Merargil and Litlaþvergil in an area that is called Surtstaðatunga. There are several minor and speculative deformation signals in the Borgarfjörður area. First, there appear to be two signals in Lambadalur, and the probably correspond to minor movement on the Innri- and Ytri-Þverhryggir landslides. The motion of the Innri-Þverhryggir landslide is stronger. A speculative signal is also seen in Breiðuvík on the north side of Móhöttur mountain. And finally, two small but clear signals are seen on the east side of Beinageitarfjall in Hvannstöðsdalur. There is LOS range increase is observed on the east-facing slope of Þingmúli in Skriðdalur, near Múlastekkur. The signal seems to be significant but the interferogram is somewhat noisy in this area. There is also a small hint of displacement on the south side of Suðurdalur in the Breiðdalur area, just below the Kistufell mountain above Innri-Ljósá gully, however, here the interferogram is quite noisy, so this signal is classified as speculative.

040912-040808

This interferogram has a small perpendicular baseline of 35 m and spans one month from August to September 2004. The quality of this interferogram is very good and it is one of the few interferograms that has good correlation up to over 1000 m, indicating no snow cover at all, not even at the highest elevations. The Loðmundarfjörður landslide shows no movement in this interferogram, nor do I detect any other major movement during this month. The only minor hint of displacement is in Surtstaðatunga, above Litlaþverárgil. This is a similar signal as is seen in interferogram 040704-040808, but at a different location than is seen in interferogram 040704-050724. This interferogram shows also a small hint of displacement above Innri-Ljósá gully in Breiðdalur.

040912-050828

This one-year interferogram has a perpendicular baseline of 150 m and retains a fair amount of correlation at all elevations. It is, however, not of comparable quality to the 040704-050724. Still, some of the signals in that interferogram can here be confirmed in this noisy image, e.g. the ones in Surtstaðatunga, Loðmundarfjörður, and maybe in Þingmúli.

050619-050515

This 35-day interferogram from early summer in 2005 has a perpendicular baseline of 60 m, but it is rather noisy and does not provide a lot of information, probably due to spring snow melt. No deformation is seen in Loðmundarfjörður nor at other locations in this interferogram.

050724-050515

This 70-day interferogram from 2005 has a long perpendicular baseline of 340 m that results in too many topographic artifacts so that this interferogram does not provide any useful information.

050724-050619

This 35-day interferogram has better correlation than the previous interferogram discussed above, but it also has too many topographic artifacts due to the long perpendicular baseline of 280 m.

050724-050828

Unfortunately, this 35-day interferogram exhibits the same problems as the two interferograms above, i.e. too many topographic artifacts due to the long baseline of 310 m.